

lek. Katarzyna Samelska

**Analiza zmian morfologii fotoreceptorów w rzadkich
dziedzicznych dystrofiach siatkówki z uwzględnieniem choroby
Stargardta i dystrofii czopkowo-pręcikowej na podstawie 6-letniej
obserwacji metodą optyki adaptatywnej**

**Rozprawa na stopień doktora nauk medycznych i nauk o zdrowiu
w dyscyplinie nauki medyczne**

Promotor: prof. dr hab. n. med. Jacek P. Szaflik
Promotor pomocniczy: dr n. med. Anna K. Kurowska

Katedra i Klinika Okulistyki Wydziału Lekarskiego
Warszawskiego Uniwersytetu Medycznego



Obrona rozprawy doktorskiej przed Radą Dyscypliny Nauk Medycznych
Warszawskiego Uniwersytetu Medycznego

Warszawa 2024

Słowa kluczowe:

choroba Stargardta; dystrofia czopkowa; dystrofia czopkowo-pręcikowa; dziedziczne dystrofie siatkówki; fotoreceptory; optyka adaptacyjna

Keywords:

adaptive optics; cone-rod dystrophy; cone dystrophy; photoreceptors; Stargardt disease

Składam wyrazy wdzięczności
Promotorowi - Profesorowi Jackowi P. Szaflikowi,
a także Promotor Pomocniczej –
Doktor Annie K. Kurowskiej
oraz Współautorom artykułów za udział
w przygotowaniu w niniejszej pracy.

Szczególne podziękowania kieruję do
Pani Docent Anny Zaleskiej-Żmijewskiej
za nadzór merytoryczny i mobilizację do
działania.

Pracę doktorską dedykuję mojej Rodzinie.

Wykaz publikacji stanowiących rozprawę doktorską:

1. Samelska K, Kupis M, Zaleska-Żmijewska A, Szaflik J. Adaptive optics imaging in the most common inherited retinal degenerations. *Klinika Oczna / Acta Ophthalmologica Polonica*. 2021;123(2):74-79.
<https://doi.org/10.5114/ko.2021.107769>
Praca poglądowa
Punktacja MEiN: 40.
2. Samelska K, Szaflik JP, Guskowska M, Kurowska AK, Zaleska-Żmijewska A. Characteristics of Rare Inherited Retinal Dystrophies in Adaptive Optics—A Study on 53 Eyes. *Diagnostics*. 2023; 13(15):2472.
<https://doi.org/10.3390/diagnostics13152472>
Praca oryginalna
Punktacja IF: 3,6. Punktacja MEiN: 70.
3. Samelska K, Szaflik JP, Śmigielska B, Zaleska-Żmijewska A. Progression of Rare Inherited Retinal Dystrophies May Be Monitored by Adaptive Optics Imaging. *Life*. 2023; 13(9):1871. <https://doi.org/10.3390/life13091871>
Praca oryginalna
Punktacja IF: 3,2. Punktacja MEiN: 70.

Łączna punktacja artykułów wchodzących w skład proponowanego cyklu:

Impact factor: 6,8

Punktacja MEiN: 180

Spis treści:

1.	Wykaz stosowanych skrótów.....	Str. 6
2.	Streszczenie w języku polskim.....	Str. 7 - 8
3.	Streszczenie w języku angielskim.....	Str. 9 - 10
4.	Wstęp uzasadniający połączenie wskazanych publikacji w jeden cykl i komentujący osiągnięcie naukowe kandydata na tle dotychczasowego stanu wiedzy.....	Str. 11-18
5.	Założenia i cel pracy.....	Str. 19
6.	Kopie opublikowanych prac Adaptive optics imaging in the most common inherited retinal degenerations.....	Str. 20 - 25
	Characteristics of Rare Inherited Retinal Dystrophies in Adaptive Optics—A Study on 53 Eyes.....	Str. 26 - 48
	Progression of Rare Inherited Retinal Dystrophies May Be Monitored by Adaptive Optics Imaging.....	Str. 49 - 66
7.	Podsumowanie i wnioski.....	Str. 67
8.	Piśmiennictwo.....	Str. 68 - 70
9.	Opinia Komisji Bioetycznej.....	Str. 71 - 72
10.	Oświadczenia współautorów.....	Str. 73 – 85

Wykaz stosowanych skrótów

AO	optyka adaptacyjna; ang. adaptive optics
BCVA	ostrość wzroku z najlepszą korekcją; ang. best-corrected visual acuity
CD	dystrofia czopkowa; ang. cone dystrophy
CRD	dystrofia czopkowo-pręcikowa; ang. cone-rod dystrophy
DM	gęstość czopków; ang. cone density
ERG	elektroretinografia
IRDs	dziedziczne dystrofie/degeneracje siatkówki; ang. inherited retinal dystrophies/degenerations
FA	angiografia fluoresceinowa; ang. fluorescein angiography
FAF	autofluorescencja dna; ang. fundus autofluorescence
mfERG	elektroretinografia wieloogniskowa; ang. multifocal electroretinography
N%6	analiza Voronoia czopków heksagonalnych
OCT	optyczna koherentna tomografia; ang. optical coherence tomography
OCTA	angiografia optycznej koherentnej tomografii; ang. optical coherence tomography angiography
RCD	dystrofia pręcikowo-czopkowa; ang. rod-cone dystrophy
REG	regularność czopków; ang. regularity
RNFL	warstwa włókien nerwowych siatkówki; ang. retinal nerve fibre layer
RP	zwyrodnienie barwnikowe siatkówki; ang. retinitis pigmentosa
RPE	nabłonek barwnikowy siatkówki; ang. retinal pigment epithelium
SM	odległość między czopkami; ang. cone spacing
STGD	choroba Stargarda; ang. Stargardt's disease

Streszczenie w języku polskim

Tytuł: Analiza zmian morfologii fotoreceptorów w rzadkich dziedzicznych dystrofiach siatkówki z uwzględnieniem choroby Stargardta i dystrofii czopkowo-pręcikowej na podstawie 6-letniej obserwacji metodą optyki adaptacyjnej

Wprowadzenie: Dziedziczne dystrofie siatkówki (IRDs) to schorzenia o podłożu genetycznym z kręgu chorób rzadkich. Prowadzą do postępującego, nieodwracalnego, obustronnego ubytku wzroku. Choroba Stargardta (STGD), dystrofia czopkowo-pręcikowa (CRD) i dystrofia czopkowa (CD) to dystrofie obejmujące pierwotnie centralny obszar siatkówki.

Sposoby obrazowania dziedzicznych chorób siatkówki są ograniczone i w wielu przypadkach niewystarczające do postawienia dokładnej diagnozy lub monitorowania progresji choroby w czasie. Optyka adaptacyjna to nowa nieinwazyjna metoda obrazowania, pozwalająca na uwidocznienie pojedynczych fotoreceptorów.

Cel pracy: Celem pracy było określenie cech charakterystycznych dla obrazu dziedzicznych dystrofii siatkówki przy użyciu optyki adaptacyjnej i porównanie ich z oczami zdrowymi, a także ocena stopnia progresji zmian czopków w dziedzicznych dystrofiach siatkówki w obserwacji 6-letniej.

Metodyka: Do badania przekrojowego włączono 36 oczu z dystrofią Stargardta i 8 oczu z dystrofią czopkowo-pręcikową oraz 14 oczu zdrowych. Badanie przeprowadzono również na 9 oczach z dystrofią czopkową.

Oceną w czasie 6-letniej obserwacji objęto 38 oczu z dystrofią Stargardta i 8 oczu z dystrofią czopkowo-pręcikową, a także 10 oczu z dystrofią czopkową.

W niniejszej pracy oceniono cechy czopków takie jak, gęstość (DM), odległość między czopkami (SM), regularność (REG) i analiza Voronoia czopków heksagonalnych (N%6). Powyższe parametry skorelowano z ostrością wzroku z najlepszą korekcją (BCVA, best-corrected visual acuity), z wiekiem i płcią pacjentów oraz z postawioną diagnozą. Dokonano ponadto analizy czynników wpływających na nieuzyskanie pełnej jakości badania.

Badanie przeprowadzono aparatem Rtx1™ (Imagine Eyes, Francja).

Wyniki: Zaobserwowano znamienne różnice w parametrach DM, SM, REG i N%6 pomiędzy oczami z IRDs a zdrowymi ($p < 0,001$ dla DM, SM i REG, $p = 0,008$ dla N%6).

Nie uwidoczniło korelacji między wartościami parametrów DM, SM i REG, a wiekiem, płcią ani BCVA w grupie badanej ($p > 0,05$).

Parametry DM i SM, a także ostrość wzroku z najlepszą korekcją w oczach z IRDs uległy znaczącej zmianie w ciągu 6-letniej obserwacji ($p < 0,001$ dla DM, $p < 0,001$ dla SM, $p = 0,001$ dla BCVA). Progresja ubytku DM i wzrostu SM była wyższa u kobiet niż u mężczyzn ($p = 0,025$ dla DM, $p = 0,021$ dla SM).

Stopień progresji zmian DM był skorelowany ze wzrostem SM, co wynika z definicji parametrów ($p < 0,001$) oraz z obniżeniem REG ($p = 0,036$). Stopień progresji zmian czopków nie był zależny od obniżenia BCVA ($p = 0,847$), od wieku ($p = 0,223$), ani od wyjściowych wartości parametrów fotoreceptorów: wyjściowego DM ($p = 0,302$), wyjściowego SM ($p = 0,231$) i wyjściowego REG ($p = 0,276$).

Parametry DM i SM różniły się znacząco w analizie trzech jednostek chorobowych: STGD, CRD i CD w jednej z analiz ($p = 0,006$ dla DM, $p = 0,002$ dla SM), co nie zostało potwierdzone w kolejnych analizach.

Nie zaobserwowano istotnej różnicy w parametrach REG i N%6 pomiędzy jednostkami chorobowymi.

Stopień progresji zmian parametrów DM, SM i REG w obserwacji 6-letniej nie wykazywał różnic w analizie porównawczej między jednostkami chorobowymi: STGD, CRD i CD ($p=0,338$ dla DM, $p=0,308$ dla SM, $p=0,475$ dla REG).

Wykonanie badania pełnego jakościowo było rzadsze w oczach z niższymi wartościami DM ($p=0,004$) i wyższymi wartościami SM ($p=0,013$).

Wnioski: Na podstawie uzyskanych wyników można stwierdzić, że parametry morfologiczne fotoreceptorów siatkówki w rzadkich dziedzicznych chorobach siatkówki różnią się od parametrów morfologicznych fotoreceptorów w zdrowych oczach. Ponadto, analiza progresji zmian wykazuje postęp degeneracji w obserwacji 6-letniej.

Zmiana parametrów fotoreceptorów w oczach z IRDs jest niezależna od ostrości wzroku z najlepszą korekcją. Możliwość uzyskania miarodajnych wyników spada w oczach z niższą gęstością czopków i wyższymi wartościami odległości między czopkami, czyli w oczach z wyższym stopniem zaawansowania choroby.

Analiza progresji w czasie jest możliwa do obserwacji za pomocą optyki adaptatywnej.

Streszczenie w języku angielskim

Title: Analysis of photoreceptor morphology in rare inherited retinal dystrophies, including Stargardt disease and cone-rod dystrophy – a 6-year observation with the use of adaptive optics

Background: Inherited retinal dystrophies (IRDs) are genetic disorders recognized as rare diseases. They lead to progressive, bilateral and irreversible vision loss. Stargardt disease (STGD), cone-rod dystrophy (CRD) and cone dystrophy (CD) are conditions affecting primarily macula.

Visualization of IRDs tends to be challenging. In many cases, it is not precise enough to state a diagnosis and to monitor the progression. Adaptive optics is a new non-invasive imaging technique enabling to visualize single photoreceptors.

Objectives: The aim of this dissertation was to determine characteristic features of macular cones in inherited retinal dystrophies with the use of adaptive optics, and to compare them with healthy eyes. Another aim was to track the progression of cone changes in inherited retinal degenerations in 6-year observation.

Methods: The cross-sectional study comprised of 36 eyes with STGD, 8 eyes with CRD and 14 healthy controls. The study was held on 9 eyes with CD as well.

6-year observation was conducted in 38 eyes with STGD, 8 eyes with CRD and also in 10 eyes with CD.

Cone parameters were evaluated, such as density (DM), spacing (SM), regularity (REG) and Voronoi analysis of hexagonal cells (N%6). The parameters were correlated with best corrected visual acuity (BCVA). An analysis to identify the factors that increase the probability of incomplete data acquisition was performed.

The images were obtained with the use of adaptive optics camera Rtx1™ (Imagine Eyes, France).

Results: There were significant differences in the DM, SM, REG, and N%6 parameters between the healthy and IRD-affected eyes ($p < 0.001$ for DM, SM, and REG; $p = 0.008$ for N%6).

No correlation was found between DM, SM and REG parameters compared to age, sex and BCVA in the study group ($p > 0,05$).

DM, SM and BCVA changed significantly over a 6-year observation period ($p < 0,001$ for DM, $p < 0.001$ for SM, $p = 0.001$ for BCVA). The decrease in the DM and increase in the SM parameters were significantly higher in females than in males ($p = 0.025$ for DM, $p = 0.021$ for SM).

There was a correlation found between DM change and SM change ($p < 0.001$), which stems from the definition of SM and DM and between DM change and REG change ($p = 0,036$). DM deterioration was not correlated with BCVA change ($p = 0.847$), age ($p = 0.223$) nor from initial DM ($p = 0.302$), initial SM ($p = 0.231$) and initial REG ($p = 0.276$).

The mean DM and SM differed significantly between the diagnoses of STGD, CRD and CD ($p = 0.006$ for DM, $p = 0.002$ for SM), which has not been confirmed in following analyses. There was no significant difference noted between photoreceptor parameters (REG and N%6) and the diagnoses.

Progression rate in DM, SM and REG did not differ significantly in the analysis between STGD, CRD and CD ($p = 0,338$ for DM, $p = 0,308$ for SM, $p = 0,475$ for REG).

Complete data acquisition was less frequent in eyes with lower DM ($p = 0.004$) and higher SM ($p = 0.013$).

Conclusions: The results outlined above lead to conclusion that photoreceptors' morphology in rare inherited retinal dystrophies differ from the ones in healthy eyes. Longitudinal analysis shows progression of degeneration in 6-years observation.

The change in cones' parameters is not correlated with best corrected visual acuity.

Low cone density and high cone spacing are risk factors for incomplete data acquisition.

Data obtained with adaptive optics offer the potential for the long-term observation of disease progression.

Wstęp uzasadniający połączenie wskazanych publikacji w jeden cykl i komentujący osiągnięcie naukowe kandydata na tle dotychczasowego stanu wiedzy

Proponowany cykl artykułów składa się z trzech manuskryptów: jednej pracy pogładowej oraz dwóch prac oryginalnych dotyczących zagadnień obrazowania z użyciem optyki adaptatywnej w kontekście diagnozowania i monitorowania rzadkich chorób siatkówki. Przedmiotem zainteresowania prac oryginalnych są: choroba Stargardta (STGD), dystrofia czopkowo-pręcikowa (CRD). Badaniem objęto również oczy z dystrofią czopkową (CD).

Wstęp teoretyczny

Rzadkie dziedziczne dystrofie siatkówki, opisywane angielskim skrótem IRDs (inherited retinal dystrophies), to heterogenna grupa chorób uwarunkowanych genetycznie. Są to schorzenia obuoczne i skutkują nieodwracalnym upośledzeniem widzenia. Podłoże genetyczne IRDs jest niejednorodne, różne dla każdej z jednostek chorobowych. Mechanizm uszkodzenia narządu wzroku w dystrofiach również nie jest jednorodny – w niektórych podłożem patologii jest pierwotne uszkodzenie fotoreceptorów siatkówki, a w innych nieprawidłowa akumulacja produktów przemiany materii w obrębie siatkówki.

Najczęstszą spośród dziedzicznych dystrofii siatkówki jest zwyrodnienie barwnikowe, znane jako *retinitis pigmentosa* (RP). Jest to zwyrodnienie pręcikowo-czopkowe – dotykające fotoreceptorów, w którym pręciki ulegają degeneracji w większym stopniu niż czopki. Uszkodzenie obejmuje pierwotnie obwodowe regiony siatkówki, w dalszych etapach schorzenia zmiany obejmują również plamkę żółtą i naczynia krwionośne – dochodzi m.in. do obrzęku plamki i ścięczenia naczyń.

Inne dystrofie przebiegające z degeneracją fotoreceptorów to dystrofia czopkowo-pręcikowa (ang. cone-rod dystrophy; CRD) oraz dystrofia czopkowa (ang. cone dystrophy; CD). Model dziedziczenia chorób CD i CRD może być autosomalny dominujący, autosomalny recesywny, związany z chromosomem X lub nieustalony. Zidentyfikowano powyżej 32 mutacje prowadzących do tego typu dystrofii [1]. Dystrofie CD i CRD występują z częstotliwością szacowaną na 1:30000 – 1:40000 [2]. Geny, których mutacje odpowiadają za wystąpienie CD i CRD, mogą kodować białka odpowiedzialne za odbiór impulsów świetlnych oraz fototransdukcję w obrębie czopków, białka strukturalne zewnętrznych segmentów fotoreceptorów, transport rzęskowy oraz transport neurotransmiterów [1].

W dystrofii czopkowo-pręcikowej dochodzi do uszkodzenia czopków w większym stopniu niż pręcików, w dystrofii czopkowej natomiast uszkodzone są jedynie czopki. Plamka żółta jest regionem siatkówki charakteryzującym się największym nagromadzeniem czopków, a co za tym idzie, odpowiadającym za widzenie centralne i barwne. Stąd choroby te są określane mianem makulopatii – chorób obejmujących plamkę żółtą oraz prowadzących do uszkodzenia widzenia centralnego oraz widzenia barw. Obrazem klinicznym CD i CRD jest obraz typu „bawolego oka” w obrębie plamki żółtej, a także depozyty typu komórek kostnych na bliskim i średnim obwodzie siatkówki. Zostały opisane różnice przebiegu choroby między CD a CRD – zaburzenia widzenia zmierzchowego objawiają się wcześniej w dystrofii czopkowej oraz progresja choroby jest gwałtowniejsza w dystrofii czopkowej w porównaniu z dystrofią czopkowo-pręcikową [1,3].

Choroba Stargardta (STGD) jest najpowszechniejszą makulopatią spośród IRDs. Jej częstość występowania szacuje się na 1:10000 [4,5]. Model dziedziczenia, podobnie jak w przypadku innych opisywanych wcześniej dystrofii, może być różnorodny. W przypadku choroby Stargardta najczęstszym dziedziczeniem jest autosomalnie recesywne, obejmujące mutację genu *ABCA4*. Gen ten jest odpowiedzialny za białko transportowe - ATP-azę obecną w ścianie fotoreceptorów [5,6].

Opisano ponad 900 mutacji chorobotwórczych w obrębie genu *ABCA4*. Jednakże nie wszystkie mutacje tego genu fenotypowo odpowiadają chorobie Stargardta. Część mutacji *ABCA4* opisano jako przyczynę postaci innych dystrofii: czopkowo-pręcikowej, czopkowej i

pręcikowo-czopkowej [6], co wpływa na trudność diagnostyki genetycznej choroby Stargarda, jak i innych chorób z grupy IRDs.

Za patogenezę zmian w STGD odpowiedzialny jest nieprawidłowy metabolizm białka fotoreceptorów – lipofuscyny, która gromadzi się w nieprawidłowy sposób w tylnym biegunie siatkówki. Wtórnie do nieprawidłowej akumulacji lipofuscyny w obrębie nabłonka barwnikowego siatkówki (ang. retinal pigment epithelium; RPE) dochodzi do uszkodzenia fotoreceptorów i zaburzeń przewodzenia bodźców wzrokowych. W miejscach gromadzenia lipofuscyny w badaniu angiografii fluoresceinowej (ang. fluorescein angiography; FA) widoczny jest objaw ciszy naczyniówkowej (ang. dark choroid) charakterystyczny dla tej jednostki chorobowej.

Z racji różnorodnej etiologii genetycznej, diagnoza IRDs opiera się w dużej mierze na obrazie klinicznym. Objawy obejmują obustronne pogorszenie ostrości wzroku przypadające najczęściej na drugą-trzecią dekadę życia. W przypadku dystrofii obejmujących plamkę, obserwowane jest pogorszenie widzenia centralnego i barwnego. W dystrofiach pręcikowo-czopkowych (oraz w mniejszym stopniu, w czopkowo-pręcikowych) obserwuje się zawężanie pola widzenia, co można zbadać przy użyciu perymetrii.

Obraz IRDs w badaniu dna oka może być niejednoznaczny i subtelnie wyrażony na wczesnych etapach choroby. W obrębie plamki żółtej mogą występować obszary zaniku. Charakterystyczny dla dystrofii obejmujących plamkę obraz „bawolego oka” nie jest specyficzny dla danego typu dystrofii. W rejonach paracentralnych obserwuje się m.in. ciemne struktury – „komórki kostne”, które często występują w dystrofii pręcikowo-czopkowej, ale i w czopkowo-pręcikowej oraz czopkowej. W celu poszerzenia diagnostyki oraz wyodrębnienia konkretnej jednostki chorobowej, poza diagnostyką genetyczną, wykonuje się badania dodatkowe.

Głównym badaniem obrazowym ukazującym zaburzoną strukturę w IRDs jest optyczna koherentna tomografia (ang. optical coherent tomography; OCT) tylnego odcinka oka oraz autofluorescencja dna oka (ang. fundus autofluorescence, FAF), za pomocą których można uwidoczniać m.in. rejony atrofii siatkówki. Celem obrazowania unaczynienia oraz perfuzji w obrębie siatkówki można wykonać badanie angio-OCT (OCTA) oraz angiografię fluoresceinową (FA) – szczególnie przydatną w diagnozowaniu choroby Stargarda [7].

Szczególne informacje funkcjonalne, poza badaniem ostrości wzroku i perymetrią, wnoszą badania elektrofizjologiczne: wzrokowe potencjały wywołane (ang. visual evoked potentials; VEP) dostarczające informacji o przewodzeniu sygnału wzrokowego na odcinku plamka żółta-kora wzrokowa, jak i ERG (elektroreginografia) dostarczająca informacji o zaburzeniu przepływu sygnału w obrębie konkretnych typów fotoreceptorów lub w obrębie konkretnych lokalizacji w biegunie tylnym [4,5,7-9].

Metody diagnostyczne wyszczególnione powyżej nie zawsze dają możliwość postawienia pewnej diagnozy, a sam proces diagnostyczny niejednokrotnie trwa miesiącami lub latami. W związku z tym istnieje zapotrzebowanie na inne, nowocześniejsze metody badania, które pozwolą na ułatwienie procesu diagnostycznego IRDs. Należą do nich między innymi optoretinografia (ang. *optoretinography*), pozwalająca na obserwację odpowiedzi na bodziec, metoda *laser speckle flowgraphy* służąca do wizualizacji krążenia w obrębie dna oka, oksymetria siatkówkowa (ang. *retinal oxymetry*) – obrazująca metabolizm i dyfuzję tlenu w obrębie naczyniówki oraz funkcjonalny rezonans magnetyczny (ang. *functional magnetic resonance*), dzięki któremu możemy obserwować odpowiedzi na bodziec wzrokowy w obrębie kory wzrokowej [9,10].

Inną metodą diagnostyki okulistycznej jest optyka adaptacyjna (ang. *adaptive optics*; AO), którą zastosowano do badania oczu z chorobami z kręgu IRDs (chorobą Stargarda, dystrofią czopkowo-pręcikową i dystrofią czopkową).

Optyka adaptacyjna i jej założenia

Optyka adaptacyjna (ang. *adaptive optics*, AO) jest metodą diagnostyczną użytą w niniejszej pracy. Jest to technika pierwotnie zaprojektowana w celu wizualizacji obiektów astronomicznych dokonująca korekcji aberracji spowodowanych zjawiskami atmosferycznymi.

Użycie AO w okulistyce zostało zapoczątkowane w 1989 [1] i opisane przez Drehera i wsp. [11] Obejmowało korektę aberracji wywołanych przez rogówkę i soczewkę w celu obrazowania warstwy nerwowych siatkówki (ang. *retinal nerve fiber layer*, RNFL). Pierwsze użycie AO w celu wizualizacji pojedynczych komórek w obrębie ludzkiej siatkówki zostało opisane w 1997 roku [12]. Od tego czasu opisywana jest analiza mikrostruktur siatkówki w oczach ze schorzeniami takimi jak jaskra, retinopatia cukrzycowa, zwyrodnienie plamki związane z wiekiem, choroby zapalne siatkówki i naczyńówki, odwarstwienie siatkówki oraz rzadkie dziedziczne dystrofie siatkówki.

Obrazowanie siatkówki z pomocą optyki adaptacyjnej odbywa się dzięki obecności dwóch źródeł światła: jedno z nich oświetla siatkówkę, a drugie dokonuje pomiaru i korekcji aberracji frontu falowego. Tak uzyskany obraz pozwala na ocenę struktur tak niewielkich, jak pojedyncze fotoreceptory [1,13]. W IRDs obserwowana jest nieprawidłowa struktura mozaiki czopków. Ocena pręcików jest utrudniona i możliwa jedynie w wybranych modelach sprzętu [14,15].

Metodyka badań

Do badania użyto aparatu Rtx1™ (Imagine Eyes, Orsay, France), który jest oftalmoskopem typu AOFIO (ang. *adaptive optics flood illuminated ophthalmoscope*). W badaniu użyte zostaje światło podczerwone o długości fali 850 nm. Jego rozdzielczość to 1,6 μm . Wymiary uzyskanego obrazu wynoszą $4^\circ \times 4^\circ$, co odpowiada w przybliżeniu obszarowi 1,2 mm x 1,2 mm w obrębie siatkówki.

Lokalizacja badanego obszaru jest możliwa do wyboru podczas dokonywania obrazowania (np. 2° powyżej, poniżej, skroniowo lub nosowo od dołeczka). Obrazowanie mikrostruktur dołeczka nie jest miarodajne w aparacie Rtx1™ [16], stąd przyjęto powszechną, również u innych badaczy, praktykę badania lokalizacji okołodołeczkowych.

Charakterystyczne cechy dla obrazowania siatkówki z pomocą optyki adaptacyjnej to zaburzenie struktury mozaiki fotoreceptorów, ciemne obszary, a także obszary z utrudnioną wizualizacją fotoreceptorów [14,15,17,18], co zostało zobrazowane na ilustracjach nr 3, 6 i 7 drugiego artykułu z serii. Zmiany morfologiczne struktury czopków występują we wczesnych fazach chorób IRDs oraz mogą zostać wykryte wcześniej niż pogorszenie funkcji wzrokowej [19]. Powyżej opisane cechy nie poddają się jednak analizie ilościowej, a jedynie opisowej.

W niniejszej pracy dokonano ilościowej analizy następujących pomiarów określających strukturę mozaiki fotoreceptorów:

- DM: gęstość czopków (ang. *cone density*) [$1/\text{mm}^2$],
- SM: odległość między czopkami (ang. *cone spacing*) [μm],
- N%6: analiza Voronoia czopków heksagonalnych [%],
- REG: regularność [%].

Spośród powyższych, DM i SM opisują ilościowo cechy mozaiki czopków. N%6 i REG są parametrami pozwalającymi na ocenę struktury mozaiki oraz prawidłowości wykonania obrazowania. W opisie parametrów, a także w opublikowanych pracach, użyto skrótów wyszczególnionych powyżej, zaproponowanych przez producenta oprogramowania.

Podczas każdej z wizyt wykonano także ocenę ostrości wzroku z najlepszą korekcją (BCVA, ang. *best-corrected visual acuity*) oraz przeprowadzono pełne badanie okulistyczne z

oceną dna oka po mydriazie (1% tropicamid), badanie OCT plamki oraz autofluorescencji dna oka (ang. fundus autofluorescence, FAF).

Badanie zostało przeprowadzone w Katedrze i Klinice Okulistyki Wydziału Lekarskiego Warszawskiego Uniwersytetu Medycznego. Badanie uzyskało pozytywną opinię Komisji Bioetycznej przy Warszawskim Uniwersytecie Medycznym (KB/87/2015). Wszyscy pacjenci wyrazili pisemną zgodę na przeprowadzenie badania.

W oparciu o zebrane dane została przeprowadzona analiza statystyczna. Dystrybucja pod względem normalności została przeanalizowana za pomocą testu Shapiro-Wilka. Do danych podlegających dystrybucji normalnej został użyty *Student's t-test*. W przypadku dystrybucji normalnej użyto testu *U Mann-Whitney'a* do porównania dwóch grup. W przypadku dystrybucji normalnej i porównania więcej niż dwóch grup użyto testu *ANOVA* (dane parametryczne) lub *Kruskala-Wallis* (dane nieparametryczne). Testem „post hoc” użytym po teście *ANOVA* był *post-hoc HSD Tukey's*, a testem użytym po teście *Kruskala-Wallis* był test *post-hoc Dunna*. Wyniki z testów były dopasowane z użyciem korekcji Bonferroniego. Model jednoczynnikowej regresji logistycznej był użyty do oceny czynników wpływających na zebranie niepełnych danych, model bazował na kryterium Akaike Information Criterion (AIC). Poziom istotności statystycznej ustalono na $p=0,05$. Obliczeń dokonywano w programie R (wersja 4.0.2).

Do niniejszej pracy włączono oczy z dystrofiami, które objawiają się pierwotnie uszkodzeniem w obrębie plamki żółtej, tj. z chorobą Stargardta, dystrofią czopkowo-pręcikową i dystrofią czopkową. Choroby te charakteryzują się zmianami możliwymi do zaobserwowania w strukturze czopków, na co pozwala obrazowanie z użyciem optyki adaptywnej.

Dystrofie pręcikowo-czopkowe (jak np. *retinitis pigmentosa*, RP) nie były przedmiotem badania z dwóch przyczyn. Po pierwsze, początek i nasilenie objawów w ich przypadku dotyczy siatkówki obwodowej. Pod drugie, zwyrodnieniu ulegają przede wszystkim pręciki, których obrazowanie przy pomocy optyki adaptywnej jest ograniczone.

Podsumowanie artykułów

Pierwszy z artykułów z proponowanego cyklu to artykuł poglądowy opublikowany na łamach kwartalnika *Klinika Oczna/Acta Ophthalmologica Polonica* (ISSN 0023-2157), będącego organem Polskiego Towarzystwa Okulistycznego od 1899 r. W artykule tym dokonano przeglądu literatury dotyczącej rzadkich dziedzicznych chorób siatkówki: choroby Stargardta i dystrofii czopkowo-pręcikowej, a także zwyrodnienia barwnikowego siatkówki oraz uwzględniono aktualne doniesienia dotyczące charakterystyki obrazowania wyżej wymienionych schorzeń za pomocą optyki adaptywnej.

Drugi i trzeci artykuł są pracami oryginalnymi opublikowanymi w indeksowanych czasopismach posiadających współczynnik oddziaływania (IF, ang. *impact factor*). Drugi z artykułów opisuje cechy dystrofii CD, CRD i STGD w badaniu AO. Porównano parametry czopków pomiędzy oczami ze zdiagnozowanymi IRDs a oczami zdrowymi oraz dokonano porównania pomiędzy poszczególnymi jednostkami chorobowymi. W badaniu dokonano także zestawienia cech morfologicznych czopków z oceną funkcjonalną siatkówki – BCVA. Trzeci artykuł opisuje analizę zmian parametrów czopków w oczach z IRDs w czasie 6-letniej obserwacji.

Obie prace oryginalne zawierają wstęp teoretyczny, w którym zawarto opis cech charakterystycznych w obrazie mozaiki fotoreceptorów uwidocznione w AO. Umieszczono także ilustracje pochodzące z badań własnych obrazujące zmiany w przebiegu dystrofii. Są to: zaburzenia architektury mozaiki, „czarne przestrzenie” (ang. „dark spaces”) odpowiadające obszarom braku zobrazowanych fotoreceptorów, a także obszary z niepełną wizualizacją fotoreceptorów. Zmiany te nie podlegały analizie ilościowej, a jedynie opisowi jakościowemu.

Drugi artykuł proponowanego cyklu opublikowany został w czasopiśmie *Diagnostics* (ISSN 2075-4418). Dokonano w nim oceny właściwości parametrów czopków: DM, SM, REG, N%6 przy użyciu aparatu Rtx1™ oraz oceniono ostrość wzroku (BCVA) na tablicy Snellena.

Do badania włączono 53 oczu 28 pacjentów ze stwierdzonymi chorobami: chorobą Stargardta (36 oczu, 19 pacjentów), dystrofią czopkowo-pręcikową (8 oczu, 4 pacjentów) i dystrofią czopkową (9 oczu, 5 pacjentów). Grupę kontrolną stanowiło 14 oczu 14 pacjentów bez stwierdzonych chorób okulistycznych.

Potwierdzono hipotezę, że parametry DM, SM, REG i N%6 różnią się pomiędzy oczami z dziedzicznymi dystrofiami siatkówki i oczami zdrowymi. Średnia gęstość czopków (parametr DM) badana dla oczu prawych wynosiła 10111,33/mm² w grupie badanej, a 25656,42/mm² w grupie kontrolnej (p<0,001). Parametr SM wyniósł średnio 12,11 um dla grupy badanej, zaś 6,91 um dla grupy kontrolnej (p<0,001). Regularność fotoreceptorów (parametr REG) wyniosła 83,74% w grupie badanej i 90,98% w grupie kontrolnej (p<0,001). Analiza Voronia (N%6) wykazała brak istotnej różnicy między grupą badaną a kontrolną (45,21% dla grupy badanej, 48,43% dla grupy kontrolnej; p=0,008).

Istotną statystycznie różnicę w parametrach DM, SM i REG wykazano również biorąc pod uwagę pomiary w poszczególnych lokalizacjach obojga oczu: w pomiarze skroniowym, nosowym, górnym i dolnym. Różnica w analizie Voronia była nieistotna statystycznie w lokalizacji skroniowej i nosowej, co zobrazowano w Tabeli nr 3 artykułu.

Nie wykazano różnic w pomiarach: DM, SM i REG ani w BCVA pomiędzy prawymi a lewymi oczami pacjentów z dziedzicznymi dystrofiami siatkówki (p=0,172 dla DM, p=0,812 dla SM, p= 0,156 dla REG, p=0,218 dla BCVA).

Średnia gęstość fotoreceptorów (DM) w CD, CRD i STGD wynosiła odpowiednio 8900,39/mm², 9296,32/mm² i 16209,66/mm². Średnia odległość pomiędzy fotoreceptorami (SM) w CD, CRD i STGD to odpowiednio 12,37 um, 14,82 um i 9,65 um. Wartości te wykazały znamienne różnicę pomiędzy powyższymi jednostkami chorobowymi (p=0,006 dla DM, p=0,002 dla SM). Różnica między poszczególnymi dystrofiami nie była znamienne dla regularności (REG) (p=0,334) ani analizy Voronia (N%6) (p=0,828). Powyższy wynik nie został potwierdzony w analizach zawartych w *artykule trzecim*, przez co niemożliwe jest określenie wartości parametrów DM i SM specyficznych dla poszczególnych jednostek chorobowych.

W innych pracach opisano różnice w parametrach czopków zbadanych za pomocą AO pomiędzy oczami zdrowymi a oczami z IRDs [17, 20-26]. Zaburzony obraz mozaiki fotoreceptorów w CRD opisali jako pierwsi Wolfing i wsp. w 2006 r. [20]. Stwierdzono wówczas 6,6-krotne obniżenie gęstości czopków w CRD w stosunku do zdrowego oka. Song i wsp. [25] raportowali istnienie polimorfizmu przebiegu CRD między pacjentami, zasugerowali większy stopień ubytku pręcików w siatkówce obwodowej w porównaniu z centralną, a także obecność ubytku czopków zarówno w siatkówce obwodowej, jak i centralnej.

Badania Chena [22] i Songa [17, 23] i wsp. wykazały zmiany *spacingu* – czyli średniej odległości - między czopkami, ale także między pręcikami w oczach z rozpoznaną dystrofią STGD. Pomiary parametrów pręcików są utrudnione w aparacie użytym do opisywanego w niniejszej pracy doktorskiej badania.

Palejwala i wsp [27] podkreślają rolę optyki adaptacyjnej we wczesnym diagnozowaniu chorób z kręgu IRDs. Opisali oni zmiany obecne w badaniu u 7-letniego bezobjawowego pacjenta, u którego występowała mutacja w genie *ELOVL4* odpowiedzialnego za dystrofię plamki żółtej.

Badanie opisane w niniejszej pracy doktorskiej wykazało brak istotnej zależności pomiędzy ostrością wzroku z najlepszą korekcją BCVA a parametrami czopków DM

($p=0,612$), SM ($p=0,436$), REG ($p=0,170$) i N%6 ($p=0,924$). Wnioski płynące z otrzymanych wyników nie wskazują na bezpośrednią korelację obrazu fotoreceptorów z funkcją widzenia. Brak korelacji może być spowodowany znacznym upośledzeniem BCVA w badanych oczach i istnieniem niewystarczającego zróżnicowania BCVA między probandami.

Badania raportowane przez Duncana i wsp. [24] wykazały związek ze zmianami morfologicznymi w obrębie fotoreceptorów ze zmianami funkcjonalnymi w przebiegu CDR i CRD, zestawiając analizę badania AO siatkówki z perymetrią, zmianami w mfERG oraz ostrością wzroku. Podobnie, korelacja między obrazem fotoreceptorów w AO z funkcjonalnymi zmianami w perymetrii, badaniu elektrofizjologicznym i badaniu poczucia kontrastu została potwierdzona przez Choi i wsp. [28]. Pozostałe cytowane prace nie zawierają analizy korelacji oceny morfologicznej z funkcjonalną.

Trzeci artykuł proponowanego cyklu został opublikowany w czasopiśmie *Life* (ISSN 2075-1729). Jest on opisem analizy zmian w czasie parametrów czopków oczu z IRDs. Badaniem objęto 56 oczu 28 pacjentów: 38 oczu 19 pacjentów z STGD, 10 oczu 5 pacjentów z CD i 4 oczu 2 pacjentów z CD. Ocenie poddano 3 parametry mierzone za pomocą optyki adaptatywnej: DM, SM i REG oraz oceniono BCVA na tablicy Snellena. Badanie zostało wykonane po raz pierwszy w 2015 roku („badanie 1”), a następnie przeprowadzono je ponownie w 2021 roku („badanie 2”), uzyskując 6-letni czas obserwacji.

Potwierdzono, że w okresie obserwacji uległy istotnej zmianie parametry czopków: doszło do obniżenia gęstości czopków - wartości DM ($12828/\text{mm}^2$ podczas „badania 1”, $10073,42/\text{mm}^2$ podczas „badania 2”, $p<0,001$) oraz zwiększenia odległości między czopkami - wartości SM ($9,83\ \mu\text{m}$ „badanie 1”, $12,16\ \mu\text{m}$ „badanie 2”, $p<0,001$). Nie wykazano zmian w regularności - wartości REG ($86,44\%$ „badanie 1”, $84,37\%$ „badanie 2”, $p=0,089$). Znamienne statystycznie pogorszeniu uległa ostrość wzroku wyrażona jako BCVA ($0,16$ „badanie 1”, $0,12$ „badanie 2”, $p=0,001$).

Wykazano, że zmiana DM w czasie była skorelowana ze zmianą SM ($p<0,001$), co wynika z definicji obu parametrów, a także ze zmianą REG ($p=0,036$). Zmiana DM podczas 6-letniej obserwacji była niezależna od zmiany w BCVA ($p=0,847$), a także od wyjściowej wartości BCVA ($p=0,302$), DM ($p=0,302$), SM ($p=0,231$) i REG ($p=0,276$).

Powyższe wyniki odnoszą się do parametrów obojga oczu (prawych i lewych) całej grupy badanej (bez podziału względem diagnozy). Istotność statystyczna zmiany parametrów DM, SM i BCVA w czasie obserwacji została potwierdzona w analizie oczu z podziałem na prawe i lewe. Istotność statystyczna zmiany tych wartości (DM, SM i BCVA) wynosiła dla oczu prawych odpowiednio: $p=0,006$, $p=0,002$, $p=0,025$, a dla oczu lewych odpowiednio: $p<0,001$, $p=0,001$, $p=0,021$.

Dokonano analizy zmiany w czasie parametrów AO: DM, SM i REG z podziałem na jednostki chorobowe: CD, CRD i STGD. Zaobserwowano, że ubytek gęstości czopków (DM) wynosił w CD $3697,39/\text{mm}^2$, w CRD $1883,46/\text{mm}^2$ oraz $3092,98/\text{mm}^2$ w STGD. Średni wzrost odległości między czopkami (SM) wynosił w CD $1,96\ \mu\text{m}$, w CRD $1,87\ \mu\text{m}$ oraz $2,8\ \mu\text{m}$ w STGD. Zmiany regularności czopków (REG) to utrata o $3,44\%$ w CD, $2,76\%$ w CRD i $1,89\%$ w STGD. Różnica pomiędzy zmianami w parametrach była nieistotna statystycznie ($p=0,338$ dla DM; $p=0,308$ dla SM; $p=0,475$ dla REG).

W dostępnych publikacjach [29-31] potwierdzono ubytek gęstości czopków w czasie w RCD i innych chorobach z kręgu IRDs. Według aktualnej wiedzy, niniejsza praca doktorska jest pierwszym badaniem obrazującym progresję w czasie zmian czopków obserwowanych przy pomocy AO w dystrofiach takich jak CRD, CD i STGD.

W niniejszej pracy wykazano, że ubytek DM i wzrost SM w czasie 6-letniej obserwacji były wyższe u kobiet niż u mężczyzn (ubytek o $3804,8/\text{mm}^2$ vs. $1908,26/\text{mm}^2$, $p=0,025$ dla DM; wzrost o $3,25\ \mu\text{m}$ vs. $1,46\ \mu\text{m}$ dla SM, $p=0,021$). Różnica w zmianie w BCVA i REG nie

była znamienne statystycznie (spadek o 0,05 vs. 0,03 dla BCVA, $p=0,748$; spadek o 2,86% vs. 1,54% dla REG, $p=0,507$). Jest to pierwsze doniesienie o różnicy progresji zmian w IRDs pomiędzy płciami. Z tego powodu wymaga ostrożnej weryfikacji w innych badaniach w przyszłości.

Podczas wykonywania badań aparatem Rtx1™, badacze napotkali trudność w uzyskaniu dobrego jakościowo obrazu mozaiki fotoreceptorów u niektórych pacjentów. W oczach, w których wykonanie pomiaru w czterech lokalizacjach było niemożliwe, do analizy wzięto uśredniony wynik w trzech lub dwóch lokalizacjach. Oczy z niepełnymi pomiarami przeanalizowano pod kątem czynników, które wpływają na ryzyko niemożności wykonania pełnego badania.

Opis tej analizy znajduje się w akapicie 3.8 *artykułu trzeciego*. Wykazano, że ryzyko niepełnej jakości badania wzrastało wraz ze wzrostem DM i spadkiem SM, co wykazało istotność statystyczną zarówno w „badaniu 1”, jak i „badaniu 2” *artykułu trzeciego* ($p<0,001$ i $p=0,004$ dla DM; $p<0,001$ i $p=0,013$ dla SM kolejno dla „badania 1” i „badania 2”). Ryzyko niepełnej akwizycji danych było wyższe w oczach z niższą wartością REG w „badaniu 1” ($p<0,001$), co nie zostało potwierdzone w „badaniu 2” ($p=0,367$). Nie wykazano, aby zmienne takie jak wiek, płeć, diagnoza oraz BCVA wpływały na ryzyko wykonania niemiarodajnego badania.

W *drugim artykule* cyklu opisano analogiczną analizę. Na podstawie zgromadzonych danych zaobserwowano, że w analizie regresji logistycznej czynnikiem ryzyka niepełnej akwizycji danych była niska wartość DM. Spadek DM o 1000/mm² zwiększał częstotliwość niepełnej jakości badania 1,39 raza (OR=0.72, CI 0.55-0.90, $p=0,008$).

Analiza doniesień literaturowych wykazała, że jest to pierwsza opublikowana analiza zależności akwizycji niepełnych danych od konkretnych czynników. Wcześniej autorzy cytowanych publikacji [10] wskazywali na trudności w uzyskaniu miarodajnego obrazu w oczach z IRDs. Wyniki opisane w pracy naszego autorstwa sugerują, że zebranie niepełnych danych jest częstsze w oczach z silniej zaznaczonymi zmianami w obrębie fotoreceptorów (niższa gęstość czopków – DM i wyższa odległość między czopkami – SM). Czynniki takie jak wiek i ostrość wzroku z najlepszą korekcją nie wpłynęły w niniejszej analizie na ryzyko niepełnego badania. Jest możliwe, że na istotność statystyczną wpłynęła liczebność grupy oraz niewielkie różnice w BCVA między badanymi oczami.

Badanie będące przedmiotem niniejszej pracy jest unikalne pod względem liczebności grupy badanej. Spośród cytowanych artykułów, żaden nie prezentuje opisu cech czopków w IRDs na grupie tak licznej. Wolfing i wsp. opisali swe obserwacje na podstawie jednego pacjenta z CRD [20]. Song i wsp. analizowali troje spokrewnionych ze sobą pacjentów [25]. Badanie Duncana i wsp. [24] obejmowało 8 oczu: 5 z diagnozą RP i 3 z CRD. Doniesienia Choi i wsp. [28] bazowały na analizie oczu pięciorga pacjentów: trojga z RCD, jednego z CRD i jednego z rozpoznaniem młodzieńczej dystrofii plamki żółtej. Artykuł Gianniniego i wsp. [32] opisuje obserwacje 12 oczu z 5 różnymi diagnozami z kręgu IRDs oraz 20 oczu zdrowych.

Prace opisujące chorych z STGD opierają się niekiedy na większej grupie pacjentów: Chen i wsp. [22] bazowali na 23 pacjentach. Song i wsp. w swoich dwóch pracach [17,23] formułują wnioski na podstawie obserwacji dwóch oraz trzech pacjentów.

Kolejną unikatową cechą prac wchodzących w skład proponowanego cyklu publikacji jest odstęp 6 lat pomiędzy obserwacjami. Opisy zmian fotoreceptorów w czasie w badaniu z użyciem optyki adaptatywnej zostały opublikowane przez innych autorów [21,26, 29-31,33]. Artykuł Foote’go i wsp. [21] opisuje brak zdefiniowanej zmiany w zdrowych oczach w obserwacji 3-letniej. Publikacje Uedy-Consolvo i wsp. [29], Ziccardiego i wsp. [30] i Roshandel’a i wsp. [31] raportują obniżenie gęstości czopków w dystrofii pręcikowo-czopkowej, w tym w zwyrodnieniu barwnikowym siatkówki na podstawie obserwacji 2-letniej

i 6-miesięcznej. Jedna z prac [33] opisuje zmiany fotoreceptorów obserwowane w AO po leczeniu operacyjnym odwarstwienia siatkówki. Ciekawe założenie przedstawili Sahel i wsp. [26], przedstawiając możliwość monitorowania w czasie zmian fotoreceptorów u pacjentów z RCD, w tym u pacjentów poddanych leczeniu genetycznemu.

Podsumowanie wstępu i implikacje kliniczne

Wszystkie trzy prace przedstawione powyżej stanowią spójny cykl tematyczny dotyczący diagnostyki, a także monitorowania rzadkich chorób siatkówki za pomocą optyki adaptacyjnej. Zagadnienie jest istotne w kontekście wdrożonej w ostatnich latach rozwoju terapii genowej wrodzonej ślepoty Lebera (LCA, Lebers' congenital amaurosis) - dystrofii pręcikowo-czopkowej, która jest chorobą z kręgu IRDs. Lekiem stosowanym w leczeniu LCA o potwierdzonej mutacji w obrębie genu *RPE65* jest *voretigene neparvovec-rzyl* dostępny pod nazwą handlową Luxturna™. Została zaaprobowana po raz pierwszy w USA w grudniu 2017 r. [34,35]. W 2021 r. opublikowano pierwszy artykuł uwzględniający monitorowanie pacjentów poddanych terapii Luxturną™ [26]. Wraz z rozwojem terapii genowych dla innych rzadkich dziedzicznych dystrofii siatkówki, optyka adaptacyjna daje szansę na pogłębienie obserwacji efektów leczenia o obserwację zmian anatomicznych.

Założenia i cel pracy

Założeniem niniejszej pracy jest możliwość oceny zmian morfometrycznych czopków obszaru plamkowego w oczach z dziedzicznymi dystrofiami siatkówki (IRDs) z użyciem optyki adaptywnej (AO) oraz możliwość monitorowania w czasie progresji zmian w obrębie fotoreceptorów w tych chorobach.

Wykazanie wiarygodności pomiarów uzyskanych dzięki AO w dystrofiach siatkówki może pozwolić na szczegółowe monitorowanie postępu tych chorób z pomocą nowej technologii, jak i monitorowanie skuteczności nowych terapii.

Celem pracy jest ocena parametrów czopków obszaru okołodołeczkowego w oczach z IRDs: dystrofii czopkowo-pręcikowej (CRD), dystrofii czopkowej (CD) i chorobie Stargardta (STGD).

Dokonano porównania parametrów gęstości czopków (DM), odległości między czopkami (SM), regularności (REG) i analizy Voronoia (N%6) między oczami z IRDs a zdrowymi oraz pomiędzy wymienionymi jednostkami chorobowymi. Dokonano analizy zależności parametrów od funkcjonalnego parametru: ostrości wzroku z najlepszą korekcją (BCVA).

Ponadto, wykonano analizę zmian wymienionych parametrów w okresie 6-letniej obserwacji, a także sprawdzono, czy czynniki ryzyka takie jak płeć, wiek, wyjściowa ostrość wzroku, rozpoznanie oraz parametry morfometryczne czopków wpływają na stopień progresji zmian chorobowych zbadanych w AO.

Cele główne:

- Porównanie morfologii receptorów siatkówki w oczach z rzadkimi dziedzicznymi dystrofiami siatkówki z obrazem receptorów siatkówki w oczach zdrowych przy zastosowaniu optyki adaptywnej.
- Analiza morfologii receptorów siatkówki w rzadkich dziedzicznych dystrofiach siatkówki w odniesieniu do stopnia klinicznej progresji.
- Ocena stopnia progresji rzadkich dziedzicznych dystrofii siatkówki określonej zmianami w badaniu optyki adaptywnej w obserwacji 6-letniej i odniesienie jej do funkcjonalnej progresji.
- Porównanie stopnia progresji zmian w obrębie fotoreceptorów siatkówki w chorobie Stargardta, dystrofii czopkowo-pręcikowej i dystrofii czopkowej w obserwacji 6-letniej.

Cele poboczne:

- Ocena czynników wpływających na tempo progresji zmian w morfologii receptorów siatkówki w oczach z rzadkimi dziedzicznymi dystrofiami siatkówki.
- Analiza czynników wpływających na nieuzyskanie pełnej jakości badania optyki adaptywnej w oczach z rzadkimi dziedzicznymi dystrofiami siatkówki.

Access this article online	
	Website: www.klinikaoczna.pl
	DOI: https://doi.org/10.5114/ko.2021.107769

Adaptive optics imaging in the most common inherited retinal degenerations

Katarzyna Samelska, Magdalena Kupis, Anna Zaleska-Żmijewska, Jacek P. Szaflik

Department of Ophthalmology, Medical University of Warsaw, Poland
SPKSO Ophthalmic University Hospital, Warsaw, Poland

ABSTRACT

Adaptive optics is the imaging technique of the retina. It finds use in visualizing microscopic changes in the retinal photoreceptors and the retinal blood vessels. Introducing adaptive optics as a diagnostic tool facilitated diagnosing inherited retinal diseases, such as Stargardt disease, cone-rod dystrophy, and retinitis pigmentosa. These diseases are often inherited in a heterogenous pattern. Thus, genetic testing often fails to give a certain diagnosis. Optical coherence tomography, fundus autofluorescence, fluorescein angi-

ography, visual field examination and electrophysiological testing are vital for diagnosing patients with inherited retinal diseases. Adaptive optics imaging complements diagnosing and monitoring conditions such as Stargardt disease and cone-rod dystrophy. In this article we sum up the main characteristics of inherited retinal diseases in adaptive optics imaging.

KEY WORDS: adaptive optics, Stargardt disease, cone-rod dystrophy, retinitis pigmentosa.

INTRODUCTION AND BASICS OF ADAPTIVE OPTICS

Adaptive optics (AO) is a powerful tool in *in vivo* imaging of the microstructures of the retina. This imaging technique was primarily developed in astronomical telescopes in order to diminish atmospheric irregularities. The aberration-correcting system provided a high-quality image of distant objects [1].

The attempts to eliminate the optical aberrations of the eye were started by Dreher *et al.* [2]. The first use of AO in imaging the microstructures of the retina was reported in 1997 [3]. There are two main technologies of adaptive optics used in visualizing the retina's photoreceptors: split-detector (SD-AOSLO; split-detector adaptive optics scanning light ophthalmoscopy) and confocal (cSLO; confocal scanning laser ophthalmoscopy) – both confocal and spectral images may be taken simultaneously [4, 5]

The classical retinal imaging adaptive optics camera consists of three main pieces: a wavefront sensor, a wavefront corrector and a control system. The aberrations are measured by a wavefront sensor and a corrector, whereas the controller interprets the sensor-collected data and controls the interaction between the sensor and corrector. There are two sources of light: one of them used to illuminate the retina and the second to measure and correct the wavefront aberrations [1, 4].

Lately, improved sensorless adaptive optics technology with enhanced quality parameters has been introduced [6]. The imaging is non-invasive and safe. It provides resolution of 2 μ m. It may be performed with or without dilation of the patient's pupil; however, the pupil dilation is usually performed before the examination. The combination of AO and optical coherence tomography provides even greater resolution of the image and enables 3D visualization [6, 7].

PRINCIPLES OF ADAPTIVE OPTICS IN OPHTHALMOLOGY

One of the main goals of AO in ophthalmology is visualization of the photoreceptors: rods and cones. The photoreceptors' parameters examined in AOSLO are: cone density, cone spacing, Voronoi analysis, reflectivity, regularity, metrics for the preferred orientation of cones and local spatial anisotropy [5, 7-12]. The regions of photoreceptor loss allow visualization of the underlying retinal pigment epithelium (RPE) cells [13, 14]. Photoreceptor pathologies are found in e.g. diabetic retinopathy (DM) and age-related macular degeneration (AMD) [15, 16]. Figure 1 shows an adaptive optics image of photoreceptors in a normal retina.

Adaptive optics provides, non-invasively, a precise image of the retinal microvasculature. Early changes in the microcirculation, e.g. in the course of DM and AMD, are detected

CORRESPONDING AUTHOR

Katarzyna Samelska, MD, Department of Ophthalmology, Medical University of Warsaw, 13 Sierakowskiego St., 03-709, Warsaw, Poland, e-mail: samelskakatarzyna@gmail.com

in AO imaging [4, 15]. The imaging of RNFL (retinal nerve fiber layer) and its glaucomatous changes is also a target of AOSLO – the image of hyperreflective bundles surrounded by dark lines depicts nerve fiber bundles and Muller cell septa [4].

Adaptive optics scanning laser ophthalmoscopy finds use in IRDs – inherited retinal degenerations. Photoreceptor visualization is a novel way to monitor the early and advanced stages of retinal diseases.

CHARACTERISTICS OF INHERITED RETINAL DISEASES: STARGARDT DISEASE, CONE-ROD DYSTROPHY, RETINITIS PIGMENTOSA

Stargardt disease

Stargardt disease is one of the most common inherited retinal diseases with a prevalence of around 1 in 10 000 [5, 17]. It is a bilateral dystrophy which affects mainly the macu-

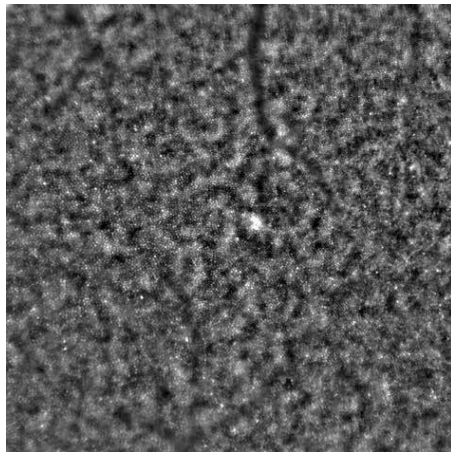


Figure 1. Photoreceptors in perifoveal area of a healthy eye imaged by adaptive optics



Figure 2. Stargardt disease: a photograph of the posterior pole

la. It leads to loss of central vision and dyschromatopsia. The dynamics of vision deterioration differs individually depending on the location of the foveal lesion [18]. The presence of central scotoma is seen in visual field examination. Microperimetry be used for monitoring the progression of the disease [19]. Macular abnormalities in Stargardt disease are shown in Figure 2.

Stargardt maculopathy is a genetic condition in most cases associated with mutations in the ABCA4 gene (MIM601691) coding a protein located in outer segments of the photoreceptors. There are more than 200 identified pathogenic variants of ABCA4 mutations leading to Stargardt disease while the three most common mutations are responsible for only 27% of the cases [20]. SD-OCT (spectral-domain optical coherence tomography) shows changes in the central macula such as loss of the outer retina structure. The dynamics of Stargardt disease progression can be defined using SD-OCT through ellipsoid zone loss evaluation [21].

Fundus autofluorescence (FAF) shows loss of central autofluorescence in the central macula and an increased signal in surrounding regions resembling bulls-eye maculopathy. With the use of FAF testing we can monitor progression of the morphological changes of the macula. The mean progression of definitely decreased autofluorescence lesions is determined as 0.51-0.76 mm²/year, and of total decreased FAF as 0.35 mm²/year [22, 23]. According to the FAF image characteristics of the fovea (including foveal sparing) and homogeneity of the background, Stargardt disease eyes may be divided into three subtypes. The RAE (rate of atrophy enlargement) differs between the three subtypes [24].

Fluorescein angiography (FFA), used more commonly in the past, showed a “dark choroid” sign in the central macula due to blocking of the choroid signal by lipofuscin deposits in the central macula. Electrophysiological tests, such as mfERG (multifocal electroretinography), show decreased macular function with a preserved peripheral signal [5, 17]. An FFA image of Stargardt disease is shown in Figure 3.

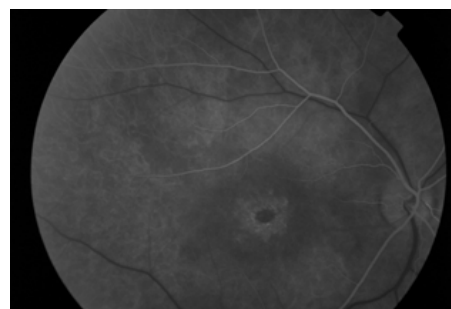


Figure 3. Stargardt disease: FFA image. Note the “dark choroid” sign in the central macula

Characteristics of adaptive optics imaging in Stargardt disease

Spectral as well as confocal AO imaging is a potent tool in imaging pathologies in photoreceptors' morphology of eyes with Stargardt disease. The cone spacing is increased and cone density is decreased in Stargardt subjects' retina compared to normal retina [5, 17, 25], as shown in Figure 4. The confocal AO images show "dark spaces" within photoreceptors' structure, which represent non-wave guiding cones visualized in SD-AOSLO. The AOSLO changes may be found before the OCT and FAF detectable changes [25].

The development of the SD-AOSLO technique revealed that the cone density in Stargardt disease is in fact higher than was expected based on confocal AOSLO imaging and improves the quality of the imaging, making it more accurate in IRDs [5, 17].

There is a correlation between increased autofluorescence and loss of photoreceptor cells. It has been found however that AOSLO image reflectivity does not correlate with lipofuscin accumulation. AOSLO images show a hyperreflective perifoveal ring and its margin marks the margin of the scotoma [26].

Adaptive optics however meets some difficulties in Stargardt disease evaluation. The central scotoma and poor fixation make it unable to examine some eyes thoroughly. The accumulation of lipofuscin prevents AOSLO photoreceptor visualization in certain areas [27]. The cone spacing and density differ between the examined areas within the same eye and there has not been established a universal way to evaluate the degree of cone atrophy [26]. A possible solution may be creating cone density deviation (CDD) maps that present variation in foveal structure and may be compared with OCT and microperimetry results [28].

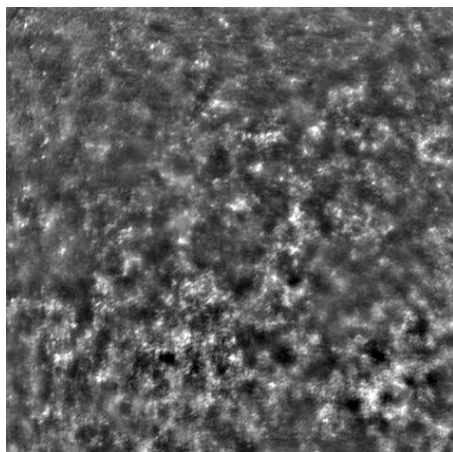


Figure 4. Stargardt disease: AO image of the perifoveal photoreceptors. Note the dark spaces and decreased cone density

Adaptive optics enables visualization of the photoreceptors' morphology in Stargardt disease which complements FAF visualization of lipofuscin accumulation and OCT cross-section of the retinal layers [27].

Cone-rod dystrophy

Cone-rod dystrophy (CRD) is a retinal dystrophy where the dysfunction is higher in cones than in rods. The prevalence ranges from 1/30 000-1/40 000 [29]. It is genetically polymorphic with multiple variants of inheritance [30, 31]. The eye fundus examination shows perifoveal atrophy and "bull's eye" appearance (Figure 5). The changes include loss of RPE, photoreceptor loss and lipofuscin accumulation. The symptoms include photoaversion, progressive visual acuity deterioration and poor color vision due to cone dysfunction. In advanced stages, CRD leads to bilateral blindness [29, 31]. The diagnostic process of CRD includes genetic testing, OCT,

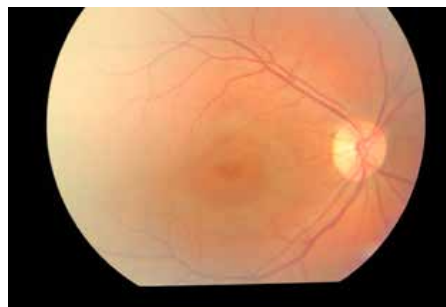


Figure 5. Cone-rod dystrophy: a photograph of the posterior pole

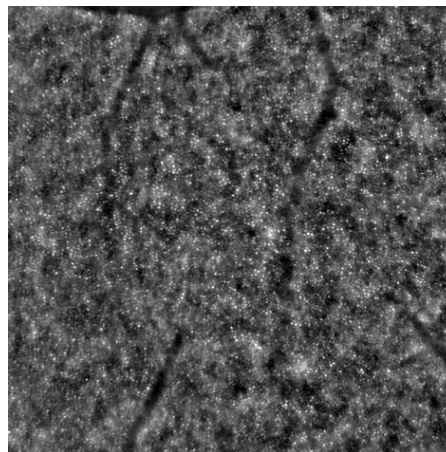


Figure 6. Cone-rod dystrophy: AO image of the perifoveal photoreceptors. Note the decreased cone density

ERG and FAF. The scotopic and photopic ERG cone and rod responses are extinguished in CRD [31].

Characteristics of adaptive optics imaging in cone-rod dystrophy

The photoreceptor AO imaging in CRD seen in AOSLO shows disruption of its mosaic and increased cone spacing and rod spacing, as seen in Figure 6. The level of the changes increases with the age of the subject. The photoreceptors in CRD show higher spacing, lower density, and lack of waveguiding cones within atrophic regions. The lowered-density regions' cone spacing measurements correlate with mfERG, microperimetry results and visual acuity changes [7, 13, 30, 32, 33].

The AOSLO imaging of the nine AD-CRD (autosomal-dominant cone-rod dystrophy) confirmed patients from the same family showed that the pattern of photoreceptor damage varies between the subjects with the same type of mutation, regardless of age [34].

Retinitis pigmentosa

Retinitis pigmentosa (RP) is an inherited progressive bilateral degeneration of the photoreceptors. Like other IRDs mentioned above, the disease may be caused by mutations in multiple genes, with a heterogenous inheritance pattern [35]. The rod loss precedes the cones loss; the changes result in reduced visual acuity, a constricted visual field and, eventually, blindness [11, 32, 36, 37]. Retinitis pigmentosa may be isolated or a part of another syndrome, e.g. Usher syndrome, where sensorineural hearing loss is also present. The characteristics of RP in the ophthalmoscopic examination include presence of bone cells, which starts in the outer regions of the retina and proceeds to the macular region in more advanced stages, blood vessel narrowing, optic nerve atrophy and macular changes: signs of dystrophy or tapetal macular reflex. An eye fundus image of RP is shown in Figure 7. The phenotype differs even within subjects with the same type of mutation [38].

Visual field examination shows progressive narrowing of the visual field. SD-OCT and time-domain OCT are used to



Figure 7. Retinitis pigmentosa: a photograph of the posterior pole

visualize the photoreceptor layers. It shows thinning or loss of outer retinal layers throughout the macula and hyper-reflective profiles in the subretinal space at the fovea. However, it lacks resolution for single photoreceptor visualization and evaluation [36, 38]. The ERG responses are distinguished, in more advanced stages, below the level of test reliability [38].

Changes in the macula in retinitis pigmentosa eyes are not uncommon. Diseases such as epiretinal membrane and macular hole may be found due to ischemia of macular RPE as well as changes in the vitreous body structure. Such conditions may be treated surgically [37, 39].

Characteristics of adaptive optics imaging in retinitis pigmentosa

Cone loss is observed in retinitis pigmentosa as well as Usher syndrome. The cone spacing in RP eyes is higher than in healthy eyes [14, 32, 35, 38]. Regions of photoreceptor atrophy and hyper-reflective structures in outer retinal layers are visualized [38], as seen in Figure 8.

The interpretation of the images of the photoreceptors in retinitis pigmentosa shows a high level of variability between interpreters due to the cone loss areas in the retina. The image interpretation quality seems to be higher in SD-AOSLO compared to confocal AO [5, 40].

Foveal visual acuity loss and foveal sensitivity changes in retinitis pigmentosa are noted when morphological changes in the retina are already in an advanced stage [41].

The efforts to determine the rate of disease progression with AOSLO seem to be successful – it has been confirmed as consistent with the progression in SD-OCT and microperimetry findings [36] and as a successful tool in monitoring disease progression during experimental treatment [11].

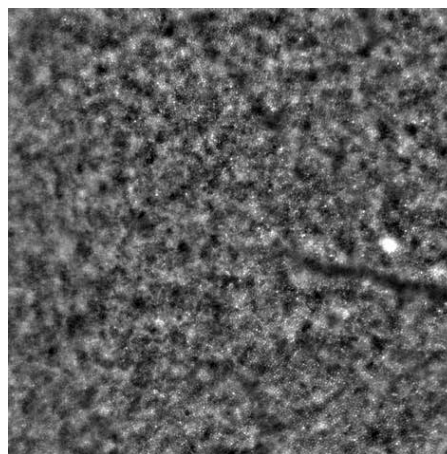


Figure 8. Retinitis pigmentosa: AO image of the perifoveal photoreceptors. Note the dark spaces, decreased cone density and hyper-reflective structures

THE USE OF ADAPTIVE OPTICS IN OTHER INHERITED RETINAL DEGENERATIONS

The AOSLO images of patients with BED (Bornholm eye disease), an X-linked cone dysfunction, prove the disruption of the cone mosaic with a high level of intersubject variability between patients with different disease-causing mutations [42].

Achromatopsia (ACHM) is also a subject of AO retinal studies. Split-detector images demonstrate a decreased number of photoreceptors as well as variations in cone density maps between the regions within the retina and between the eyes of ACHM subjects [9, 43].

The AO studies of patients with occult macular dystrophy (OMD) show regions of loss of photoreceptors, RPE visualization and lower cone density than in healthy eyes and a correlation of the morphological changes with the microperimetry [44-46].

LIMITATIONS

The challenges of adaptive optics include obtaining good-quality images in poor fixation, as well as in nystagmus – the eye tracking devices overcome those difficulties [47-49].

The interpretation of the images is also prone to mistakes made by non-experienced examiners. The machine learning

of AO interpretation is vital to establish objective interpretation and forming right conclusions.

The need for larger study cohorts in IRDs is emphasized [50].

SUMMARY

Numerous ophthalmic researchers emphasize the role of longitudinal studies of patients with inherited retinal diseases. The research is limited by the low prevalence and difficult diagnostic process in some cases. The classical and well-known techniques, such as OCT, fundus autofluorescence, fluorescein angiography, and electroretinography used in diagnosing and monitoring IRD patients play a vital role. With the course of scientific development, the role of novel ophthalmic diagnostic solutions is becoming more significant. Adaptive optics imaging gives hopes for better understanding of the morphological basics and natural course of retinal diseases and with the introduction of experimental therapies also for monitoring the effectiveness of introduced treatment. Being able to monitor rare retinal conditions is crucial for the further development of medical solutions.

DISCLOSURE

The authors declare no conflict of interest.

REFERENCES

1. Gill JS, Moosajee M, Dubis AM. Cellular imaging of inherited retinal diseases using adaptive optics. *Eye (Lond)* 2019; 33: 1683-1698.
2. Dreher AW, Bille JF, Weinreb RN. Active optical depth resolution improvement of the laser tomographic scanner. *Appl Opt* 1989; 28: 804-808.
3. Liang J, Williams DR, Miller DT. Supernormal vision and high-resolution retinal imaging through adaptive optics. *J Opt Soc Am A Opt Image Sci Vis* 1997; 14: 2884-2892.
4. Lombardo M, Serrao S, Devaney N, et al. Adaptive Optics Technology for High-Resolution Retinal Imaging. *Sensors (Basel)* 2012; 13: 334-366.
5. Tanna P, Kasilian M, Strauss R, et al. Reliability and repeatability of cone density measurements in patients with Stargardt disease and RPGR-associated retinopathy. *Invest Ophthalmol Vis Sci* 2017; 58: 3608-3615.
6. Polans J, Keller B, Carrasco-Zevallos OM, et al. Wide-field retinal optical coherence tomography with wavefront sensorless adaptive optics for enhanced imaging of targeted regions. *Biomed Opt Express* 2017; 8: 16-37.
7. Georgiou M, Kalitzeos A, Patterson EJ, et al. Adaptive optics imaging of inherited retinal diseases. *Br J Ophthalmol* 2018; 102: 1028-1035.
8. Zaleska-Żmijewska A, Wawrzyniak ZM, Ulińska M, et al. Human photoreceptor cone density measured with adaptive optics technology (rtx1 device) in healthy eyes: Standardization of measurements. *Medicine (Baltimore)* 2017; 96: e7300.
9. Dubis AM, Cooper RF, Aboshiha J, et al. Genotype-dependent variability in residual cone structure in achromatopsia: toward developing metrics for assessing cone health. *Invest Ophthalmol Vis Sci* 2014; 55: 7303-7311.
10. Godara P, Wagner-Schuman M, Rha J, et al. Imaging the photoreceptor mosaic with adaptive optics: beyond counting cones. *Adv Exp Med Biol* 2012; 723: 451-458.
11. Talcott KE, Ratnam K, Sundquist SM, et al. Longitudinal study of cone photoreceptors during retinal degeneration and in response to ciliary neurotrophic factor treatment. *Invest Ophthalmol Vis Sci* 2011; 52: 2219-2226.
12. Lombardo M, Serrao S, Lombardo G. Technical factors influencing cone packing density estimates in adaptive optics flood illuminated retinal images. *PLoS One* 2014; 9: e107402.
13. Roorda A, Zhang Y, Duncan JL. High-resolution in vivo imaging of the RPE mosaic in eyes with retinal disease. *Invest Ophthalmol Vis Sci* 2007; 48: 2297-2303.
14. Ratnam K, Västinsalo H, Roorda A, et al. Cone structure in patients with usher syndrome type III and mutations in the *Clarín 1* gene. *JAMA Ophthalmol* 2013; 131: 67-74.
15. Zaleska-Żmijewska A, Wawrzyniak ZM, Dąbrowska A, et al. Adaptive Optics (rtx1) High-Resolution Imaging of Photoreceptors and Retinal Arteries in Patients with Diabetic Retinopathy. *J Diabetes Res* 2019; 2019: 9548324.
16. Zaleska-Żmijewska A, Piątkiewicz P, Śmigielńska B, et al. Retinal Photoreceptors and Microvascular Changes in Prediabetes Measured with Adaptive Optics (rtx1™): A Case-Control Study. *J Diabetes Res* 2017; 4174292.
17. Tanna P, Strauss RW, Fujinami K, et al. Stargardt disease: clinical features, molecular genetics, animal models and therapeutic options. *Br J Ophthalmol* 2017; 101: 25-30.
18. Kong X, Fujinami K, Strauss RW, et al. Visual Acuity Change Over 24 Months and Its Association with Foveal Phenotype and Genotype in Individuals With Stargardt Disease: ProgStar Study Report No. 10. *JAMA Ophthalmol* 2018; 136: 920-928.

19. Schönbach EM, Strauss RW, Ibrahim MA, et al. Faster Sensitivity Loss around Dense Scotomas than for Overall Macular Sensitivity in Stargardt Disease: ProgStar Report No. 14. *Am J Ophthalmol* 2020; S0002-9394(20)30120-3.
20. Fujinami K, Strauss RW, Chiang JP, et al. Detailed genetic characteristics of an international large cohort of patients with Stargardt disease: ProgStar study report 8. *Br J Ophthalmol* 2019; 103: 390-397.
21. Tanna P, Georgiu M, Strauss RW, et al. Cross-Sectional and Longitudinal Assessment of the Ellipsoid Zone in Childhood-Onset Stargardt Disease. *Transl Vis Sci Technol* 2019; 8: 1.
22. Strauss RW, Muñoz B, Ho A, et al. Progression of Stargardt Disease as Determined by Fundus Autofluorescence in the Retrospective Progression of Stargardt Disease Study (ProgStar Report No. 9). *JAMA Ophthalmol* 2017; 135: 1232-1241.
23. Strauss RW, Kong X, Ho A, et al. Progression of Stargardt Disease as Determined by Fundus Autofluorescence Over a 12-Month Period: ProgStar Report No. 11. *JAMA Ophthalmol* 2019; 137: 1134-1145.
24. Fujinami K, Lois N, Mukherjee R, et al. A longitudinal study of Stargardt disease: quantitative assessment of fundus autofluorescence, progression, and genotype correlations. *Invest Ophthalmol Vis Sci* 2013; 54: 8181-8190.
25. Song H, Rossi EA, Latchney L, et al. Cone and rod loss in Stargardt disease revealed by adaptive optics scanning light ophthalmoscopy. *JAMA Ophthalmol* 2015; 133: 1198-1203.
26. Chen Y, Ratnam K, Sundquist SM, et al. Cone photoreceptor abnormalities correlate with vision loss in patients with Stargardt disease. *Invest Ophthalmol Vis Sci* 2011; 52: 3281-3292.
27. Chen Y, Roorda A, Duncan JL. Advances in imaging of Stargardt disease. *Adv Exp Med Biol* 2010; 664: 333-340.
28. Razeen MM, Cooper RF, Langlo CS, et al. Correlating photoreceptor mosaic structure to clinical findings in Stargardt disease. *Transl Vis Sci Technol* 2016; 5: 6.
29. Hamel CP, Griffoin JM, Bazalgette C, et al. Molecular genetics of pigmentary retinopathies: identification of mutations in CHM, RDS, RHO, RPE65, USH2A and XLR51 genes. *J Fr Ophtalmol* 2000; 23: 985-995.
30. Wolfing JI, Chung M, Carroll J, et al. High-resolution retinal imaging of cone-rod dystrophy. *Ophthalmology* 2006; 113: 1014-1019.
31. Wawrocka A, Skorzycyk-Werner A, Wicher K, et al. Novel Variants Identified with Next-Generation Sequencing in Polish Patients With Cone-Rod Dystrophy. *Mol Vis* 2018; 24: 326-339.
32. Duncan JL, Zhang Y, Gandhi J, et al. A High-Resolution imaging with adaptive optics in patients with inherited retinal degeneration. *Invest Ophthalmol Vis Sci* 2007; 48: 3283-3291.
33. Choi SS, Doble N, Hardy JL, et al. In vivo imaging of the photoreceptor mosaic in retinal dystrophies and correlations with visual function. *Invest Ophthalmol Vis Sci* 2006; 47: 2080-2092.
34. Song H, Rossi EA, Stone E, et al. Phenotypic diversity in autosomal-dominant cone-rod dystrophy elucidated by adaptive optics retinal imaging. *Br J Ophthalmol* 2018; 102: 136-141.
35. Park SP, Lee W, Bae EJ, et al. Early structural anomalies observed by high-resolution imaging in two related cases of autosomal-dominant retinitis pigmentosa. *Ophthalmic Surg Lasers Imaging Retin* 2014; 45: 469-473.
36. Foote KG, De la Huerta I, Gustafson K, et al. Cone Spacing Correlates With Retinal Thickness and Microperimetry in Patients With Inherited Retinal Degenerations. *Invest Ophthalmol Vis Sci* 2019; 60: 1234-1243.
37. Nowosielska A. Vitrectomy for macular lesions in eyes with retinitis pigmentosa. *Klin Oczna* 2018; 3: 155-158.
38. Duncan JL, Biswas P, Kozak I, et al. Ocular phenotype of a family with FAM161A-associated retinal degeneration. *Ophthalmic Genet* 2016; 37: 44-52.
39. Jin ZB, Gan DK, Xu GZ, et al. Macular hole formation in patients with retinitis pigmentosa and prognosis of pars plana vitrectomy. *Retina* 2008; 28: 610-614.
40. Giannini D, Lombardo G, Mariotti L, et al. Reliability and agreement between metrics of cone spacing in adaptive optics images of the human retinal photoreceptor mosaic. *Invest Ophthalmol Vis Sci* 2017; 58: 3127-3137.
41. Ratnam K, Carroll J, Porco TC, et al. Relationship between foveal cone structure and clinical measures of visual function in patients with inherited retinal degenerations. *Invest Ophthalmol Vis Sci* 2013; 54: 5836-5847.
42. Patterson EJ, Tee J, Neitz J, et al. Assessing cone mosaic disruption in patients with X-linked cone dysfunction. *Invest Ophthalmol Vis Sci* 2015; 56: 88-88.
43. Litts KM, Georgiou M, Langlo CS, et al. Interocular Symmetry of Foveal Cone Topography in Congenital Achromatopsia. *Curr Eye Res* 2020; 13: 1-8.
44. Nakanishi A, Ueno S, Kawano K, et al. Pathologic changes of cone photoreceptors in eyes with occult macular dystrophy. *Invest Ophthalmol Vis Sci* 2015; 56: 7243-7249.
45. Tojo N, Nakamura T, Ozaki H, et al. Analysis of macular cone photoreceptors in a case of occult macular dystrophy. *Clin Ophthalmol* 2013; 7: 859-864.
46. Viana KI, Messias A, Siqueira RC, et al. Structure-functional correlation using adaptive optics, OCT, and microperimetry in a case of occult macular dystrophy. *Arq Bras Oftalmol* 2017; 80: 118-121.
47. Sheehy CK, Tiruveedhula P, Sabesan R, et al. Active eye-tracking for an adaptive optics scanning laser ophthalmoscope. *Biomed Opt Express* 2015; 7: 2412-2423.
48. Privitera CM, Sabesan R, Winter S, et al. Eye-tracking technology for real-time monitoring of transverse chromatic aberration. *Opt Lett* 2016; 41: 1728-1731.
49. Tam J, Roorda A. Speed quantification and tracking of moving objects in adaptive optics scanning laser ophthalmoscopy. *J Biomed Opt* 2011; 16: 036002.
50. Strauss RW, Ho A, Munoz B, et al. The Natural History of the Progression of Atrophy Secondary to Stargardt Disease (ProgStar) Studies: Design and Baseline Characteristics: ProgStar Report No. 1. *Ophthalmology* 2016; 123: 817-828.

Article

Characteristics of Rare Inherited Retinal Dystrophies in Adaptive Optics—A Study on 53 Eyes

Katarzyna Samelska ^{1,2,*}, Jacek Paweł Szaflik ^{1,2}, Maria Guskowska ², Anna Katarzyna Kurowska ^{1,2}
and Anna Zaleska-Żmijewska ^{1,2}¹ Department of Ophthalmology, Medical University of Warsaw, 02-091 Warsaw, Poland² SPKSO Ophthalmic University Hospital, 00-576 Warsaw, Poland

* Correspondence: samelskakatarzyna@gmail.com

Abstract: Inherited retinal dystrophies (IRDs) are genetic disorders that lead to the bilateral degeneration of the retina, causing irreversible vision loss. These conditions often manifest during the first and second decades of life, and their primary symptoms can be non-specific. Diagnostic processes encompass assessments of best-corrected visual acuity, funduscopy, optical coherence tomography, fundus autofluorescence, fluorescein angiography, electrophysiological tests, and genetic testing. This study focuses on the application of adaptive optics (AO), a non-invasive retinal examination, for the assessment of patients with IRDs. AO facilitates the high-quality, detailed observation of retinal photoreceptor structures (cones and rods) and enables the quantitative analysis of parameters such as cone density (DM), cone spacing (SM), cone regularity (REG), and Voronoi analysis (N%6). AO examinations were conducted on eyes diagnosed with Stargardt disease (STGD, $N = 36$), cone dystrophy (CD, $N = 9$), and cone-rod dystrophy (CRD, $N = 8$), and on healthy eyes ($N = 14$). There were significant differences in the DM, SM, REG, and N%6 parameters between the healthy and IRD-affected eyes ($p < 0.001$ for DM, SM, and REG; $p = 0.008$ for N%6). The mean DM in the CD, CRD, and STGD groups was 8900.39/mm², 9296.32/mm², and 16,209.66/mm², respectively, with a significant inter-group difference ($p = 0.006$). The mean SM in the CD, CRD, and STGD groups was 12.37 μm , 14.82 μm , and 9.65 μm , respectively, with a significant difference observed between groups ($p = 0.002$). However, no significant difference was found in REG and N%6 among the CD, CRD, and STGD groups. Significant differences were found in SM and DM between CD and STGD ($p = 0.014$ for SM; $p = 0.003$ for DM) and between CRD and STGD ($p = 0.027$ for SM; $p = 0.003$ for DM). Our findings suggest that AO holds significant potential as an impactful diagnostic tool for IRDs.

Keywords: adaptive optics; cone dystrophy; cone-rod dystrophy; inherited retinal diseases; inherited retinal dystrophies; photoreceptors; retinal imaging; Stargardt disease



Citation: Samelska, K.; Szaflik, J.P.; Guskowska, M.; Kurowska, A.K.; Zaleska-Żmijewska, A. Characteristics of Rare Inherited Retinal Dystrophies in Adaptive Optics—A Study on 53 Eyes. *Diagnostics* **2023**, *13*, 2472. <https://doi.org/10.3390/diagnostics13152472>

Academic Editors: Mario Damiano Toro, Daniele Tognetto and Rosa Giglio

Received: 16 May 2023
Revised: 21 July 2023
Accepted: 24 July 2023
Published: 25 July 2023



Copyright: © 2023 by the authors. Licensee MDPI, Basel, Switzerland. This article is an open access article distributed under the terms and conditions of the Creative Commons Attribution (CC BY) license (<https://creativecommons.org/licenses/by/4.0/>).

1. Introduction

Inherited retinal dystrophies (IRDs), also known as inherited retinal diseases, are genetic disorders characterized by a variety of inheritance patterns, all leading to bilateral, irreversible vision loss. Recognized as rare diseases, the IRD group is highly heterogeneous, comprising over 20 phenotypically distinct conditions. Each condition may arise from different mutations in distinct genes. To date, around 271 genes have been linked with IRDs. The disease progression may vary among patients, with functional blindness occurring at different ages. The genetic basis of the IRDs of different phenotypes is detailed on RetNet (<https://web.sph.uth.edu/RetNet/home.htm> (accessed on 9 July 2023)). The genetic characteristics of patients with IRDs have been described in various populations, such as in Taiwan [1]. Only one successful therapy has been introduced so far, voretigene neparvovec-rzyl—Luxturna™—limited to patients with mutations in the *RPE65* gene. Other treatments, including stem cell therapy, retinal pigment transplantation, photoreceptor transplantation, and anti-inflammatory approaches, are under development [2–8]. However, none of these therapies have seen widespread use.

1.1. Retinitis Pigmentosa

Retinitis pigmentosa (RP) is the most common IRD, with a prevalence of 1/3000 to 1/5000, accounting for approximately half of all IRDs. RP is a rod-cone dystrophy (RCD) in which the deterioration of rod function exceeds that of cone function, leading to the loss of photoreceptor and pigment epithelium function. RP's heterogeneous origin involves more than 3100 mutations in over 50 genes, including the non-syndromic form. The disease may be inherited in an autosomal (dominant or recessive) or X-linked pattern, with mitochondrial inheritance uncommon in the non-syndromic form [9,10]. The age of onset varies among patients with different forms of the disease, with RP potentially affecting visual function in early infancy, as well as in the second to third decades of life. Retinitis pigmentosa presents heterogeneous genetics, clinical phenotypes, and presentations. A single gene mutation may lead to different clinical presentations, even among members of the same family [10].

RP may manifest as an independent disease or as part of a syndrome, such as Usher syndrome, which includes hearing loss, or Bardet-Biedl syndrome, which features RP accompanied by kidney failure, polydactyly, and obesity. These syndromic forms are also genetically heterogeneous: there are at least 12 gene mutations leading to Usher syndrome and at least 17 gene mutations causing Bardet-Biedl syndrome [10].

A crucial symptom of RP is the narrowing of the visual field, which occurs in the advanced stages of the disease. Since the degeneration primarily affects the peripheral retina, the central vision is not impacted in the early stages, and potential findings include nyctalopia and photophobia. The clinical image is characterized by peripheral bone spicule deposits, attenuation of the retinal blood vessels, optic disc pallor, and, in later stages, the development of macular edema. Some RP patients develop subcortical posterior cataracts [11].

Leber congenital amaurosis (LCA) is a form of RP present in infancy, resulting in vision loss in early infancy. One of the genes that may be affected in LCA is *RPE65*. Mutations in this gene usually cause the autosomal recessive form of the disease but can also lead to the dominant form [10]. LCA caused by *RPE65* mutation may be treated with voretigene neparvovec-rzyl (Luxturna™). Luxturna™ is the first commercially available gene therapy, approved by the FDA in December 2017 and now globally available [12,13].

The cone spacing in RP has been found to be increased compared to healthy eyes, correlating with microperymetry changes [14].

Despite RP being the most common condition among IRDs, we chose not to include RP patients in our study for two reasons. Firstly, in retinitis pigmentosa, the morphological changes primarily affect the rods, which are challenging to quantitatively visualize with adaptive optics. Secondly, the morphological changes predominantly affect the peripheral retina; hence, we opted for conditions primarily affecting the macular region.

1.2. Characteristics of Stargardt Disease (STGD), Cone Dystrophy (CD), and Cone-Rod Dystrophy (CRD)

1.2.1. Stargardt Disease (STGD)

Stargardt disease (STGD) is the most common maculopathy among IRDs, with a prevalence of approximately 1 in 10,000. STGD is characterized by central vision loss, dyschromatopsia, and macular abnormalities, often forming a 'bull's eye' sign. Yellow-white flecks in fundus autofluorescence (FAF) indicate abnormal lipofuscin accumulation within the retinal pigment epithelium (RPE). An eye fundus image of STGD is presented in Figure 1.

Typically, symptoms of the disease begin in the second decade of life. Maculopathy arises from abnormal lipofuscin deposits in the central macula. These deposits block the signal from the underlying choroid, causing the characteristic 'dark choroid' sign in fluorescein angiography (FFA) [15,16].

Diagnosis is based on clinical signs and can be confirmed by genetic testing. The most common mutations in Stargardt's disease affect the *ABCA4* gene (MIM601691), which codes for a protein located in the outer segments of the photoreceptors [17]. Disease monitoring

includes functional tests, such as best-corrected visual acuity (BCVA) assessment, multifocal electroretinography (mfERG), and microperimetry, and imaging tests such as spectral-domain optical coherent tomography (SD-OCT), FAF, and FFA [16,18–20].

Disease progression can be determined by tracking the ellipsoid zone loss in SD-OCT [21] and the rate of atrophy enlargement (RAE) monitored in FAF [22–24].

AO imaging (both spectral and confocal) has been utilized to assess photoreceptor abnormalities in Stargardt disease. Studies have found increased cone spacing (SM) and decreased cone density (DM) compared to the normal retina [18,21,25,26]. Cone reflectivity changes have been described but do not correspond with lipofuscin accumulation [25]. Moreover, confocal AO images show changes in retinal photoreceptor morphology, detectable even before OCT and FAF can identify changes. These images reveal ‘dark spaces’ within photoreceptor structures. These ‘dark spaces’ indicate abnormal cones with decreased core reflectance and a disrupted outer segment structure, although their inner structure appears intact. These ‘dark spaces’ could potentially be a target for treatment. It is worth noting that ‘dark spaces’ are not pathognomonic for STGD and can also be found in other IRDs [26–28]. Adaptive optics studies have suggested that photoreceptor loss in patients with type STGD1 Stargardt disease precedes clinically detectable retinal pigment epithelial disease [26]. Conversely, the highly reflective structures observed in AO might represent flecks or areas of atrophy [29].

An additional study analyzing the AO visualization of Stargardt disease illustrated differences in cone morphology between the perifoveal area, the transition zone, and the outer retina [30]. In macular atrophy regions, the RPE mosaic was not clearly identifiable in two of the three patients, and the photoreceptors were unidentifiable in the remaining patient. In transition regions, the cones appeared dark, enlarged, and sparse, and the cone spacing was increased. The AO image of the peripheral retina showed cone spacing and an appearance similar to those of a healthy retina, but the RPE cell contrast was lower than in normal eyes.

Figure 2 depicts an AO image of a healthy retina, and Figure 3 presents an AO image of an STGD retina.

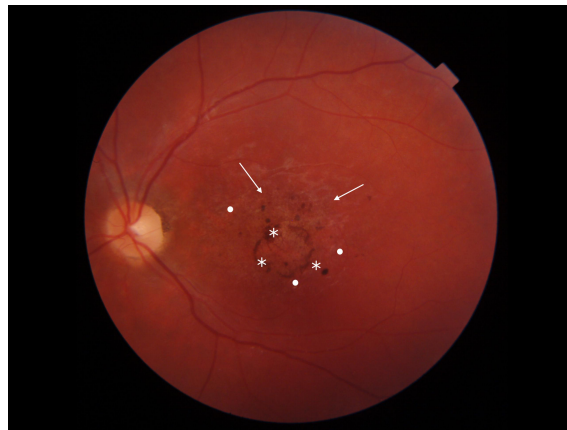


Figure 1. Eye fundus image of a patient with Stargardt disease (DRI OCT Triton; Topcon). Observe the ‘bull’s eye’ maculopathy (indicated by arrows), pigment deposits (indicated by asterisks), and the presence of yellow-white flecks (highlighted with dots) in the perifoveal area.

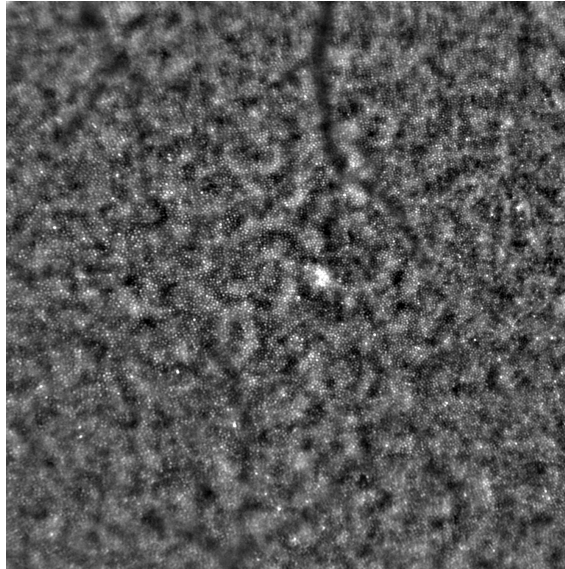


Figure 2. Adaptive optics image showcasing the photoreceptors of a healthy eye (Rtx1™; Imagine Eyes, France). Individual cones are distinctly visualized (visible as white and grayish dots), and the cone mosaic image appears undisrupted.

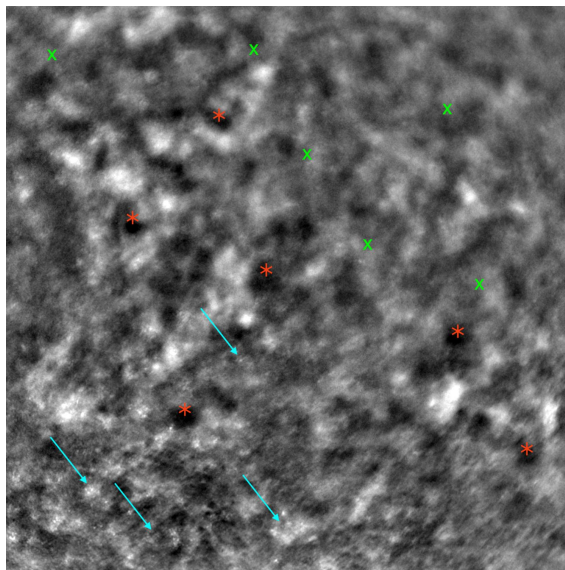


Figure 3. Adaptive optics image demonstrating the photoreceptors of an eye with Stargardt disease (Rtx1™; Imagine Eyes, France). Observe the disruption in the cone mosaic (examples indicated by light blue arrows) and the presence of 'dark spaces' (examples highlighted with red asterisks). The area with inadequate visualization of the cone mosaic is marked with green X symbols.

Among other IRDs, cone-rod dystrophy (CRD) and cone dystrophy (CD) are notable for their primary cone dysfunction, which supersedes rod dysfunction. In these disorders, the macula, being the retinal region with the highest cone concentration, is primarily affected.

1.2.2. Cone-Rod Dystrophy and Cone Dystrophy

Cone-rod dystrophy (CRD) and cone dystrophy (CD) are IRDs that occur less frequently than Stargardt disease. CRD involves both cones and rods, while CD affects only cones. Both primarily impact the macula, leading to central vision disturbances. The clinical presentation is similar in both CD and CRD, showcasing a bull's eye maculopathy and bone spicule deposits in the outer retina. Inheritance patterns can be autosomal dominant, autosomal recessive, X-linked, or unresolved. At least 32 gene mutations associated with these dystrophies have been identified. Symptoms of CD encompass central vision deterioration, nystagmus, photophobia, and color vision deficits [31,32]. Early nyctalopia is not a feature of CD [32]. CRD symptoms appear later than CD symptoms and often result in legal blindness in later life [33]. Fundus photographs of eyes with CD and CRD are shown in Figures 4 and 5, respectively.

The characteristic AO imaging pattern in CRD has been described as areas devoid of cones, although it has also been reported as a diminished cone mosaic with reduced cone density and increased cone spacing [34–36]. Other studies have noted that eyes with CRD exhibit increased cone spacing compared to healthy eyes and those with RP. Correlations between CRD and the deterioration of mfERG peak amplitudes have also been reported [37]. An AO scanning laser ophthalmoscopy (AOSLO) study highlighted greater cone loss than rod loss, reflecting the disease's nature [38]. AO images from CD and CRD cases are presented in Figures 6 and 7.

A study on AO imaging in cone dystrophy with supernormal rod electroretinogram (CDSR) depicted reduced cone density, disruption of the cone photoreceptor mosaic, and the presence of cones surrounded by patches of either absent or present non-wave-guiding cones [31].

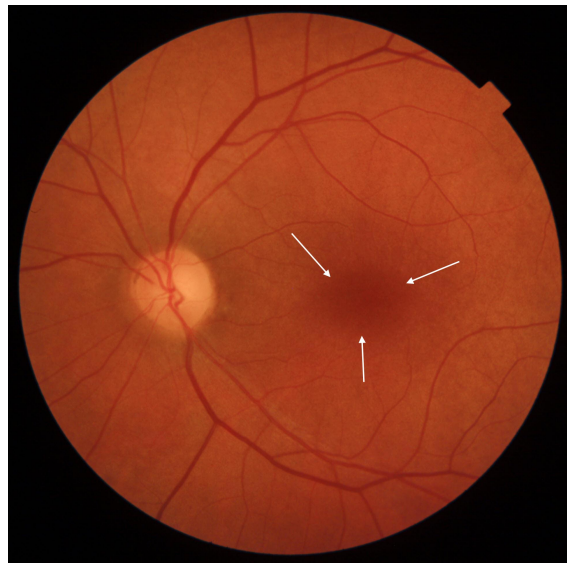


Figure 4. Eye fundus image of a macula with cone dystrophy (DRI OCT Triton; Topcon). Observe the 'bull's eye' maculopathy (indicated by arrows).

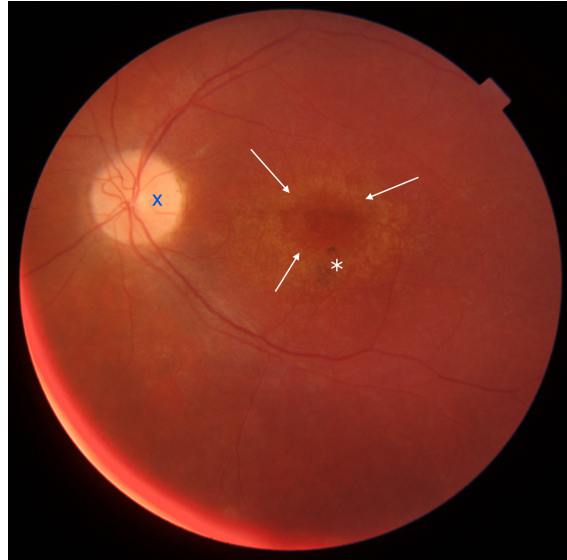


Figure 5. Eye fundus image of a macula with cone-rod dystrophy (DRI OCT Triton; Topcon). Note the ‘bull’s eye’ maculopathy (indicated by arrows), pigment deposits in the perifoveal area (marked with an asterisk), and the pallor of the optic nerve disc (marked with dark blue X symbol).

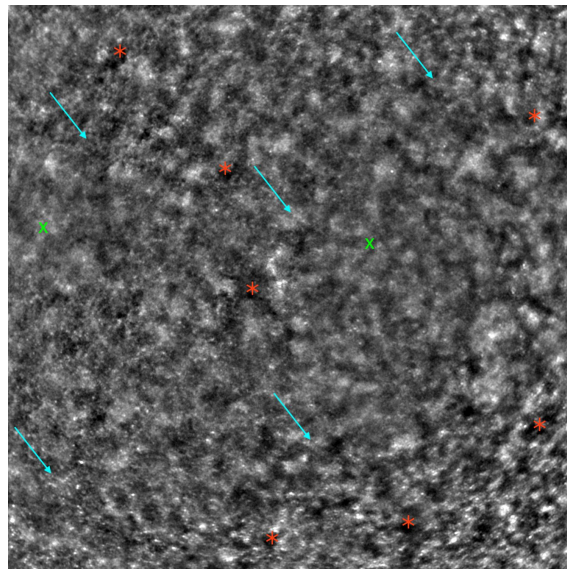


Figure 6. Adaptive optics image of the photoreceptors in an eye with cone dystrophy (Rtx1™; Imagine Eyes, France). Observe the disruption of the cone mosaic (examples indicated by light blue arrows) and the presence of ‘dark spaces’ (examples indicated by red asterisks). The areas with poor visualization of the cone mosaic are marked with green X symbols.

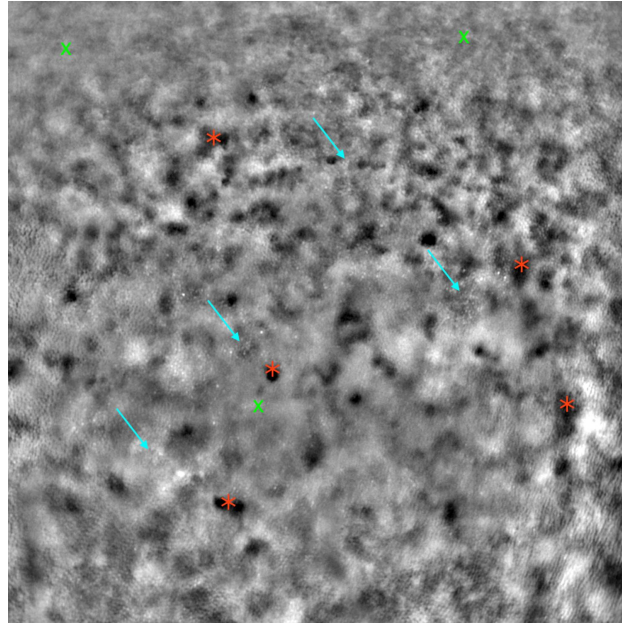


Figure 7. Adaptive optics image of the photoreceptors in an eye with cone-rod dystrophy (Rbx1™; Imagine Eyes, France). Observe the disruption of the cone mosaic (examples indicated by light blue arrows) and the presence of ‘dark spaces’ (examples indicated by red asterisks). Areas with poor visualization of the cone mosaic are marked with green X symbols.

Cone-rod dystrophy, cone dystrophy, and Stargardt disease primarily affect the macula and central visual field, resulting in progressive central vision loss. This differs from RCDs, which initially impact peripheral vision. The clinical implications of central vision loss are significant, as patients and their families must confront the possibility of progressive vision deterioration.

Retinal imaging, designed to assess the stage and monitor the progression of maculopathies, is achievable using OCT, AF, FAF, electrophysiological testing (such as mfERG), and perimetry (such as 10-2 macular perimetry).

However, monitoring with the above-mentioned methods can often prove challenging and imprecise. As a more recent imaging technique, AO allows the visualization of the retina’s microstructures, such as the cones, expanding the diagnostic and monitoring capabilities for IRDs. Studies confirm that morphological changes in the cone microstructure, as visualized by AO, can be detected earlier than the onset of functional visual deterioration [39].

1.2.3. Adaptive Optics

Adaptive optics (AO) is an imaging technique originally developed for precise visualization in astronomy, capable of correcting atmospheric irregularities. This aberration-correcting system provided high-quality imaging of distant objects [40,41]. In 1989, Dreher et al. [42] developed improvements in laser scanning tomography, enabling the compensation of corneal and lens aberrations to assess the retinal nerve fiber layer (RNFL) thickness and optic disc topography of the human eye. It was not until 1997, however, that Liang et al. first utilized adaptive optics to visualize single cells in the human retina [43].

The retinal imaging AO camera uses two light sources: one to illuminate the retina and the second to measure and correct wavefront aberrations. The wavefront sensor and corrector measure these aberrations. The control system then interprets the data collected by the sensor and orchestrates the interaction between the sensor and corrector [41,44]. There are two main AO technologies used in visualizing retinal photoreceptors: split detector (SD-AOSLO) and confocal (cSLO). Both confocal and spectral images can be taken simultaneously. Some AO imaging devices capture three channels simultaneously (confocal, split detection, and dark-field), each highlighting different retinal structures [18,44,45].

AO permits the visualization of rods and cones, the two types of retinal photoreceptors. AO can measure parameters such as cone density, cone spacing, Voronoi analysis, reflectivity, regularity, the preferred orientation of cones, and local spatial anisotropy [18,46–48]. While rod visualization is possible in healthy individuals, determining their spacing is generally impractical. However, in retinas with a disrupted cone mosaic, it can reveal the presence of often-enlarged rods. The cone-to-rod ratio can be measured [26,27]. For our project, we opted not to take rod measurements.

Beyond photoreceptor visualization, AO also provides images of the retinal microvasculature. Studies examining the arteriole morphology in angiopathies, such as diabetic retinopathy, and in systemic conditions such as hypertension, obesity, and prediabetes, offer an innovative perspective on retinal blood circulation [49–53].

AO's capability to visualize individual photoreceptors due to aberration correction is a breakthrough in modern ophthalmic imaging. Research on its application in IRDs is emerging, as existing diagnostic techniques (SD-OCT, FAF, FA, and microperimetry) are not sufficiently precise for comprehensive assessments. Several studies confirm that IRDs can present morphological changes detectable by AO preceding functional vision loss, which could greatly impact IRDs' diagnostic processes [36,39,44].

The evaluation of RNFL and optic nerve microvasculature microchanges in glaucoma has also been a subject of study. Age-related macular degeneration (AMD), a condition causing morphological changes in the macula, has been a focus in numerous studies. AMD, along with diabetic retinopathy and glaucoma, remains one of the leading causes of vision loss in developed countries [44,54].

While there are numerous studies examining AO images in IRDs, there is still much to discover and describe. AO has been in use in ophthalmology for over two decades, and there is still a need for longitudinal studies monitoring cone density in IRDs [55].

1.2.4. Rtx1™

Rtx1™ (Imagine Eyes, Orsay, France) is an adaptive optics flood illuminated ophthalmoscope (AOFIO) that utilizes infrared light with a wavelength of 850 nm and offers a resolution of 1.6 μm . The image dimensions that it captures are $4^\circ \times 4^\circ$, corresponding approximately to 1.2 mm \times 1.2 mm of the retina. The location under examination can be selected (for example, 2° superior, inferior, temporal, or nasal). Image acquisition in a single position takes between 2 and 4 s, during which 40 individual images are acquired [44,49,53,56]. The Rtx1™ software (*version 3.4*, also called *AO Image 3.4*, Imagine Eyes, Orsay, France) includes two programs for data evaluation: AO Detect for photoreceptor parameter analysis and AO Detect Artery for vessel parameter analysis.

2. Materials and Methods

This study focused on examining the characteristic images and parameters of the macular cones in three conditions predominantly affecting the posterior pole, STGD, CRD, and CD, using AO device Rtx1™.

The investigation focused on the photoreceptor parameters, namely cone density (DM), cone spacing (SM), Voronoi analysis of hexagonal cones (N%6), and regularity (REG), all of which can be evaluated in the AO Detect program. DM, SM, N%6, and REG are abbreviations employed by AO Detect. DM, expressed in $[1/\text{mm}^2]$, has an inverse correlation with SM, which measures the neighbor distance of each cone [μm]. The N%6

analysis is performed by dividing the number of Voronoi cells (i.e., six-sided cells) by the total number of cells, expressing the percentage of hexagonal cells in the image. REG, along with the $N\%6$ parameter (both expressed in [%]), is crucial in excluding inaccuracies resulting from cell identification errors [48].

Patients diagnosed with CD, CRD, or STGD, confirmed previously through clinical history, eye fundus imaging, electrophysiological testing, perimetry, FAF, and, in some cases, fluorescein angiography, had their eyes included in the study. Genetic testing was performed on all patients in the Stargardt group, revealing *ABCA4* gene mutations in 12 individuals. Gene mutations leading to STGD or another IRD were not confirmed in other patients.

Patients with other ocular pathologies (such as glaucoma, cataract), those with a history of ocular surgeries or uveitis, and diabetic patients were excluded from the study. Cases where AO data collection was impossible due to poor visual acuity, nystagmus, or a lack of fixation were also excluded. This led to the exclusion of one eye each from the STGD and CD groups.

The study group included 53 eyes from 28 patients: 36 eyes (from 19 patients) with STGD, 8 eyes (from 4 patients) with CRD, and 9 eyes (from 5 patients) with CD. The control group comprised 14 healthy right eyes from 14 patients. Exclusion criteria for the control group included past ocular pathologies, increased body weight ($BMI > 25 \text{ kg/m}^2$), systemic hypertension, and diabetes. All eyes in the control group had a BCVA of 1.0.

Table 1 presents the demographic data and BCVA of the study and control groups.

Table 1. Demographic data, diagnosis, eye laterality (left/right), and BCVA for both the study group and the control group. BCVA: best-corrected visual acuity; CD: cone dystrophy; CRD: cone-rod dystrophy; STGD: Stargardt disease.

	Study Group (N = 53)	Control Group (N = 14)
Age		
Mean (SD)	44.02 (14.24)	46.93 (9.28)
Median (IQR)	44 (35–54)	47.5 (42.25–55.25)
Range	19–73	31–59
Sex		
Female	60.4% (N = 32)	92.9% (N = 13)
Male	39.6% (N = 21)	7.1% (N = 1)
Diagnosis		
CD	17% (N = 9)	-
CRD	15.1% (N = 8)	-
STGD	67.9% (N = 36)	-
Eye		
Right	28	14
Left	25	0
BCVA		
Mean (SD)	0.13 (0.14)	1.0
Median (IQR)	0.07 (0.05–0.16)	1.0
Range	0.01–0.7	1.0

All patients provided written consent for their participation in the study, which adhered to the tenets of the Declaration of Helsinki and was approved by the bioethics commission of the Medical University of Warsaw (KB/87/2015). The exams were conducted in the Department of Ophthalmology of the Medical University of Warsaw, in the SPKSO Ophthalmic University Hospital in Warsaw.

Patients with IRDs had both eyes examined, while the control group had their right eyes examined, using the Rtx1™. Measurements were taken at four positions: 2° from the foveola in the superior, inferior, temporal, and nasal quadrants.

Before each examination, the BCVA was checked using a Snellen chart, and the axial length of each eye was measured using the LS 900 (Haag Streit, Wedel, Germany).

After administering one drop of topical 1% tropicamide to dilate the pupils, the Rtx1™ test was performed. After image acquisition, the images were processed with AO Detect to analyze the photoreceptor parameters DM, SM, REG, and N%6.

Data were assessed for a normal distribution using the Shapiro–Wilk test. If data were normally distributed, Student’s *t*-test for independent variables was used to compare mean values. If the data did not follow a normal distribution, the non-parametric U Mann–Whitney test was used to compare continuous variables between two groups of observations. If there were more than two groups, one-way ANOVA (parametric test) or the Kruskal–Wallis test (non-parametric) was used to compare differences, depending on the assumptions. ANOVA was followed by the HSD Tukey’s post-hoc test and the Kruskal–Wallis test was followed by Dunn’s post-hoc test. The results from both post-hoc tests were adjusted using Bonferroni correction.

A multivariate logistic model was used to examine the relationship between the existence of missing data for respective quadrants and the available variables. The model with the best fit was selected based on the Akaike Information Criterion (AIC). The exponents of the β coefficients ($\exp(\beta)$) were calculated to express the unit odds ratio. When a predictor was a dichotomous categorical variable, one was assumed for the event and zero otherwise. The odds ratio represented the ratio of probability of the occurrence and non-occurrence of a given event.

In this analysis, the level of statistical significance was set to $p = 0.05$. All calculations were conducted using R (version 4.0.2).

The values of DM, SM, REG, and N%6 for both the study and control groups are presented in Table 2.

Table 2. Comparison of DM, SM, REG, and N%6 between the study and control groups. DM: cone density [$1/\text{mm}^2$]; SM: cone spacing [μm]; REG: cone regularity [%]; N%6: Voronoi analysis [%]. The bold was used in all *p*-Values lower than 0.05 (=with statistical significance).

	Study Group (N = 53)	Control Group (N = 14)	<i>p</i> -Value (U Mann–Whitney)
DM			<0.001
Mean (SD)	10,111.33 (3198.77)	25,656.42 (2132.93)	
Median (IQR)	10,228.25 (7943.67–12,341.25)	24,961.54 (24,046.79–27,320.94)	
Range	3830–16,341.25	22,977.75–29,455.25	
SM			<0.001
Mean (SD)	12.11 (4.17)	6.91 (0.29)	
Median (IQR)	10.91 (9.92–12.24)	7 (6.68–7.13)	
Range	8.59–35.08	6.42–7.3	
REG			<0.001
Mean (SD)	83.74 (8.54)	90.98 (1.8)	
Median (IQR)	86.09 (80.81–88.96)	91.25 (89.64–92.18)	
Range	48.28–96.77	87.81–94.07	
N%6			0.008
Mean (SD)	45.21 (8.21)	48.43 (3.25)	
Median (IQR)	43.5 (40.5–48)	48.88 (48.18–49.58)	
Range	27.65–73.75	41.8–53.27	

3. Outcomes

3.1. Differences in Cone Density (DM), Cone Spacing (SM), Cone Regularity (REG), and Voronoi Analysis (N%6) between the Study and Control Groups

A statistically significant difference was observed between the control group and those with IRDs concerning DM ($10,111.33/\text{mm}^2$ vs. $25,646.42/\text{mm}^2$, $p < 0.001$), SM ($12.11 \mu\text{m}$ vs. $6.91 \mu\text{m}$, $p < 0.001$), REG (83.74% vs. 90.98% , $p < 0.001$), and N%6 (45.21% vs. 48.43% , $p = 0.008$) collectively across all quadrants, as detailed in Table 2. Additionally, a significant difference between the study group and the control group was noted in DM, SM, and REG for each quadrant, and in N%6 in the superior and inferior quadrants, as shown in Table 3.

Table 3. Comparison between the control and study groups, with evaluations made in each quadrant: temporal, nasal, superior, and inferior. DM_T: cone density in the temporal quadrant; SM_T: cone spacing in the temporal quadrant; REG_T: cone regularity in the temporal quadrant; N%6_T: Voronoi analysis in the temporal quadrant; DM_N: cone density in the nasal quadrant; SM_N: cone spacing in the nasal quadrant; REG_N: cone regularity in the nasal quadrant; N%6_N: Voronoi analysis in the nasal quadrant; DM_S: cone density in the superior quadrant; SM_S: cone spacing in the superior quadrant; REG_S: cone regularity in the superior quadrant; N%6_S: Voronoi analysis in the superior quadrant; DM_I: cone density in the inferior quadrant; SM_I: cone spacing in the inferior quadrant; REG_I: cone regularity in the inferior quadrant; N%6_I: Voronoi analysis in the inferior quadrant. The bold was used in all *p*-Values lower than 0.05 (=with statistical significance).

	Study Group (N = 53)	Control Group (N = 14)	<i>p</i> -Value (U Mann–Whitney)
Mean DM [1/mm ²] (SD)			
DM_T	10,893.92 (6038.18)	26,729.98 (2058.61)	<0.001
DM_N	9718.94 (4263.11)	25,585.69 (2153.57)	<0.001
DM_S	9673.34 (3648.9)	25,386.9 (2768.69)	<0.001
DM_I	10,159.14 (4408.24)	24,923.12 (3023.91)	<0.001
Mean SM [μm] (SD)			
SM_T	11.32 (3.07)	6.76 (0.27)	<0.001
SM_N	11.82 (3.71)	6.91 (0.3)	<0.001
SM_S	11.8 (3.39)	6.94 (0.37)	<0.001
SM_I	13.52 (13.13)	7.03 (0.42)	<0.001
Mean REG [%] (SD)			
REG_T	81.37 (15)	94.11 (3.2)	<0.001
REG_N	85.44 (11.41)	94.48 (2.58)	0.001
REG_S	82.41 (14.18)	81.05 (3.6)	0.029
REG_I	85.53 (10.25)	94.28 (3.18)	<0.001
Mean N%6 [%] (SD)			
N%6_T	43.02 (9.05)	48.02 (6.03)	0.061
N%6_N	47.04 (15.39)	47.41 (3.96)	0.162
N%6_S	45.88 (13.24)	50.73 (6.11)	0.036
N%6_I	44.91 (14.09)	47.56 (5.27)	0.031

3.2. Differences in DM, SM, REG, and N%6 between the Right Eyes of the Study Group and Controls

The analysis of data specifically from the right eyes revealed statistically significant differences between patients and the control groups in the mean values of DM, SM, and REG ($p = 0.003$, $p = 0.017$, $p = 0.035$, respectively). However, there was no significant difference observed in N%6 ($p = 0.220$) between these groups, as demonstrated in Table 4.

Table 4. Comparison of the mean values of DM, SM, REG, and N%6 between the study group and the control group for the right eye. DM: cone density [1/mm²]; SM: cone spacing [μm]; REG: cone regularity [%]; N%6: Voronoi analysis [%]. The bold was used in all *p*-Values lower than 0.05 (=with statistical significance).

	Study Group (N = 29)	Control Group (N = 14)	<i>p</i> -Value (U Mann–Whitney)
DM	10,154.52 (3641.81)	25,656.42 (2132.93)	0.003
SM	11.64 (2.83)	6.91 (0.29)	0.017
REG	82.69 (8.32)	90.98 (1.8)	0.035
N%6	45.2 (10.35)	48.43 (3.25)	0.220

3.3. Differences in BCVA, DM, SM, and REG between Right and Left Eyes with IRDs

No statistically significant differences were observed in BCVA ($p = 0.218$), DM ($p = 0.172$), SM ($p = 0.812$), or REG ($p = 0.156$) between the right and left eyes in the study group, as evidenced in Table 5.

Table 5. Characteristics of BCVA, DM, SM, REG in right and left eyes with IRDs. BCVA: best-corrected visual acuity; DM: cone density [$1/\text{mm}^2$]; SM: cone spacing [μm]; REG: cone regularity [%]; IRDs: inherited retinal dystrophies.

	Right Eye (N = 28)	Left Eye (N = 25)	p-Value (Test)
BCVA			
Mean (SD)	0.14 (0.17)	0.11 (0.16)	0.218 (<i>t</i> -test)
Median (IQR)	0.06 (0.04–0.2)	0.05 (0.04–0.12)	
Range	0.01–0.8	0.01–0.8	
DM			
Mean (SD)	10,357.02 (3246.84)	9767.12 (3224.25)	0.172 (<i>t</i> -test)
Median (IQR)	9396.5 (8420.12–12,993.88)	10,480.5 (6807–12,074.25)	
Range	3830–15,499.88	4584.33–16,341.25	
SM			
Mean (SD)	12.4 (5.13)	11.9 (2.95)	0.812 (Wilcoxon)
Median (IQR)	11.31 (9.91–12.11)	10.53 (10.06–13.21)	
Range	8.85–35.08	8.59–21.18	
REG			
Mean (SD)	83.25 (7.53)	85.57 (6.21)	0.156 (Wilcoxon)
Median (IQR)	85.66 (78.39–88.39)	86.17 (84.48–88.96)	
Range	60.66–96.77	66.67–95.84	

3.4. Differences in DM and SM among Eyes with CD, CRD, and STGD

The mean DM values were $8900.39/\text{mm}^2$, $9296.32/\text{mm}^2$, and $16,209.66/\text{mm}^2$ for eyes with CD, CRD, and STGD, respectively. Meanwhile, the average SM was $12.37 \mu\text{m}$ for CD, $14.82 \mu\text{m}$ for CRD, and $9.65 \mu\text{m}$ for STGD.

In eyes with IRDs, the mean SM and DM values showed significant differences based on the diagnosis: CD, CRD, or STGD ($p = 0.006$ and $p = 0.002$ for DM and SM, respectively), as demonstrated in Table 6. The highest average DM was observed in eyes with Stargardt's disease (mean DM $16,209.66/\text{mm}^2$, SD $8024.64/\text{mm}^2$), which also exhibited the lowest average SM ($9.65 \mu\text{m}$, SD $2.87 \mu\text{m}$).

However, differences in REG and N%6 among the CD, CRD, and STGD groups were not statistically significant ($p = 0.334$ and $p = 0.828$). Furthermore, the aforementioned correlations were not statistically significant when analyzing each quadrant.

REG was significantly correlated ($p = 0.044$) with the diagnosis of STGD, CD, or CRD in the temporal quadrant for the right eye, as depicted in Table 7. No such correlation was found in the remaining quadrants of the right eye or in any quadrant of the left eye.

Dunn's post-hoc analysis revealed a statistically significant difference in DM and SM between CD and STGD (mean DM $8,900.39/\text{mm}^2$ (SD $3022.87/\text{mm}^2$) vs. $16,209.66/\text{mm}^2$ (SD $8024.64/\text{mm}^2$), $p = 0.002$; mean SM $12.37 \mu\text{m}$ (SD $2.96 \mu\text{m}$) vs. $9.65 \mu\text{m}$ (SD $2.87 \mu\text{m}$), $p = 0.014$).

Likewise, a statistically significant difference in DM and SM was found between CRD and STGD (mean DM $9296.32/\text{mm}^2$ (SD $2965.31/\text{mm}^2$) vs. $16,209.66/\text{mm}^2$ (SD $8024.64/\text{mm}^2$), $p = 0.003$; mean SM $14.82 \mu\text{m}$ (SD $8.28 \mu\text{m}$) vs. $9.65 \mu\text{m}$ (SD $2.87 \mu\text{m}$), $p = 0.027$).

The data discussed above are illustrated in Figures 8 and 9.

Table 6. Comparison of mean DM, SM, REG, and N%6 values among eyes with CD, CRD, and STGD. DM: cone density [1/mm²]; SM: cone spacing [μm]; REG: cone regularity [%]; N%6: Voronoi analysis [%]; CD: cone dystrophy; CRD: cone-rod dystrophy; STGD: Stargardt disease. The bold was used in all *p*-Values lower than 0.05 (=with statistical significance).

	CD (N = 9)	CRD (N = 8)	STGD (N = 36)	<i>p</i> -Value (Kruskal–Wallis)
DM	8900.39 (3022.87)	9296.32 (2965.31)	16,209.66 (8024.64)	0.006
SM	12.37 (2.96)	14.82 (8.28)	9.65 (2.87)	0.002
REG	87.22 (4.98)	82 (10.31)	83.47 (10.82)	0.334
N%6	46.18 (5.4)	45.43 (12.89)	46.29 (9.38)	0.828

Table 7. Correlation of REG in each quadrant with the diagnosis for right eye. REG_T [%]: cone regularity in temporal quadrant; REG_N [%]: cone regularity in nasal quadrant; REG_S [%]: cone regularity in superior quadrant; REG_I [%]: cone regularity in inferior quadrant. CD: cone dystrophy; CRD: cone-rod dystrophy; STGD: Stargardt disease. The bold was used in all *p*-Values lower than 0.05 (=with statistical significance).

	CD (N = 5)	CRD (N = 4)	STGD (N = 19)	<i>p</i> -Value (Kruskal–Wallis)
REG_T				0.044
Mean (SD)	0.91 (0.05)	0.89 (0.05)	0.76 (0.2)	
Median (IQR)	0.92 (0.86–0.95)	0.91 (0.88–0.92)	0.85 (0.75–0.88)	
Range	0.84–0.96	0.82–0.94	0.33–0.94	
REG_N				0.953
Mean (SD)	0.85 (0.12)	0.86 (0.04)	0.87 (0.08)	
Median (IQR)	0.85 (0.84–0.87)	0.87 (0.85–0.89)	0.85 (0.81–0.92)	
Range	0.67–1	0.8–0.89	0.75–1	
REG_S				0.681
Mean (SD)	0.87 (0.07)	0.8 (0.14)	0.81 (0.14)	
Median (IQR)	0.87 (0.86–0.89)	0.85 (0.76–0.89)	0.87 (0.74–0.88)	
Range	0.77–0.96	0.6–0.9	0.5–1	
REG_I				0.511
Mean (SD)	0.87 (0.04)	0.87 (0.03)	0.85 (0.07)	
Median (IQR)	0.89 (0.86–0.89)	0.88 (0.86–0.89)	0.85 (0.81–0.88)	
Range	0.8–0.9	0.82–0.9	0.71–1	

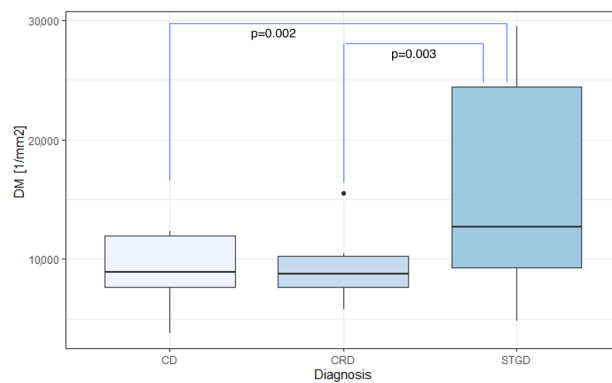


Figure 8. Comparison of DM among CD, CRD, and STGD groups. DM: cone density [1/mm²]; CD: cone dystrophy; CRD: cone-rod dystrophy; STGD: Stargardt disease.

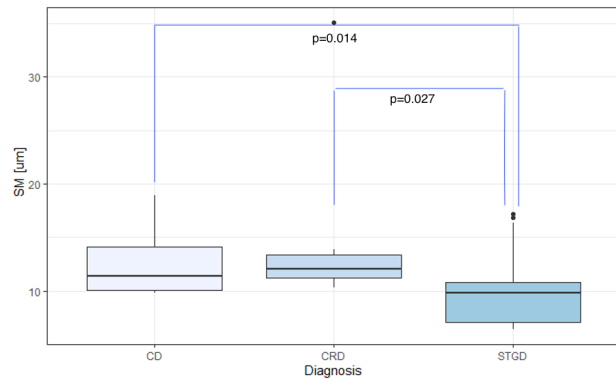


Figure 9. Comparison of SM among the CD, CRD, and STGD groups. SM: cone spacing [μm]; CD: cone dystrophy; CRD: cone-rod dystrophy; STGD: Stargardt disease.

3.5. Correlation between Photoreceptor Parameters and BCVA

No significant correlation was observed between BCVA and any of the measured parameters (DM, SM, REG, or N%6) in the study group, as illustrated in Table 8. Since all eyes in the control group had a BCVA of 1.0, no correlation calculations were conducted between BCVA and the AO cone parameters (DM, SM, REG, N%6) in the controls.

Similarly, no significant correlation was found between BCVA and DM, SM, and REG in the right eye ($p = 0.877$, $p = 0.737$, and $p = 0.130$ for DM, SM, and REG, respectively) or in the left eye ($p = 0.208$, $p = 0.106$, and $p = 0.349$ for DM, SM, and REG, respectively). These findings are shown in Table 9.

Table 8. Spearman’s correlation coefficients between BVCA and the mean values of DM, SM, REG, and N%6 in the eyes with IRDs. DM: cone density [1/mm²]; SM: cone spacing [μm]; REG: cone regularity [%]; N%6: Voronoi analysis [%].

	Correlation Coefficient (r)	p-Value
DM	0.07	0.612
SM	−0.109	0.436
REG	0.191	0.170
N%6	0.013	0.924

Table 9. Spearman’s correlation coefficients between BCVA and DM, SM, and REG in the right eye and the left eye with IRDs. DM: cone density [1/mm²]; IRDs: inherited retinal dystrophies; SM: cone spacing [μm]; REG: cone regularity [%]; N%6: Voronoi analysis [%].

	Correlation Coefficient (r)	p-Value
	Right eyes	
DM	0.031	0.877
SM	−0.068	0.737
REG	0.299	0.13

Table 9. Cont.

	Correlation Coefficient (r)	p-Value
Left eyes		
DM	0.261	0.208
SM	−0.331	0.106
REG	0.196	0.349

3.6. Correlation between Photoreceptor Parameters and Age

There was no significant correlation observed between age and the adaptive optics parameters (DM, SM, REG, and N%6) in either the eyes with IRDs or the control group, as illustrated in Table 10.

Table 10. Spearman’s correlation coefficients between age and DM, SM, REG, and N%6 in eyes with IRDs and in healthy eyes. DM: cone density [$1/\text{mm}^2$]; IRDs: inherited retinal dystrophies; SM: cone spacing [μm]; REG: cone regularity [%]; N%6: Voronoi analysis [%].

	Correlation Coefficient (r)	p-Value
Study group		
DM	−0.146	0.295
SM	0.186	0.184
REG	−0.152	0.277
N%6	0.075	0.593
Control group		
DM	−0.286	0.321
SM	0.299	0.3
REG	0.133	0.65
N%6	0.325	0.257

3.7. Correlation of DM and SM with the Probability of Incomplete Data Acquisition

During data collection, cases arose where image acquisition was impossible in all four quadrants or where the image quality was insufficient for analysis. This was mainly observed in patients with poor fixation and nystagmus. We investigated the factors that could potentially reduce the likelihood of obtaining a complete, high-quality dataset. Incomplete data were defined as the acquisition of fewer than four images suitable for analysis, while complete data entailed acquiring one image in each quadrant (superior, inferior, temporal, and nasal) suitable for analysis.

Incomplete data collection did not depend on patients’ BCVA, age, sex, or diagnosis (CD, CRD, or STGD), nor was it correlated with DM, SM, or REG, as shown in Table 11.

Nonetheless, univariate logistic regression model analysis indicated that DM was a statistically significant factor ($OR = 0.72$, $CI\ 0.55 - 0.90$, $p = 0.008$) affecting incomplete data collection in the study group. A decline in DM by $1000/\text{mm}^2$ increased the odds of incomplete data collection by 1.39 times. Owing to the substantial scale of DM, this variable was rescaled (divided by 1000) to derive a more reliable estimate of the odds ratio (OR). Age, sex, BCVA, diagnosis, SM, and regularity were not identified as significant factors in the univariate logistic regression model.

In a separate analysis of the univariate logistic regression models for the right and left eyes, SM emerged as a significant factor impacting incomplete data collection for the left eye: each unit increase in SM multiplied the odds of failure by 2.14 ($p = 0.019$). DM was also identified as a significant factor ($p = 0.011$), but its overall impact was negligible ($OR = 1$).

There were no cases of incomplete data collection in the control group.

Table 11. Descriptive characteristics concerning complete or incomplete data (with complete data indicating that 4 measurements provided an image suitable for analysis). BCVA: best-corrected visual acuity; DM: cone density [$1/\text{mm}^2$]; SM: cone spacing [μm]; REG: cone regularity [%]; CD: cone dystrophy; CRD: cone-rod dystrophy; STGD: Stargardt disease.

	Incomplete Data (N = 12)	Complete Data (N = 41)	p-Value (Test)
Mean age (SD)	45.63 (14.3)	41.92 (13.95)	0.360 (t-test)
Sex			
Male	50% (N = 6)	36.6% (N = 15)	0.839
Female	50% (N = 6)	63.4% (N = 26)	(chi-squared)
Diagnosis			
CD	25.0% (N = 3)	14.6% (N = 6)	0.838
CRD	16.7% (N = 2)	14.6% (N = 6)	(Fisher)
STGD	58.3% (N = 7)	70.7% (N = 29)	
BCVA			
Mean (SD)	0.1 (0.12)	0.15 (0.19)	0.309
Median (IQR)	0.05 (0.04–0.11)	0.1 (0.04–0.2)	(U Mann–Whitney)
Range	0.01–0.4	0.01–0.8	
DM			
Mean (SD)	9667.5 (3092.92)	10,673.83 (3263.13)	0.284
Median (IQR)	9180 (8083–10,990.75)	10,228.25 (8593–13,400.5)	(U Mann–Whitney)
Range	5292.75–15,499.88	3830–15,499.88	
SM			
Mean (SD)	13.28 (5.93)	11.99 (4.67)	0.103
Median (IQR)	11.39 (10.91–13.89)	10.91 (9.76–11.99)	(U Mann–Whitney)
Range	9.04–35.08	8.85–35.08	
REG			
Mean (SD)	84.19 (7.3)	82.82 (7.59)	0.889
Median (IQR)	85.66 (77.46–88.31)	85.66 (79.05–88.47)	(U Mann–Whitney)
Range	72.81–96.77	60.66–91.31	

4. Discussion

4.1. Evaluation of Cones and Rods in IRDs

There exist several studies providing thorough analyses of adaptive optics (AO) imaging and numeric parameters in healthy populations. Using the Rtx1™, the mean values of the AO parameters in a healthy population are as follows: DM 19,453/ mm^2 , SM 7.96 μm , and N% 46.7%, with no significant difference found between the right and left eyes [46].

The characteristics of IRDs in adaptive optics are known to differ from those of healthy eyes [14,25,26,30,37,38,57].

Wolfgang et al.'s study [34], the first to describe photoreceptor image disruption in CRD, focused on imaging the retina of a single patient. This revealed an abnormal cone density with a 6.6-fold reduction compared to normative data for healthy eyes.

An investigation of three patients with CRD and their three healthy relatives using AOSLO demonstrated that the cone-to-rod spacing ratio was increased in all the CRD patients. This suggests the dominance of cone loss over rod loss in CRD. Despite the symptoms of CRD, one patient (aged 18) showed no abnormalities in cone spacing compared to normative data. Another patient (aged 12), however, displayed increased cone spacing in all measured eccentricities. Rod loss increased with eccentricity. These data suggest a polymorphic course of CRD in patients, even within the same family, and a higher degree of rod loss in more peripheral areas of the retina [38].

Sahel et al. [57] assessed AOFIO in 10 eyes of 10 patients with RCD. While changes in cone morphology were described, no numeric parameters were reported. A study by

Duncan et al. [37] reported significant changes in SM between healthy retinas and those with retinitis pigmentosa (5 eyes) and cone-rod dystrophy (3 eyes). Foote et al. [14] analyzed cone spacing in 15 eyes of 14 patients with RCD and found a correlation between SM and macular sensitivity.

Chen et al. [25] reported cone abnormalities, such as increased cone spacing in regions of abnormal FAF imaging, in 12 patients with Stargardt disease. The study by Song et al. [26] reported changes not only in cone spacing but also in rod spacing in two patients with Stargardt disease. The cone density in the foveal region peaked at around 48,300/mm² in one patient and was impossible to measure in the other patient since no cones were identified in the foveal region.

In another study, Song et al. [30] reported a 50% increase in cone spacing and a 30% increase in rod spacing in patients with STGD. Photoreceptor changes did not uniformly correspond with FAF abnormalities. The study included three patients with STGD compared to a healthy control. The authors highlighted abnormalities in photoreceptor appearance and the presence of dark spots ('dark spaces') in the mosaic.

There have been studies, including ours, that have confirmed the correlation of AO findings with functional and structural changes. Duncan et al. [37] found a significant correlation of cone spacing in patients with RP and CRD with the foveal threshold in perimetry, electrophysiological changes in mfERG, and BCVA. This study group included eight eyes with IRDs.

Another study compared AO imaging with perimetrical and electrophysiological changes, as well as contrast sensitivity. The correlation of these parameters was confirmed. The study group was heterogeneous and consisted of three patients with RCD, one patient with CRD, and one with juvenile macular dystrophy [35].

4.2. Early Diagnosis of IRDs

Several studies highlight the potential role of adaptive optics in the early diagnosis of retinal dystrophies. For instance, Palejwala et al. reported that cone loss measured by adaptive optics flood illumination ophthalmoscopy (AOFIO) can show signs of inherited retinal dystrophy before the symptoms of vision loss appear, as evidenced in a 7-year-old patient [58]. This patient was diagnosed with a mutation in the *ELOVL4* gene, which is responsible for autosomal dominant Stargardt-like macular dystrophy.

The case studies described by Ito et al. [59] and Kubota et al. [60] underscore the importance of assessing cone density in the diagnosis of cone dystrophy and atypical Usher syndrome.

Understanding the phenotypes of cones and rods, along with their changes during the progression of retinal diseases, is considered to be vital for future studies on inherited retinal dystrophies (IRDs) [61].

4.3. Potential for Future Advancement in Adaptive Optics

The loss of central vision and unstable fixation pose challenges to obtaining high-quality images. Furthermore, in IRDs, the cone spacing (SM) and cone density (DM) vary within the same eye, a factor described in the context of Stargardt disease [62]. Chen et al. [25] reported difficulties in obtaining AO images in 4 out of 12 patients with STGD.

The accumulation of lipofuscin may also lead to the aberrant acquisition of a cone mosaic appearance in certain regions. To circumvent this issue, we calculated results based on average measurements from four different regions. Other proposed solutions include generating cone density deviation maps and correlating them with OCT and microperimetry data [63]. Conversely, some studies suggest that in patients with RP, the repeatability of AO measurements is comparable to that in healthy subjects when measured with the i2K Retina device [64]. However, we found no data for maculopathies similar to the ones investigated in our study.

Rtx1™, despite its widespread use and the existence of population data, has some limitations, such as difficulty in examining foveal cones, which are crucial in IRDs [48]. We, as with other researchers using Rtx1™, circumvented this problem by taking measurements two degrees away from the fovea in different directions.

One difficulty concerning the adaptive optics scanning laser ophthalmoscopy (AOSLO) imaging of IRDs is the possible imprecision in detecting photoreceptors in abnormal retinas [65]. Deep learning solutions are being developed to facilitate the automatic recognition of cones in IRDs, even in microscopic pathologies previously unseen [45].

The diagnostic process for IRDs is often lengthy and challenging due to the overlapping symptoms and multiple gene mutations causing each dystrophy. Artificial intelligence models have been proposed to facilitate the diagnosis of IRDs based on clinical images. The model assessment includes AO imaging of the retina, as well as fundus imaging, fluorescein and indocyanine-green angiography, autofluorescence, and OCT. This highlights the potential role of adaptive optics as a crucial tool in diagnosing rare retinal diseases [29,66,67].

AO imaging, however, has universal limitations: it does not assess foveal cones or rods and is a costly solution. The need for the precise visualization of the photoreceptor mosaics has spurred the development of other imaging techniques. For instance, a study comparing AOSLO images with those from the Heidelberg Engineering SPECTRALIS High Magnification Module (HMM) in Stargardt disease showed promising quality and potential for HMM development [48].

4.4. The Research Group

Our study underscores significant differences in cone parameters, specifically in cone density (DM) and cone spacing (SM), between STGD, CD, and CRD. These findings could potentially streamline the differential diagnosis among IRDs that affect the macula.

The molecular etiology of STGD differs from that of CD and CRD, primarily impacting the retinal pigment epithelium (RPE) instead of the photoreceptors. In our study, the DM and SM parameters in the STGD group demonstrated the highest standard deviations among all groups.

A limitation of our study is the absence of a confirmed genetic etiology of IRD in all participants.

In several other studies [34,37], the genetic mutations causing CRD or RP were not reported for the majority of the patients examined. Similarly, more recent reports [14,57] do not provide precise information on mutations in all subjects.

Since the clinical symptoms of IRDs can overlap, diagnosis without confirming the genetic mutation may be questionable. There is a need for studies focusing on the differences in photoreceptor changes, as seen in AO, between eyes with varying genetic causes of retinal degeneration.

Studying rare conditions such as IRDs is challenging due to the difficulty in gathering a sufficiently large research group for reliable statistical analysis. However, we mitigated this issue by successfully assembling a large study group and comparing their data with outcomes from healthy retinas.

Ratnam et al. [55] described foveal changes in 18 eyes from 18 patients diagnosed with various types of IRDs. Tuten et al. [68] examined 12 eyes from 12 patients diagnosed with choroideremia using AO-SLO and AO-microperimetry. To the best of our knowledge, our study represents the largest research group in terms of AO imaging in IRDs.

4.5. Longitudinal Observation

Adaptive optics (AO) is a relatively recent advancement in the field of ophthalmic imaging. As such, there are still few studies examining changes over time. Roshandel et al. [69] conducted a six-month observation study on photoreceptor changes, confirming significant parafoveal cone loss over the observation period in rod-cone dystrophy (RCD). Foote et al. [14] documented an increase in cone spacing in 15 eyes of 14 RCD

patients over a three-year observation period. Furthermore, Chen et al. [25] described the longitudinal progression of photoreceptor changes in two Stargardt disease patients over 27 months. However, we found no such studies for cone-rod dystrophy or cone dystrophy.

Ziccardi et al. explored the possibility of monitoring the progression of retinitis pigmentosa (RP) associated with a mutation in the *RP1L1* gene in three patients [70]. Over a two-year follow-up, they noted a significant reduction in DM in the proband, with the most substantial reduction observed 2° from the fovea.

Other retinal conditions, such as retinal detachment, are also subjects of investigation for photoreceptor damage. Potic et al. [71] used AO to examine visual acuity and cone density in eyes after retinal detachment repair, with a follow-up time of three months.

5. Conclusions

Our study confirmed that photoreceptor parameters in eyes with IRDs distinctly diverge from those in healthy eyes. An examination utilizing adaptive optics could potentially facilitate the differentiation between STGD and CD, as well as between STGD and CRD.

We advocate for more studies focused on the adaptive optics parameters unique to each genetic mutation. These research efforts could yield fresh insights into the etiology of photoreceptor degeneration in varying conditions.

From our perspective, there exists a significant demand for longitudinal studies that assess the progression of photoreceptor changes over extended periods.

Author Contributions: Conceptualization, J.P.S. and A.Z.-Ż.; methodology, A.Z.-Ż.; software, K.S.; validation, A.Z.-Ż., K.S. and A.K.K.; formal analysis, A.Z.-Ż.; investigation, M.G., K.S. and A.Z.-Ż.; resources, K.S.; data curation, M.G. and K.S.; writing—original draft preparation, K.S.; writing, K.S. and A.Z.-Ż.; review and editing, K.S., J.P.S., A.Z.-Ż. and A.K.K.; visualization, J.P.S. and A.Z.-Ż.; supervision, A.Z.-Ż.; project administration, J.P.S.; funding acquisition, J.P.S. All authors have read and agreed to the published version of the manuscript.

Funding: This research received no external funding.

Institutional Review Board Statement: The study was conducted in accordance with the Declaration of Helsinki and approved by the Bioethics Committee of the Medical University of Warsaw (KB/87/2015, 7 April 2015).

Informed Consent Statement: Informed consent was obtained from all subjects involved in the study.

Data Availability Statement: Not applicable.

Conflicts of Interest: The authors declare no conflict of interest.

Abbreviations

The following abbreviations are used in this manuscript:

AMD	Age-related macular degeneration
AO	Adaptive optics
AOFIO	Adaptive optics flood illuminated ophthalmoscope
AOSLO	Adaptive optics scanning laser ophthalmoscopy
CD	Cone dystrophy
CDSR	Cone dystrophy with supernormal rod electroretinogram
CRD	Cone-rod dystrophy
BCVA	Best-corrected visual acuity
MDPI	Multidisciplinary Digital Publishing Institute
DOAJ	Directory of Open Access Journals
DM	Cone density [1/mm ²]
FAF	Fundus autofluorescence
FFA	Fluorescein angiography
HMM	High Magnification Module
IQR	Interquartile range

IRD	Inherited retinal dystrophy
LCA	Leber congenital amaurosis
mFERG	Multifocal electroretinography
N%6	Voronoi analysis of hexagonal cones [%]
RCD	Rod-cone dystrophy
REG	Cone regularity [%]
RNFL	Retinal nerve fiber layer
RP	Retinitis pigmentosa
RPE	Retinal pigment epithelium
SD	Standard deviation
SD-OCT	Spectral-domain optical coherent tomography
SM	Cone spacing [μm]
STGD	Stargardt disease
OR	Odds ratio

References

- Chen, T.C.; Huang, D.S.; Lin, C.W.; Yang, C.H.; Yang, C.M.; Wang, V.Y.; Lin, J.W.; Luo, A.C.; Hu, F.R.; Chen, P.L. Genetic characteristics and epidemiology of inherited retinal degeneration in Taiwan. *NPJ Genom. Med.* **2021**, *6*, 16. [\[CrossRef\]](#) [\[PubMed\]](#)
- Schwartz, S.D.; Regillo, C.D.; Lam, B.L.; Elliott, D.; Rosenfeld, P.J.; Gregori, N.Z.; Hubschman, J.P.; Davis, J.L.; Heilwell, G.; Spirm, M.; et al. Human embryonic stem cell-derived retinal pigment epithelium in patients with age-related macular degeneration and Stargardt's macular dystrophy: Follow-up of two open-label phase 1/2 studies. *Lancet* **2015**, *385*, 509–516. [\[CrossRef\]](#) [\[PubMed\]](#)
- Sung, Y.; Lee, M.J.; Choi, J.; Jung, S.Y.; Chong, S.Y.; Sung, J.H.; Shim, S.H.; Song, W.K. Long-term safety and tolerability of subretinal transplantation of embryonic stem cell-derived retinal pigment epithelium in Asian Stargardt disease patients. *Br. J. Ophthalmol.* **2021**, *105*, 829–837.
- Lingam, S.; Liu, Z.; Yang, B.; Wong, W.; Parikh, B.H.; Ong, J.Y.; Goh, D.; Wong, D.S.L.; Tan, Q.S.W.; Tan, G.S.W.; et al. cGMP-grade human iPSC-derived retinal photoreceptor precursor cells rescue cone photoreceptor damage in non-human primates. *Stem Cell Res. Ther.* **2021**, *12*, 464. [\[CrossRef\]](#) [\[PubMed\]](#)
- Girach, A.; Audo, I.; Birch, D.G.; Huckfeldt, R.M.; Lam, B.L.; Leroy, B.P.; Michaelides, M.; Russell, S.R.; Sallum, J.M.F.; Stingl, K.; et al. RNA-based therapies in inherited retinal diseases. *Ther. Adv. Ophthalmol.* **2022**, *14*, 25158414221134602. [\[CrossRef\]](#)
- John, M.C.; Quinn, J.; Hu, M.L.; Cehajic-Kapetanovic, J.; Xue, K. Gene-agnostic therapeutic approaches for inherited retinal degenerations. *Front. Mol. Neurosci.* **2022**, *15*, 1068185. [\[CrossRef\]](#) [\[PubMed\]](#)
- Battu, R.; Ratra, D.; Gopal, L. Newer therapeutic options for inherited retinal diseases: Gene and cell replacement therapy. *Indian J. Ophthalmol.* **2022**, *70*, 2316–2325. [\[CrossRef\]](#)
- Olivares-González, L.; Velasco, S.; Campillo, I.; Rodrigo, R. Retinal Inflammation, Cell Death and Inherited Retinal Dystrophies. *Int. J. Mol. Sci.* **2021**, *22*, 2096. [\[CrossRef\]](#)
- Pagon, R.A. Retinitis pigmentosa. *Surv. Ophthalmol.* **1988**, *33*, 137–177. [\[CrossRef\]](#)
- Daiger, S.P.; Sullivan, L.S.; Bowne, S.J. Genes and mutations causing retinitis pigmentosa. *Clin. Genet.* **2013**, *84*, 132–141. [\[CrossRef\]](#)
- Hamel, C. Retinitis pigmentosa. *Orphanet. J. Rare Dis.* **2006**, *1*, 40. [\[CrossRef\]](#) [\[PubMed\]](#)
- Maguire, A.M.; Bennett, J.; Aleman, E.M.; Leroy, B.P.; Aleman, T.S. Clinical Perspective: Treating RPE65-Associated Retinal Dystrophy. *Mol. Ther.* **2021**, *29*, 442–463. [\[CrossRef\]](#) [\[PubMed\]](#)
- Hu, M.L.; Edwards, T.L.; O'Hare, F.; Hickey, D.G.; Wang, J.H.; Liu, Z.; Ayton, L.N. Gene therapy for inherited retinal diseases: Progress and possibilities. *Clin. Exp. Optom.* **2021**, *104*, 444–454. [\[CrossRef\]](#)
- Foote, K.G.; De la Huerta, I.; Gustafson, K.; Baldwin, A.; Zayit-Soudry, S.; Rinella, N.; Porco, T.C.; Roorda, A.; Duncan, J.L. Cone Spacing Correlates With Retinal Thickness and Microperimetry in Patients With Inherited Retinal Degenerations. *Investig. Ophthalmol. Vis. Sci.* **2019**, *60*, 1234–1243. [\[CrossRef\]](#)
- Vasireddy, V.; Wong, P.; Ayyagari, R. Genetics and molecular pathology of Stargardt-like macular degeneration. *Prog. Retin. Eye Res.* **2010**, *29*, 191–207. [\[CrossRef\]](#) [\[PubMed\]](#)
- Tanna, P.; Strauss, R.W.; Fujinami, K.; Michaelides, M. Stargardt disease: Clinical features, molecular genetics, animal models and therapeutic options. *Br. J. Ophthalmol.* **2017**, *101*, 25–30. [\[CrossRef\]](#) [\[PubMed\]](#)
- Ścieżyńska, A.; Oziębło, D.; Ambroziak, A.M.; Korwin, M.; Szulborski, K.; Krawczyński, M.; Stawiński, P.; Szaflik, J.; Szaflik, J.P.; Płoski, R.; et al. Next-generation sequencing of ABCA4: High frequency of complex alleles and novel mutations in patients with retinal dystrophies from Central Europe. *Exp. Eye Res.* **2016**, *145*, 93–99. [\[CrossRef\]](#)
- Tanna, P.; Kasilian, M.; Strauss, R.; Tee, J.; Kalitzeos, A.; Tarima, S.; Visotcky, A.; Dubra, A.; Carroll, J.; Michaelides, M. Reliability and Repeatability of Cone Density Measurements in Patients With Stargardt Disease and RPGR-Associated Retinopathy. *Investig. Ophthalmol. Vis. Sci.* **2017**, *58*, 3608–3615. [\[CrossRef\]](#)
- Kong, X.; Fujinami, K.; Strauss, R.W.; Munoz, B.; West, S.K.; Cideciyan, A.V.; Michaelides, M.; Ahmed, M.; Ervin, A.M.; Schönbach, E.; et al. Visual Acuity Change Over 24 Months and Its Association With Foveal Phenotype and Genotype in Individuals With Stargardt Disease: ProgStar Study Report No. 10. *JAMA Ophthalmol.* **2018**, *136*, 920–928. [\[CrossRef\]](#)

20. Schönbach, E.M.; Strauss, R.W.; Ibrahim, M.A.; Janes, J.L.; Birch, D.G.; Cideciyan, A.V.; Sunness, J.S.; Muñoz, B.; Ip, M.S.; Sadda, S.R.; et al. Faster Sensitivity Loss around Dense Scotomas than for Overall Macular Sensitivity in Stargardt Disease: ProgStar Report No. 14. *Am. J. Ophthalmol.* **2020**, *216*, 219–225. [[CrossRef](#)]
21. Tanna, P.; Georgiou, M.; Strauss, R.W.; Ali, N.; Kumaran, N.; Kalitzeos, A.; Fujinami, K.; Michaelides, M. Cross-Sectional and Longitudinal Assessment of the Ellipsoid Zone in Childhood-Onset Stargardt Disease. *Transl. Vis. Sci. Technol.* **2019**, *8*, 1. [[CrossRef](#)]
22. Strauss, R.W.; Muñoz, B.; Ho, A.; Jha, A.; Michaelides, M.; Cideciyan, A.V.; Audo, I.; Birch, D.G.; Hariri, A.H.; Nittala, M.G.; et al. Progression of Stargardt Disease as Determined by Fundus Autofluorescence in the Retrospective Progression of Stargardt Disease Study (ProgStar Report No. 9). *JAMA Ophthalmol.* **2017**, *135*, 1232–1241. [[CrossRef](#)] [[PubMed](#)]
23. Strauss, R.W.; Kong, X.; Ho, A.; Jha, A.; West, S.; Ip, M.; Bernstein, P.S.; Birch, D.G.; Cideciyan, A.V.; Michaelides, M.; et al. Progression of Stargardt Disease as Determined by Fundus Autofluorescence Over a 12-Month Period: ProgStar Report No. 11. *JAMA Ophthalmol.* **2019**, *137*, 1134–1145. [[CrossRef](#)] [[PubMed](#)]
24. Fujinami, K.; Lois, N.; Mukherjee, R.; McBain, V.A.; Tsunoda, K.; Tsubota, K.; Stone, E.M.; Fitzke, F.W.; Bunce, C.; Moore, A.T.; et al. A longitudinal study of Stargardt disease: Quantitative assessment of fundus autofluorescence, progression, and genotype correlations. *Investig. Ophthalmol. Vis. Sci.* **2013**, *54*, 8181–8190. [[CrossRef](#)] [[PubMed](#)]
25. Chen, Y.; Ratnam, K.; Sundquist, S.M.; Lujan, B.; Ayyagari, R.; Gudiseva, V.H.; Roorda, A.; Duncan, J.L. Cone photoreceptor abnormalities correlate with vision loss in patients with Stargardt disease. *Investig. Ophthalmol. Vis. Sci.* **2011**, *52*, 3281–3292. [[CrossRef](#)]
26. Song, H.; Rossi, E.A.; Latchney, L.; Bessette, A.; Stone, E.; Hunter, J.J.; Williams, D.R.; Chung, M. Cone and rod loss in Stargardt disease revealed by adaptive optics scanning light ophthalmoscopy. *JAMA Ophthalmol.* **2015**, *133*, 1198–1203. [[CrossRef](#)]
27. Scoles, D.; Sulai, Y.N.; Langlo, C.S.; Fishman, G.A.; Curcio, C.A.; Carroll, J.; Dubra, A. In vivo imaging of human cone photoreceptor inner segments. *Investig. Ophthalmol. Vis. Sci.* **2014**, *55*, 4244–4251. [[CrossRef](#)]
28. Song, H.; Latchney, L.; Williams, D.; Chung, M. Fluorescence adaptive optics scanning laser ophthalmoscope for detection of reduced cones and hypoautofluorescent spots in fundus albipunctatus. *JAMA Ophthalmol.* **2014**, *132*, 1099–1104. [[CrossRef](#)]
29. Al-Khuzaei, S.; Shah, M.; Foster, C.R.; Yu, J.; Broadgate, S.; Halford, S.; Downes, S.M. The role of multimodal imaging and vision function testing in ABCA4-related retinopathies and their relevance to future therapeutic interventions. *Ther. Adv. Ophthalmol.* **2021**, *13*, 25158414211056384. [[CrossRef](#)]
30. Song, H.; Rossi, E.A.; Yang, Q.; Granger, C.E.; Latchney, L.R.; Chung, M.M. High-Resolution Adaptive Optics in Vivo Autofluorescence Imaging in Stargardt Disease. *JAMA Ophthalmol.* **2019**, *137*, 603–609. [[CrossRef](#)]
31. Vincent, A.; Wright, T.; Garcia-Sanchez, Y.; Ksilak, M.; Campbell, M.; Westall, C.; Héon, E. Phenotypic characteristics including in vivo cone photoreceptor mosaic in KCNV2-related “cone dystrophy with supernormal rod electroretinogram”. *Investig. Ophthalmol. Vis. Sci.* **2013**, *54*, 898–908. [[CrossRef](#)]
32. Gill, J.S.; Georgiou, M.; Kalitzeos, A.; Moore, A.T.; Michaelides, M. Progressive cone and cone-rod dystrophies: Clinical features, molecular genetics and prospects for therapy. *Br. J. Ophthalmol.* **2019**, *103*, 711–720. [[CrossRef](#)] [[PubMed](#)]
33. Thiadens, A.A.H.J.; Phan, T.M.L.; Zekveld-Vroon, R.C.; Leroy, B.P.; van den Born, L.I.; Hoyng, C.B.; Klaver, C.C.W.; Roosing, S.; Pott, J.W.R.; van Schooneveld, M.J.; et al. Clinical course, genetic etiology, and visual outcome in cone and cone-rod dystrophy. *Ophthalmology* **2012**, *119*, 819–826. [[CrossRef](#)] [[PubMed](#)]
34. Wolfing, J.I.; Chung, M.; Carroll, J.; Roorda, A.; Williams, D.R. High-resolution retinal imaging of cone-rod dystrophy. *Ophthalmology* **2006**, *113*, 1019.e1. [[CrossRef](#)] [[PubMed](#)]
35. Choi, S.S.; Doble, N.; Hardy, J.L.; Jones, S.M.; Keltner, J.L.; Olivier, S.S.; Werner, J.S. In vivo imaging of the photoreceptor mosaic in retinal dystrophies and correlations with visual function. *Investig. Ophthalmol. Vis. Sci.* **2006**, *47*, 2080–2092. [[CrossRef](#)]
36. Roorda, A.; Zhang, Y.; Duncan, J.L. High-resolution in vivo imaging of the RPE mosaic in eyes with retinal disease. *Investig. Ophthalmol. Vis. Sci.* **2007**, *48*, 2297–2303. [[CrossRef](#)]
37. Duncan, J.L.; Zhang, Y.; Gandhi, J.; Nakanishi, C.; Othman, M.; Branham, K.E.H.; Swaroop, A.; Roorda, A. High-resolution imaging with adaptive optics in patients with inherited retinal degeneration. *Investig. Ophthalmol. Vis. Sci.* **2007**, *48*, 3283–3291. [[CrossRef](#)]
38. Song, H.; Rossi, E.A.; Stone, E.; Latchney, L.; Williams, D.; Dubra, A.; Chung, M. Phenotypic diversity in autosomal-dominant cone-rod dystrophy elucidated by adaptive optics retinal imaging. *Br. J. Ophthalmol.* **2018**, *102*, 136–141. [[CrossRef](#)]
39. Bensinger, E.; Rinella, N.; Saud, A.; Loumou, P.; Ratnam, K.; Griffin, S.; Qin, J.; Porco, T.C.; Roorda, A.; Duncan, J.L. Loss of Foveal Cone Structure Precedes Loss of Visual Acuity in Patients With Rod-Cone Degeneration. *Investig. Ophthalmol. Vis. Sci.* **2019**, *60*, 3187–3196. [[CrossRef](#)]
40. Samelska, K.; Kupis, M.; Zaleska-Żmijewska, A.; Szaflik, J.P. Adaptive optics imaging in the most common inherited retinal degenerations. *Klin. Ocz.* **2021**, *123*, 74–79. [[CrossRef](#)]
41. Gill, J.S.; Moosajee, M.; Dubis, A.M. Cellular imaging of inherited retinal diseases using adaptive optics. *Eye* **2019**, *33*, 1683–1698. [[CrossRef](#)]
42. Dreher, A.W.; Bille, J.F.; Weinreb, R.N. Active optical depth resolution improvement of the laser tomographic scanner. *Appl. Opt.* **1989**, *28*, 804–808. [[CrossRef](#)] [[PubMed](#)]
43. Liang, J.; Williams, D.R.; Miller, D.T. Supernormal vision and high-resolution retinal imaging through adaptive optics. *J. Opt. Soc. Am. A Opt. Image Sci. Vis.* **1997**, *14*, 2884–2892. [[CrossRef](#)] [[PubMed](#)]





44. Lombardo, M.; Serrao, S.; Devaney, N.; Parravano, M.; Lombardo, G. Adaptive optics technology for high-resolution retinal imaging. *Sensors* **2012**, *13*, 334–366. [[CrossRef](#)] [[PubMed](#)]
45. Davidson, B.; Kalitzeos, A.; Carroll, J.; Dubra, A.; Ourselin, S.; Michaelides, M.; Bergeles, C. Automatic Cone Photoreceptor Localisation in Healthy and Stargardt Afflicted Retinas Using Deep Learning. *Sci. Rep.* **2018**, *8*, 7911. [[CrossRef](#)]
46. Zaleska-Żmijewska, A.; Wawrzyniak, Z.M.; Ulińska, M.; Szaflik, J.; Dąbrowska, A.; Szaflik, J.P. Human photoreceptor cone density measured with adaptive optics technology (rtx1 device) in healthy eyes: Standardization of measurements. *Medicine* **2017**, *96*, e7300. [[CrossRef](#)]
47. Polans, J.; Keller, B.; Carrasco-Zevallos, O.M.; LaRocca, F.; Cole, E.; Whitson, H.E.; Lad, E.M.; Farsiu, S.; Izatt, J.A. Wide-field retinal optical coherence tomography with wavefront sensorless adaptive optics for enhanced imaging of targeted regions. *Biomed. Opt. Express* **2017**, *8*, 16–37. [[CrossRef](#)] [[PubMed](#)]
48. Wynne, N.; Heitkotter, H.; Woertz, E.N.; Cooper, R.F.; Carroll, J. Comparison of Cone Mosaic Metrics From Images Acquired With the SPECTRALIS High Magnification Module and Adaptive Optics Scanning Light Ophthalmoscopy. *Transl. Vis. Sci. Technol.* **2022**, *11*, 19. [[CrossRef](#)]
49. Zaleska-Żmijewska, A.; Wawrzyniak, Z.M.; Dąbrowska, A.; Szaflik, J.P. Adaptive Optics (rtx1) High-Resolution Imaging of Photoreceptors and Retinal Arteries in Patients with Diabetic Retinopathy. *J. Diabetes Res.* **2019**, *2019*, 9548324. [[CrossRef](#)]
50. Zaleska-Żmijewska, A.; Piątkiewicz, P.; Śmigielka, B.; Sokołowska-Oracz, A.; Wawrzyniak, Z.M.; Romaniuk, D.; Szaflik, J.; Szaflik, J.P. Retinal Photoreceptors and Microvascular Changes in Prediabetes Measured with Adaptive Optics (rtx1™): A Case-Control Study. *J. Diabetes Res.* **2017**, *2017*, 4174292. [[CrossRef](#)]
51. Rosenbaum, D.; Mattina, A.; Koch, E.; Rossant, F.; Gallo, A.; Kachenoura, N.; Paques, M.; Redheuil, A.; Girerd, X. Effects of age, blood pressure and antihypertensive treatments on retinal arterioles remodeling assessed by adaptive optics. *J. Hypertens.* **2016**, *34*, 1115–1122. [[CrossRef](#)] [[PubMed](#)]
52. Meixner, E.; Michelson, G. Measurement of retinal wall-to-lumen ratio by adaptive optics retinal camera: A clinical research. *Graefes Arch. Clin. Exp. Ophthalmol.* **2015**, *253*, 1985–1995. [[CrossRef](#)] [[PubMed](#)]
53. Zaleska-Żmijewska, A.; Wawrzyniak, Z.; Kupis, M.; Szaflik, J.P. The Relation between Body Mass Index and Retinal Photoreceptor Morphology and Microvascular Changes Measured with Adaptive Optics (rtx1) High-Resolution Imaging. *J. Ophthalmol.* **2021**, *2021*, 6642059. [[CrossRef](#)]
54. Boretsky, A.; Khan, F.; Burnett, G.; Hammer, D.X.; Ferguson, R.D.; van Kuijk, F.; Motamedi, M. In vivo imaging of photoreceptor disruption associated with age-related macular degeneration: A pilot study. *Lasers. Surg. Med.* **2012**, *44*, 603–610. [[CrossRef](#)] [[PubMed](#)]
55. Ratnam, K.; Carroll, J.; Porco, T.C.; Duncan, J.L.; Roorda, A. Relationship between foveal cone structure and clinical measures of visual function in patients with inherited retinal degenerations. *Investig. Ophthalmol. Vis. Sci.* **2013**, *54*, 5836–5847. [[CrossRef](#)]
56. Muthiah, M.N.; Gias, C.; Chen, F.K.; Zhong, J.; McClelland, Z.; Sallo, F.B.; Peto, T.; Coffey, P.J.; da Cruz, L. Cone photoreceptor definition on adaptive optics retinal imaging. *Br. J. Ophthalmol.* **2014**, *98*, 1073–1079. [[CrossRef](#)]
57. Sahel, J.A.; Grieve, K.; Pagot, C.; Authié, C.; Mohand-Said, S.; Paques, M.; Audo, I.; Becker, K.; Chaumet-Riffaud, A.E.; Azoulay, L.; et al. Assessing Photoreceptor Status in Retinal Dystrophies: From High-Resolution Imaging to Functional Vision. *Am. J. Ophthalmol.* **2021**, *230*, 12–47. [[CrossRef](#)] [[PubMed](#)]
58. Palejwala, N.V.; Gale, M.J.; Clark, R.F.; Schlechter, C.; Weleber, R.G.; Pennesi, M.E. Insights into autosomal dominant stargardt-like macular dystrophy through multimodality diagnostic imaging. *Retina* **2016**, *36*, 119–130. [[CrossRef](#)]
59. Ito, N.; Kameya, S.; Gocho, K.; Hayashi, T.; Kikuchi, S.; Katagiri, S.; Gekka, T.; Yamaki, K.; Takahashi, H.; Tsuneoka, H. Multimodal imaging of a case of peripheral cone dystrophy. *Doc. Ophthalmol.* **2015**, *130*, 241–251. [[CrossRef](#)]
60. Kubota, D.; Gocho, K.; Kikuchi, S.; Akeo, K.; Miura, M.; Yamaki, K.; Takahashi, H.; Kameya, S. CEP250 mutations associated with mild cone-rod dystrophy and sensorineural hearing loss in a Japanese family. *Ophthalmic. Genet.* **2018**, *39*, 500–507. [[CrossRef](#)]
61. Morgan, J.I.W.; Chui, T.Y.P.; Grieve, K. Twenty-five years of clinical applications using adaptive optics ophthalmoscopy [Invited]. *Biomed. Opt. Express* **2023**, *14*, 387–428. [[CrossRef](#)] [[PubMed](#)]
62. Chen, Y.; Roorda, A.; Duncan, J.L. Advances in imaging of Stargardt disease. *Adv. Exp. Med. Biol.* **2010**, *664*, 333–340. [[CrossRef](#)] [[PubMed](#)]
63. Razeen, M.M.; Cooper, R.F.; Langlo, C.S.; Goldberg, M.R.; Wilk, M.A.; Han, D.P.; Connor, T.B.J.; Fishman, G.A.; Collison, F.T.; Sulai, Y.N.; et al. Correlating Photoreceptor Mosaic Structure to Clinical Findings in Stargardt Disease. *Transl. Vis. Sci. Technol.* **2016**, *5*, 6. [[CrossRef](#)] [[PubMed](#)]
64. Gale, M.J.; Harman, G.A.; Chen, J.; Pennesi, M.E. Repeatability of Adaptive Optics Automated Cone Measurements in Subjects With Retinitis Pigmentosa and Novel Metrics for Assessment of Image Quality. *Transl. Vis. Sci. Technol.* **2019**, *8*, 17. [[CrossRef](#)]
65. Bergeles, C.; Dubis, A.M.; Davidson, B.; Kasilian, M.; Kalitzeos, A.; Carroll, J.; Dubra, A.; Michaelides, M.; Ourselin, S. Unsupervised identification of cone photoreceptors in non-confocal adaptive optics scanning light ophthalmoscope images. *Biomed. Opt. Express* **2017**, *8*, 3081–3094. [[CrossRef](#)]
66. Esengönül, M.; Marta, A.; Beirão, J.; Pires, I.M.; Cunha, A. A Systematic Review of Artificial Intelligence Applications Used for Inherited Retinal Disease Management. *Medicina* **2022**, *58*, 504. [[CrossRef](#)]
67. Williams, D.R.; Burns, S.A.; Miller, D.T.; Roorda, A. Evolution of adaptive optics retinal imaging [Invited]. *Biomed. Opt. Express* **2023**, *14*, 1307–1338. [[CrossRef](#)]

68. Tuten, W.S.; Vergilio, G.K.; Young, G.J.; Bennett, J.; Maguire, A.M.; Aleman, T.S.; Brainard, D.H.; Morgan, J.I.W. Visual Function at the Atrophic Border in Choroideremia Assessed with Adaptive Optics Microperimetry. *Ophthalmol. Retin.* **2019**, *3*, 888–899. [[CrossRef](#)]
69. Roshandel, D.; Heath Jeffery, R.C.; Charng, J.; Sampson, D.M.; McLenachan, S.; Mackey, D.A.; Chen, F.K. Short-Term Parafoveal Cone Loss Despite Preserved Ellipsoid Zone in Rod Cone Dystrophy. *Transl. Vis. Sci. Technol.* **2021**, *10*, 11. [[CrossRef](#)]
70. Ziccardi, L.; Giannini, D.; Lombardo, G.; Serrao, S.; Dell’Omo, R.; Nicoletti, A.; Bertelli, M.; Lombardo, M. Multimodal Approach to Monitoring and Investigating Cone Structure and Function in an Inherited Macular Dystrophy. *Am. J. Ophthalmol.* **2015**, *160*, 301–312. [[CrossRef](#)]
71. Potic, J.; Bergin, C.; Giacuzzo, C.; Daruich, A.; Pournaras, J.A.; Kowalczuk, L.; Behar-Cohen, F.; Konstantinidis, L.; Wolfensberger, T.J. Changes in visual acuity and photoreceptor density using adaptive optics after retinal detachment repair. *Retina* **2020**, *40*, 376–386. [[CrossRef](#)] [[PubMed](#)]

Disclaimer/Publisher’s Note: The statements, opinions and data contained in all publications are solely those of the individual author(s) and contributor(s) and not of MDPI and/or the editor(s). MDPI and/or the editor(s) disclaim responsibility for any injury to people or property resulting from any ideas, methods, instructions or products referred to in the content.

Article

Progression of Rare Inherited Retinal Dystrophies May Be Monitored by Adaptive Optics Imaging

Katarzyna Samelska ^{1,2,*} , Jacek Paweł Szaflik ^{1,2} , Barbara Śmigielńska ^{1,2}  and Anna Zaleska-Żmijewska ^{1,2} ¹ Department of Ophthalmology, Medical University of Warsaw, 02-091 Warsaw, Poland² SPKSO Ophthalmic University Hospital, 00-576 Warsaw, Poland

* Correspondence: samelskakatarzyna@gmail.com

Abstract: Inherited retinal dystrophies (IRDs) are bilateral genetic conditions of the retina, leading to irreversible vision loss. This study included 55 eyes afflicted with IRDs affecting the macula. The diseases examined encompassed Stargardt disease (STGD), cone dystrophy (CD), and cone-rod dystrophy (CRD) using adaptive optics (Rtx1™; Imagine Eyes, Orsay, France). Adaptive optics facilitate high-quality visualisation of retinal microstructures, including cones. Cone parameters, such as cone density (DM), cone spacing (SM), and regularity (REG), were analysed. The best corrected visual acuity (BCVA) was assessed as well. Examinations were performed twice over a 6-year observation period. A significant change was observed in DM (1282.73/mm² vs. 10,073.42/mm², $p < 0.001$) and SM (9.83 μm vs. 12.16 μm, $p < 0.001$) during the follow-up. BCVA deterioration was also significant (0.16 vs. 0.12, $p = 0.001$), albeit uncorrelated with the change in cone parameters. No significant difference in REG was detected between the initial examination and the follow-up ($p = 0.089$).

Keywords: adaptive optics; cone dystrophy; cone-rod dystrophy; inherited retinal diseases; inherited retinal dystrophies; ocular imaging; photoreceptors; retina; retinal imaging; Stargardt disease



Citation: Samelska, K.; Szaflik, J.P.; Śmigielńska, B.; Zaleska-Żmijewska, A. Progression of Rare Inherited Retinal Dystrophies May Be Monitored by Adaptive Optics Imaging. *Life* **2023**, *13*, 1871. <https://doi.org/10.3390/life13091871>

Academic Editors: Michele Lanza, Jay Chhablani and Claudio Iovino

Received: 4 August 2023

Revised: 2 September 2023

Accepted: 3 September 2023

Published: 5 September 2023



Copyright: © 2023 by the authors. Licensee MDPI, Basel, Switzerland. This article is an open access article distributed under the terms and conditions of the Creative Commons Attribution (CC BY) license (<https://creativecommons.org/licenses/by/4.0/>).

1. Introduction

1.1. Inherited Retinal Dystrophies

Inherited retinal dystrophies (IRDs) comprise a heterogeneous group of rare diseases that result in bilateral, irreversible vision loss. Although IRDs are genetic conditions, they represent a diverse group with varying inheritance patterns. The most-common IRD is rod-cone dystrophy (RCD), e.g., retinitis pigmentosa (RP), which primarily affects rods, with cone degeneration in RP originating in the outer retina.

Among the IRDs primarily affecting the macula, Stargardt disease (STGD) is the most-prevalent, with an incidence rate of approximately 1 in 10,000. Its manifestations include central vision loss, dyschromatopsia, and macular abnormalities, forming a “bull’s eye” pattern. This maculopathy results from abnormal accumulation of lipofuscin deposits in the central macula, with degeneration primarily affecting the retinal pigment epithelium (RPE) in the macular region. STGD symptoms typically emerge in the second decade of life. Cone-rod dystrophy (CRD) and cone dystrophy (CD) are IRDs less common than Stargardt disease, affecting approximately 1 in 30,000 to 1 in 40,000 individuals. CRD involves the degeneration of both cones and rods, while CD affects only cones; both of these conditions are progressive. These dystrophies primarily affect the macula and disturb central vision. Clinically, both CD and CRD present similarly, with bull’s eye maculopathy and bone spicule cells in the outer retina. The inheritance of the aforementioned IRDs may be autosomal dominant, autosomal recessive, X-linked, or unresolved [1–3].

Numerous genes have been identified with mutations that can lead to various IRDs, making genetic testing complex. The most-common gene mutation in STGD is autosomal recessive, involving the *ABCA4* gene, which encodes the ATP-binding cassette transporter

protein found in photoreceptors. Over 900 *ABCA4* disease-causing sequences have been identified, most of which are autosomal recessive. Some of the *ABCA4* mutations are responsible for the occurrence of RCD, CD, and CRD [4,5]. Other genes implicated in STGD include *ELOVL4* and *PROM1*.

Pathogenic mutations leading to CD and CRD can be located in genes encoding proteins involved in photoreception and the phototransduction cascade, such as *OPN1MW* and *OPN1LW* (encoding cone opsins) or in variants of *PDE6C*, *PDE6H*, *CNGA3*, and *CNGB3* (encoding transporters involved in controlling cGMP intracellular concentration). Other mutations may occur in genes involved in photoreceptor outer segment morphogenesis, intraflagellar transport, and neurotransmitter release. Of the 32 gene mutations leading to CD or CRD, 6 exhibit a predilection for CD and 22 tend to result in CRD, but most mutations overlap. There are also forms of CD and CRD associated with mutations in *ABCA4*—the most-common gene affected in STGD—as well as mutations in *RPGR*, which most commonly leads to RCD [2]. A comprehensive list of genetic mutations leading to different IRDs can be found on RetNet (<https://web.sph.uth.edu/RetNet/home.htm>, accessed on 4 August 2023).

1.2. Diagnostic Methods in Inherited Retinal Dystrophies

A clinical diagnosis of an IRD is typically made based on the clinical image of the eye fundus, the patient's history of vision loss in the first and second decades of life, and family history. Ancillary tests that aid in diagnosing IRDs include optical coherent tomography (OCT) of the macula, OCT angiography (OCTA), perimetry, electrophysiological testing (e.g., electroretinography (ERG)), fundus autofluorescence (FAF), and fluorescein angiography (FA) [5–9].

Monitoring of IRDs is challenging, and in most cases, universal guidelines for patient management are lacking.

The emergence of new methods for IRD evaluation is ongoing. These include emerging technologies such as adaptive optics (AO), adaptive optics OCT (AO-OCT), optoretinography, laser speckle flowgraphy, retinal oximetry, and functional magnetic resonance imaging [9,10]. Optoretinography maps the optical signal in response to a stimulus, whereas laser speckle flowgraphy enables real-time visualisation of circulation within ocular fundus structures. Retinal oximetry provides measurements of oxygen metabolism and oxygen diffusion from the choroidal circulation. Functional magnetic resonance imaging is a neuroimaging technique that records responses from the visual cortex. Adaptive optics, a ground-breaking technology, enables non-invasive imaging of retinal photoreceptors at the cellular level, making it a potent tool for visualising retinal pathologies. AO-OCT improves the quality of OCT imaging by correcting aberrations and mitigating quality degradation [9,10].

1.3. Therapy Perspectives in Inherited Retinal Dystrophies

Potential therapeutic techniques under development include gene supplementation, gene editing, antisense nucleotides, optogenetics, and stem-cell-based therapies. There is particular optimism for the successful treatment of IRDs with gene therapy [10]. The aim of these potential therapies is to slow down the degeneration of photoreceptors or improve their function.

The only currently available treatment for IRDs is gene therapy with voretigene neparvovec-rzyl (Luxturna[®]), approved by the Food and Drug Administration (FDA) in 2017 and the European Commission in 2018. Luxturna[®] targets the *RPE65* gene, which is primarily responsible for Leber congenital amaurosis (LCA).

In STGD, a human treatment trial targeting the *ABCA4* gene was initiated, but it was later halted by the sponsor (ClinicalTrials.gov ID: NCT01367444). Another active trial involves optogenetic therapy incorporating the injection of multi-characteristic opsin in eyes with STGD (NCT05417126). The results of gene therapy trials in RCD targeting the *RPGR*, *RHO*, *PDE6A*, *PDE6B*, and *MCO* genes are still awaited (NCT03252847, NCT03116113, NCT03316560,

NCT05748873, NCT04945772). To our knowledge, there are no human clinical trials targeting CD and CRD listed on ClinicalTrials.gov. However, several trials target the *CNGA3* and *CNGB3* gene mutations in another IRD, achromatopsia (ACHM) (NCT03278873, NCT02610582).

1.4. The Use of Adaptive Optics in Ophthalmology

Adaptive optics (AO) is an imaging technique initially developed for precise visualisation in astronomy, where it corrected atmospheric irregularities. The aberration-correcting system provides high-quality imaging of distant objects [11,12]. This high-quality visualisation is used in ophthalmology to evaluate the microstructures of the human retina with the precision to visualise a single cell. The AO retinal exam is quick and non-invasive. The assessment of the rods, cones, and retinal pigment endothelium cells has found its application in the management of diabetic retinopathy, age-related macular degeneration, glaucoma, and IRDs. Another possible application of AO in ophthalmology is the visualisation and measurement of the parameters of retinal microvessels: veins and arteries, which may be useful in diabetic retinopathy, prediabetes, hypertension, and glaucoma [13–15]. When combined with OCT, AO enables 3D imaging of retinal structures such as photoreceptors and retinal pigment epithelium [9].

The characteristics of cone mosaic parameters in a healthy eye have been defined [16]. Cone density in the healthy adult population averages 19,453/mm²; cone spacing is 7.96 µm; Voronoi analysis of cones (which is the percentage of hexagonal cells) is 46.7%.

Adaptive optics retinal images depicting a healthy eye, CD, CRD, and STGD are presented in Figures 1–4.

Figure 1 depicts the photoreceptor mosaic in a healthy eye. The image is taken paracentrally (2° superiorly) due to the limited ability of foveal image acquisition by Rtx™ [17]. By changing the focus point, the quality of an acquired image provides the assessment of photoreceptor parameters in parafoveal cones. The aberration and noise found in Figures 2–4 are considered to be the result of poor fixation in eyes with impaired central vision in the course of macular disease. This issue has been addressed in our study. The assessment of factors predisposing for obtaining inadequate image quality was taken into consideration further in this article.

Cone mosaic disruption is an abnormality typical of IRDs. The cone and rod spacing is increased in IRDs compared to healthy retinas [18]. Additionally, poor image quality, likely resulting from inadequate fixation in eyes with low visual acuity, is a problem that, in some cases, makes image acquisition impossible [19,20]. In STGD, as well as in other IRDs, the “dark spaces” depicting areas of disrupted cone structure and abnormal cone reflectance have been described [21,22].

Rtx1™ (Imagine Eyes, Orsay, France) is an adaptive optics flood-illuminated ophthalmoscope (AOFIO) that uses infrared light (850 nm wavelength) with a 1.6 µm resolution. The image dimensions are 4° × 4°, which corresponds to approximately 1.2 mm × 1.2 mm of the retina. The observation of foveal cones in Rtx™ is limited, as mentioned above [17], so images of the extrafoveal retina are typically acquired. Researchers working with this device often bypass this limitation by choosing a parafoveal region for the analysis. The examined position can be selected (e.g., 2° superior, inferior, temporal, or nasal—as in our study). The image acquisition in a single position lasts 2–4 s, during which 40 individual images are acquired [13,23–25]. The Rtx1™ software provides two programs for data evaluation: AO Detect for the analysis of photoreceptors parameters and AO Detect Artery for the analysis of vessel parameters.

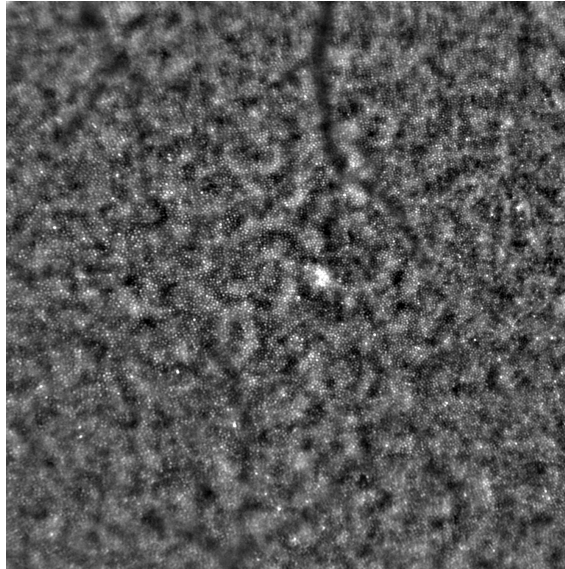


Figure 1. An adaptive optics image showing photoreceptors in a healthy eye (Rtx1™, Imagine Eyes, France). The photoreceptor mosaic appears intact (not disrupted) with individual photoreceptors visible as white and greyish spots.

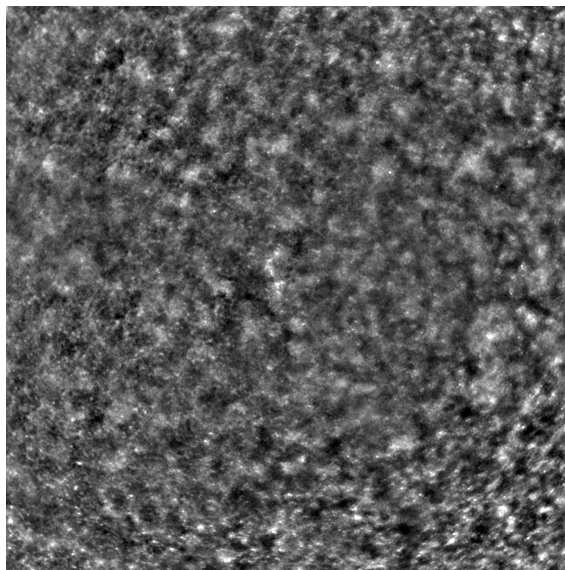


Figure 2. An adaptive optics image of the photoreceptors of an eye afflicted by cone dystrophy (Rtx1™, Imagine Eyes, France). Observe the cone disruption throughout the image with “dark spaces” apparent within the cone mosaic across different areas of the image.

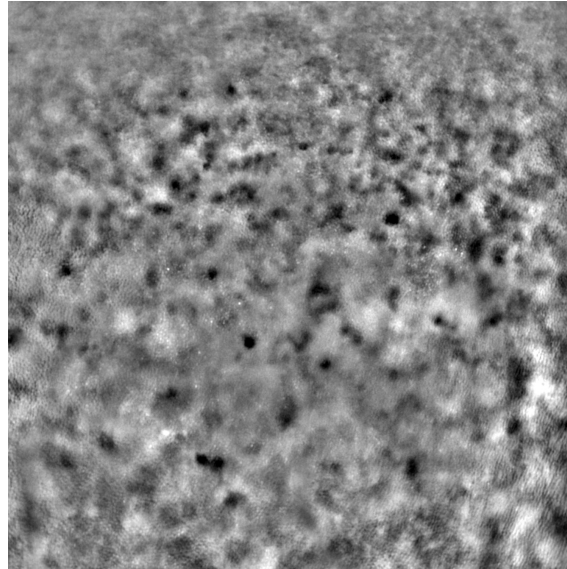


Figure 3. An adaptive optics image of photoreceptors in an eye affected by cone-rod dystrophy (Rtx1™, Imagine Eyes, France). Throughout the image, the cones are not clearly visible. Observe the “dark spaces” scattered within the cone mosaic across various regions of the picture.

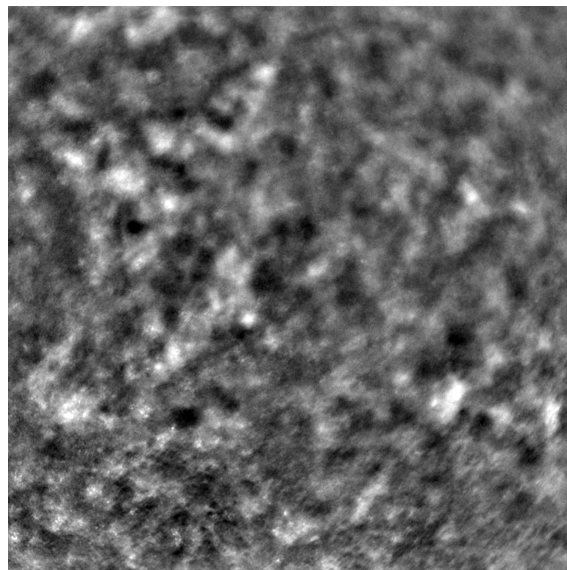


Figure 4. An adaptive optics image of the photoreceptors of the eye with Stargardt disease (Rtx1™; Imagine Eyes, France). The photoreceptor mosaic is disrupted, note the appearance “dark spaces” among the cone mosaic in various regions of the picture.

AO enables the visualisation of rods and cones, the two types of retinal photoreceptors. The parameters that adaptive optics can measure include: cone density, cone spacing, Voronoi analysis of hexagonal cells, reflectivity, regularity, metrics for the preferred orientation of cones, and local spatial anisotropy [6,16,17,26].

In our study, we analysed cone parameters: cone density (DM), cone spacing (SM), and cone regularity (REG). The abbreviations DM, SM, and REG are used by the AO Detect program and are further used in this article.

DM is expressed in $1/\text{mm}^2$; it is inversely correlated with SM, which measures the neighbour distance of each cone. REG (expressed in %) is important for providing the exclusion of inaccuracies caused by cell identification errors [17]. Our study focused on the use of AO in IRDs, specifically CD, CRD, and STGD, over a 6-year observation period. We performed AO retinal examinations twice over a 6-year observation period.

2. Materials and Methods

The study included 56 eyes from 28 patients who had been diagnosed with Stargardt disease (STGD) (38 eyes of 19 patients), cone dystrophy (CD) (10 eyes of 5 patients), or cone-rod dystrophy (CRD) (8 eyes of 4 patients). One eye, belonging to a female patient diagnosed with CD, was excluded from the analysis of photoreceptor parameters because it was not possible to obtain a good-quality image in any quadrant during the follow-up check. However, this eye was included in the analysis of factors that could potentially lead to incomplete data acquisition.

The examinations occurred in 2015 and were repeated in 2021, conducted at the Department of Ophthalmology, Medical University of Warsaw, in the SPKSO Ophthalmic University Hospital.

Each patient received his/her respective diagnosis of CD, CRD, or STGD through an evaluation that incorporated the clinical appearance of the eye fundus, FAF, AF, perimetry, and electrophysiological testing. Genetic testing was carried out in 20 patients, 13 of whom with STGD tested positive for *ABCA4* mutations. In the remaining patients, no mutation causing their conditions was found.

The exclusion criteria for the study encompassed other ocular pathologies such as glaucoma, cataract, previous ocular surgeries, history of uveitis, obesity (body mass index (BMI) $> 30 \text{ kg/m}^2$), and diabetes. Each participant, and parents of those under 18, provided written consent. This study adhered to the tenets of the Declaration of Helsinki and secured approval from the bioethics committee of the Medical University of Warsaw (KB/87/2015).

Before each examination, the best corrected visual acuity (BCVA) was checked using a Snellen chart, and the axial length of each eye was measured (LS 900; Haag-Streit; Koeniz, Switzerland). After mydriasis was induced using one drop of 1% tropicamide administered into each eye, the Rtx1™ (Imagine Eyes, France) test was performed. The acquired images were processed with the AO Detect program (version 3.4, also known as AO Image 3.4, Imagine Eyes, Orsay, France), providing numeric values for photoreceptor parameters: DM, cone density; SM, cone spacing; REG, cone regularity.

Each patient's eyes were examined using Rtx1™ (Imagine Eyes, France), measuring four positions in each eye: 2° away from the fixation point in the superior, inferior, temporal, and nasal quadrants. The area selected for analysis was taken from within the examined frame, specifically in a location where the image quality was adequate for conducting a quantitative analysis.

Due to the poor quality of some scans, the image positions were not considered for subsequent statistical analysis. Instead, we computed the average values from all positions where image acquisition was possible.

Demographic data for patients at initial presentation are detailed in Table 1. The values of BCVA, DM, SM, and cone regularity are shown in Table 2 for the initial check and in Table 3 for the follow-up check.

Data underwent normal distribution testing using the Shapiro–Wilk test. For normal distributions, Student’s *t*-test was used to compare the mean values of independent variables. If the normality assumption was violated, we employed the non-parametric Mann–Whitney U-test to compare continuous variables between two groups of observations. For comparisons involving more than two groups (as in our case, where three diagnosis types existed), we used one-way ANOVA (for parametric tests) or the Kruskal–Wallis test (for non-parametric tests). These tests were followed by either the HSD Tukey’s post hoc test (ANOVA) or Dunn’s post hoc test (Kruskal–Wallis), with results adjusted using the Bonferroni method. For this analysis, we set the level of statistical significance to $p = 0.05$. All calculations were carried out in R (Version 4.0.2).

Table 1. Demographic data of the patients during the initial check (data collected in 2015). CD: cone dystrophy. CRD: cone-rod dystrophy. STGD: Stargardt disease.

	CD (N = 9)	CRD (N = 8)	STGD (N = 38)	Total (N = 55)
Age (years)				
Mean (SD)	38.11 (7.46)	44.75 (4.17)	35.89 (14.41)	37.18 (14.18)
Median	39	43.5	35	36.5
Range	30–55	41–67	13–61	13–67
Sex				
Female	5 (55.6%)	2 (25%)	24 (63%)	31 (56.4%)
Male	4 (44.4%)	6 (75%)	14 (37%)	24 (43.6%)
Eye				
Right	5 (55.6%)	4 (50%)	19 (50%)	28 (51%)
Left	4 (44.4%)	4 (50%)	19 (50%)	27 (49%)

Table 2. Characteristics of adaptive optics parameters with respect to diagnosis during the initial check (data collected in 2015). BCVA: best corrected visual acuity; DM: cone density (1/mm²), SM: cone spacing (µm); REG: cone regularity (%); CD: cone dystrophy; CRD: cone-rod dystrophy; STGD: Stargardt disease. The bold was used in all *p*-Values lower than 0.05 (=with statistical significance).

	All Patients	CD (N = 9)	CRD (N = 8)	STGD (N = 38)	<i>p</i> -Value (Test)
BCVA					
Mean (SD)	0.16 (0.19)	0.17 (0.13)	0.32 (0.32)	0.13 (0.16)	0.102
Median	0.08 (0.04–0.2)	0.2	0.1	0.06	(Kruskal–Wallis)
Range	(0.01–0.8)	0.02–0.4	0.04–0.8	0.01–0.7	
DM					
Mean (SD)	12,828.73 (2618.96)	14,454.69 (2797)	13,594.72 (3067.63)	12,235.54 (2304.38)	0.032 (Kruskal–Wallis)
Median	13,018.33	14,523	14,434.62	12,513.33	
Range	7062–18,644.75	9368.67–18,644.75	8511.67–16,704	7062–18,080.5	
SM					
Mean (SD)	9.83 (1.01)	9.34 (1.04)	9.55 (1.12)	10.03 (0.95)	0.034 (Kruskal–Wallis)
Median	9.62	9.18	9.09	9.75	
Range	8.1–12.72	8.1–11.61	8.62–11.61	8.22–12.72	
REG					
Mean (SD)	86.44 (4.44)	90.24 (2.52)	89.02 (2.24)	84.88 (4.38)	<0.001 (Kruskal–Wallis)
Median	86.86	90.42	88.25	85.05	
Range	72.55–93.8	84.97–93.8	86.78–92.97	72.55–92.6	

Table 3. Characteristics of adaptive optics parameters with respect to diagnosis during the follow-up check (data collected in 2021). BCVA: best corrected visual acuity; DM: cone density ($1/\text{mm}^2$); SM: cone spacing (μm); REG: cone regularity (%); CD: cone dystrophy; CRD: cone-rod dystrophy; STGD: Stargardt disease.

	All Patients	CD (N = 9)	CRD (N = 8)	STGD (N = 38)	p-Value (Test)
BCVA					
Mean (SD)	0.12 (0.16)	0.15 (0.09)	0.28 (0.34)	0.09 (0.09)	0.111
Median	0.05	0.16	0.06	0.05	(Kruskal–Wallis)
Range	0.01–0.8	0.01–0.25	0.04–0.8	0.01–0.4	
DM					
Mean (SD)	10,073.42 (3217.93)	10,757.3 (3839.17)	11,711.26 (3694.61)	9523.2 (2861.4)	0.208
Median	10,213.38	10,777.25	12,140	9123	(Kruskal–Wallis)
Range	3830–16,341.25	5627.33–16,341.25	4584.33–15,494.75	3830–15,499.88	
SM					
Mean (SD)	12.16 (4.19)	11.3 (2.46)	11.42 (4.11)	12.55 (4.58)	0.219
Median	11.08	10.5	9.91	11.34	(Kruskal–Wallis)
Range	8.59–35.08	8.59–15.51	8.86–21.18	9.11–35.08	
REG					
Mean (SD)	84.37 (6.96)	86.8 (4.35)	86.26 (4.48)	83.31 (7.77)	0.262
Median	86.03	88.47	86.61	85.66	(Kruskal–Wallis)
Range	60.66–96.77	77.46–91.31	79.05–92.46	60.66–96.77	

3. Outcomes

3.1. BCVA Change during the 6-Year Observation Period

There was a significant change in BCVA observed between the examinations in 2015 and 2021: 0.16 vs. 0.12 ($p = 0.001$), as shown in Table 4. This change was also observed when analysing the right eyes ($p = 0.024$, Table 5) and left eyes ($p = 0.021$, Table 6) separately.

BCVA was not found to differ significantly between diagnoses in the initial examination ($p = 0.102$, Table 2), nor in the follow-up ($p = 0.111$, Table 3). Moreover, the BCVA change over the 6-year follow-up was not correlated with the diagnosis ($p = 0.705$, Table 7).

Table 4. Changes in adaptive optics parameters between the initial (2015) and follow-up (2021) checks. BCVA: best corrected visual acuity; DM: cone density ($1/\text{mm}^2$); SM: cone spacing (μm); REG: cone regularity (%); CD: cone dystrophy; CRD: cone-rod dystrophy; STGD: Stargardt disease. The bold was used in all p-Values lower than 0.05 (=with statistical significance).

		Initial (N = 55)	Follow-Up (N = 55)	p-Value (Test)
BCVA	Mean (SD)	0.16 (0.19)	0.12 (0.16)	0.001
	Median	0.08	0.05	(Wilcoxon)
	Range	0.01–0.8	0.01–0.8	
DM	Mean (SD)	12,828.73 (2618.96)	10,073.42 (3217.93)	<0.001
	Median	13,018.33	10,213.38	(Wilcoxon)
	Range	7062–18,644.75	3830–16,341.25	
SM	Mean (SD)	9.83 (1.01)	12.16 (4.19)	<0.001
	Median	9.62	11.08	(Wilcoxon)
	Range	8.1–12.72	8.59–35.08	
REG	Mean (SD)	86.44 (4.44)	84.37 (6.96)	0.089
	Median	86.86	86.03	(Wilcoxon)
	Range	72.55–93.8	60.66–96.77	

Table 5. Changes in adaptive optics parameters between the initial and follow-up checks for right eyes only. BCVA: best corrected visual acuity; DM: cone density (1/mm²); SM: cone spacing (μm); REG: cone regularity (%); CD: cone dystrophy; CRD: cone-rod dystrophy; STGD: Stargardt disease. The bold was used in all *p*-Values lower than 0.05 (=with statistical significance).

		Initial (N = 55)	Follow-Up (N = 55)	<i>p</i> -Value (Test)
BCVA	Mean (SD)	0.18 (0.23)	0.14 (0.17)	0.025 (Wilcoxon)
	Median	0.07	0.06	
	Range	0.01–0.8	0.01–0.8	
DM	Mean (SD)	12,595.3 (2590.99)	10,357.02 (3246.84)	0.006 (<i>t</i> -test)
	Median	12,877	9396.5	
	Range	7500–18,644.75	3830–15,499.88	
SM	Mean (SD)	9.97 (1.01)	12.4 (5.13)	0.002 (Wilcoxon)
	Median	9.82	11.31	
	Range	8.1–12.18	8.85–35.08	
REG	Mean (SD)	86.00 (5.06)	83.25 (7.53)	0.160 (Wilcoxon)
	Median	86.38	85.66	
	Range	72.55–93.8	60.66–96.77	

Table 6. Changes in adaptive optics parameters between the initial and follow-up checks for the left eyes only. BCVA: best corrected visual acuity; DM: cone density (1/mm²); SM: cone spacing (μm); REG: cone regularity (%); CD: cone dystrophy; CRD: cone-rod dystrophy; STGD: Stargardt disease. The bold was used in all *p*-Values lower than 0.05 (=with statistical significance).

		Initial (N = 55)	Follow-Up (N = 55)	<i>p</i> -Value (Test)
BCVA	Mean (SD)	0.15 (0.15)	0.11 (0.16)	0.021 (Wilcoxon)
	Median	0.1	0.05	
	Range	0.01–0.6	0.01–0.8	
DM	Mean (SD)	13,080.83 (2678.64)	9767.12 (3224.25)	< 0.001 (<i>T</i> -test)
	Median	13,152.25	10,480.5	
	Range	7062–18,080.5	4584.33–16,341.25	
SM	Mean (SD)	9.69 (1.02)	11.9 (2.95)	< 0.001 (Wilcoxon)
	Median	9.44	10.53	
	Range	8.21–12.72	8.59–21.18	
REG	Mean (SD)	86.92 (3.7)	85.57 (6.21)	0.182 (Wilcoxon)
	Median	85.95	86.17	
	Range	77.22–92.6	66.67–95.84	

Table 7. A difference in change in BCVA, DM, SM, and REG over 6-year observation between CD, CRD, and STGD groups: both eyes. BCVA: best corrected visual acuity. DM: cone density (1/mm²). SM: cone spacing (μm). REG: cone regularity (%). CD: cone dystrophy. CRD: cone-rod dystrophy. STGD: Stargardt disease.

	All Patients (N = 55)	CD (N = 9)	CRD (N = 8)	STGD (N = 38)	<i>p</i> -Value (Test)
BCVA change					
Mean (SD)	−0.04 (0.1)	−0.03 (0.08)	−0.03 (0.14)	−0.04 (0.1)	0.705 (Kruskal–Wallis)
Median	0	0	−0.04	0	
Range	(−0.4)–0.2	(−0.15)–0.1	(−0.3)–0.2	(−0.4)–0.04	
DM change					
Mean (SD)	−3008.25 (3059.45)	−3697.39 (1571.73)	−1883.46 (4462.61)	−3092.98 (2983.56)	0.338 (Kruskal–Wallis)
Median	−3600.12	−3682.75	−1139.75	−3622	
Range	(−10,290.42)–3798.33	(−6004.92)–(−1358.5)	(−10,290.42)–3798.33	(−8683.33)–3185.83	
SM change					
Mean (SD)	2.5 (4.13)	1.96 (1.76)	1.87 (4.43)	2.8 (4.56)	0.308 (Kruskal–Wallis)
Median	1.41	1.33	0.23	1.55	
Range	(−1.85)–24.39	0.38–5.66	(−1.85)–12.18	(−1.07)–24.39	
REG change					
Mean (SD)	−2.31 (7.66)	−3.44 (3.67)	−2.76 (4.36)	−1.89 (9.04)	0.475 (Kruskal–Wallis)
Median	−1.82	−4.81	−1.82	0.05	
Range	(−27.74)–18.61	(−7.57)–2.26	(−11.55)–2.01	(−27.74)–18.61	

3.2. Change in DM and SM during the 6-Year Observation Period

During the 6-year observation period, there was a significant decrease in DM ($-3008.25/\text{mm}^2$, $\text{SD} = 3059.45/\text{mm}^2$, $p < 0.001$) and an increase in SM ($2.5 \mu\text{m}$, $\text{SD} = 4.13 \mu\text{m}$, $p < 0.001$), as shown in Table 4. This significance was consistent when the calculations were performed separately for the right ($p = 0.006$ for DM and $p = 0.002$ for SM) and left eyes ($p < 0.001$ for both DM and SM), as shown in Tables 5 and 6.

3.3. Correlation between Cone Parameters and Diagnosis

The lowest mean DM and highest mean SM were found in patients with STGD. Both the DM and REG parameters differed significantly between eyes with a different diagnoses ($p = 0.032$ for DM (Kruskal–Wallis test), $p < 0.001$ for REG (Kruskal–Wallis test) in the initial examination (Table 2). However, these findings were not confirmed in the follow-up exam (Table 3).

Regarding the change in cone parameters over the 6-year observation period, the highest DM change was noted in the CD group ($-3697.39/\text{mm}^2$), compared to the STGD ($-3092.98/\text{mm}^2$) and CRD ($-1883.46/\text{mm}^2$) groups. The highest SM change was observed in the STGD group ($2.8 \mu\text{m}$), compared to the CD ($1.96 \mu\text{m}$) and CRD ($1.87 \mu\text{m}$) groups. However, the intergroup difference in the DM and SM change was not significant ($p = 0.338$ for DM change, $p = 0.308$ for SM change), as shown in Table 7.

3.4. Change in REG during 6-Year Observation Period

No significant difference was observed between REG values from the initial and follow-up checks (86.44% vs. 84.37%, $p = 0.089$ for both eyes; 86.0% vs. 83.25%, $p = 0.160$ for right eyes only; 86.92% vs. 85.57%, $p = 0.182$ for left eyes only), as shown in Tables 4–6.

3.5. Correlation between BCVA Change, Cone Parameters Change, and Patient's Sex

The decrease in the DM and increase in the SM parameters were significantly higher in females than in males, as depicted in Figures 5 and 6 and Table 8. Changes in DM and SM varied between the sexes. The mean DM change was ($-1908.26/\text{mm}^2$) for males and ($-3804.8/\text{mm}^2$) for females ($p = 0.025$). The mean SM change was $1.46 \mu\text{m}$ for males and $3.25 \mu\text{m}$ for females ($p = 0.021$). The changes in BCVA (-0.03 in males vs. -0.05 in females) and REG (-1.54% in males vs. -2.86% in females) were not significantly correlated with sex ($p = 0.748$ for BCVA change, $p = 0.507$ for REG change).

Table 8. Differences in BCVA, DM, SM, and REG changes over a 6-year observation period between males and females: both eyes. BCVA: best corrected visual acuity; DM: cone density ($1/\text{mm}^2$); SM: cone spacing (μm); REG: cone regularity (%); CD: cone dystrophy; CRD: cone–rod dystrophy; STGD: Stargardt disease. The bold was used in all p -Values lower than 0.05 (=with statistical significance).

	Males (N = 24)	Females (N = 31)	p -Value (Test)
BCVA change			
Mean (SD)	−0.03 (0.1)	−0.05 (0.1)	0.748
Median	0	0	(Mann–Whitney U)
Range	(−0.3)–0.2	(−0.4)–0.1	
DM change			
Mean (SD)	−1908.26 (3470.12)	−3804.8 (2492.9)	0.025
Median	−1528.75	−3741.33	(Mann–Whitney U)
Range	(−10,290.42)–3798.33	(−8683.33)–2622.88	
SM change			
Mean (SD)	1.46 (2.99)	3.25 (4.7)	0.021
Median	0.48	1.62	(Mann–Whitney U)
Range	(−1.85)–12.18	0.1–24.39	
REG change			
Mean (SD)	−1.54 (5.11)	−2.86 (9.12)	0.507
Median	−1.86	−1.79	(Mann–Whitney U)
Range	(−11.99)–6.91	(−27.74)–18.61	

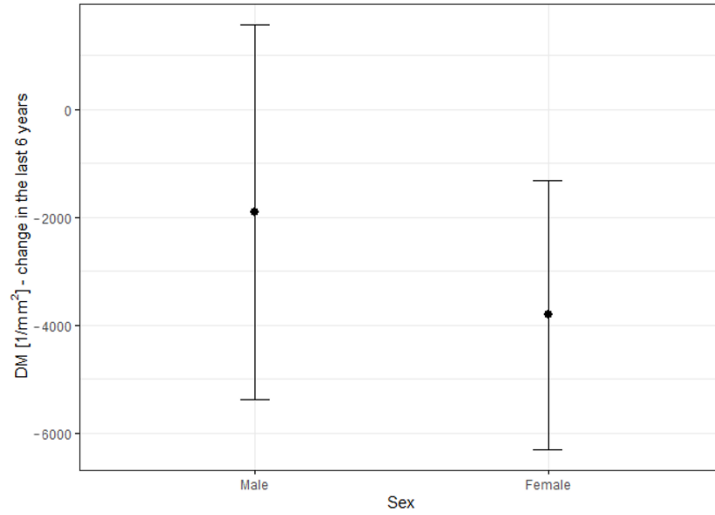


Figure 5. Difference in DM change over a 6-year observation period with respect to sex. DM: cone density (1/mm²).

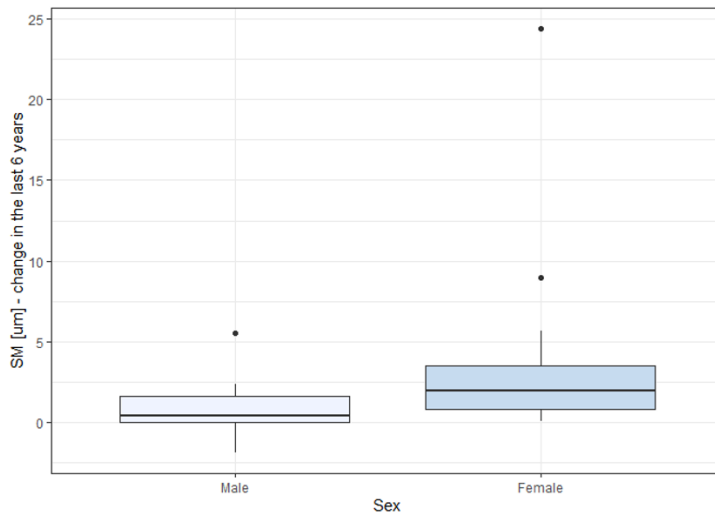


Figure 6. Difference in SM change over a 6-year observation with respect to sex. SM: cone spacing (µm).

3.6. Correlation of DM Change over 6-Year Observation with BCVA and AO Parameters

The investigation aimed to ascertain whether the decrease in DM during the observation correlated with a functional parameter: BCVA. The Spearman analysis revealed no correlation between DM change from the initial measurement to the follow-up and either initial BCVA ($p = 0.302$) or BCVA change over the 6-year observation ($p = 0.847$), as illustrated in Table 9. However, a significant correlation was noted between DM change and REG deterioration over the observation period ($p = 0.036$). A robust correlation was

also found between DM and SM change (correlation coefficient (r) = -0.856 , $p < 0.001$), which stems from the definition of SM and DM.

Table 9. Correlation between DM change over a 6-year observation and initial parameters BCVA, DM, SM, REG, and age; BCVA change, SM change, and REG change. Initial BCVA: best corrected visual acuity at initial check (2015). Initial DM: cone density at initial check (2015) ($1/\text{mm}^2$). Initial SM: cone spacing at initial check (2015) (μm). Initial REG: cone regularity at initial check (2015) (%). BCVA change: difference in best corrected visual acuity between the initial check and follow-up. SM change: difference in cone spacing between the initial check and follow-up (μm). REG change: difference in cone regularity between the initial check and follow-up (%). The bold was used in all p -Values lower than 0.05 (=with statistical significance).

Variable	Correlation Coefficient (r)	p -Value	(Test)
initial BCVA	0.149	0.302	Spearman
initial DM	0.149	0.302	Pearson
initial SM	0.172	0.231	Spearman
initial REG	-0.157	0.276	Spearman
age (years)	-0.176	0.223	Pearson
BCVA change	0.028	0.847	Spearman
SM change	-0.856	<0.001	Spearman
REG change	0.297	0.036	Pearson

3.7. Correlation of Cone Parameters with Patients' Age

There was no observed correlation between patients' age and either DM ($p = 0.290$) or SM ($p = 0.185$), as demonstrated in Table 10. Additionally, there was no correlation between DM change during the observation period and patients' age ($p = 0.223$), as shown in Table 9.

Table 10. Pearson's correlation coefficient (r) between mean values of DM, SM, and age (data collected in 2021). DM: cone density ($1/\text{mm}^2$), SM: cone spacing (μm).

Variable	Both Eyes (r)	p -Value	Right Eyes (r)	p -Value	Left Eyes (r)	p -Value
DM	-0.146	0.295	-0.328	0.110	-0.148	0.290
SM	0.197	0.157	0.316	0.124	0.185	0.185

3.8. Analysis of Factors Augmenting the Probability of Incomplete Data Acquisition

As previously mentioned, it was sometimes impossible to acquire an image of sufficient quality for analysis in all four examined quadrants. We conducted an analysis to identify the factors that increase the probability of incomplete data acquisition. The results of this analysis are presented in Tables 11 and 12.

Table 11. Descriptive characteristics concerning complete or incomplete data (with complete data indicating that 4 measurements provided an image suitable for analysis); data collected during the initial check. BCVA: best-corrected visual acuity; DM: cone density ($1/\text{mm}^2$); SM: cone spacing (μm); REG: cone regularity (%); CD: cone dystrophy; CRD: cone-rod dystrophy; STGD: Stargardt disease. The bold was used in all p -Values lower than 0.05 (=with statistical significance).

	Incomplete Data ($N = 28$)	Complete Data ($N = 28$)	p -Value (Test)
Mean age (SD)	36.4 (16.5)	37.9 (11.4)	0.694 (t -test)
Sex			
Male	42.9% ($N = 12$)	42.9% ($N = 12$)	1
Female	57.1% ($N = 16$)	57.1% ($N = 16$)	(chi-squared)
Diagnosis			
CD	7.1% ($N = 2$)	28.6% ($N = 8$)	0.118
CRD	14.3% ($N = 4$)	14.3% ($N = 4$)	(Fisher)
STGD	78.6% ($N = 22$)	57.1% ($N = 16$)	

Table 11. Cont.

	Incomplete Data (N = 28)	Complete Data (N = 28)	p-Value (Test)
BCVA			
Mean (SD)	0.15 (0.23)	0.21 (0.22)	0.112
Median (IQR)	0.05 (0.03–0.12)	0.09 (0.05–0.29)	(Mann–Whitney U)
Range	0.01–0.9	0.01–0.7	
DM			
Mean (SD)	11,078.6 (2329.58)	14,003.66 (1905.81)	<0.001
Median (IQR)	10,460.67 (9368.67–12,786.08)	13,805 (12,817.25–15,283.5)	(f-test)
Range	7500–15,949	10,540–18,644.75	
SM			
Mean (SD)	10.56 (0.98)	9.42 (0.65)	<0.001
Median (IQR)	10.78 (9.84–11.21)	9.42 (8.99–9.82)	(f-test)
Range	8.78–12.18	8.1–10.7	
REG			
Mean (SD)	83.53 (5.56)	88.29 (3.08)	<0.001
Median (IQR)	84.4 (79.47–87.03)	88.4 (86.2–90.6)	(f-test)
Range	72.55–92.97	81.77–93.8	

Table 12. Descriptive characteristics concerning complete or incomplete data (with complete data indicating that 4 measurements provided an image suitable for analysis); data collected during the follow-up. BCVA: best-corrected visual acuity; DM: cone density (1/mm²); SM: cone spacing (μm); REG: cone regularity (%); CD: cone dystrophy; CRD: cone-rod dystrophy; STGD: Stargardt disease. The bold was used in all p-Values lower than 0.05 (=with statistical significance).

	Incomplete Data (N = 19)	Complete Data (N = 37)	p-Value (Test)
Mean age (SD)	39.63 (14.3)	35.39 (13.95)	0.360 (f-test)
Sex			
Male	47.4% (N = 9)	40.5% (N = 15)	0.839
Female	52.6% (N = 10)	59.5% (N = 26)	(chi-squared)
Diagnosis			
CD	21.1% (N = 4)	16.2% (N = 6)	0.838
CRD	10.5% (N = 2)	16.2% (N = 6)	(Fisher)
STGD	68.4% (N = 13)	67.6% (N = 25)	
BCVA			
Mean (SD)	0.1 (0.12)	0.14 (0.18)	0.416
Median (IQR)	0.05 (0.04–0.11)	0.06 (0.05–0.2)	(Mann–Whitney U)
Range	0.01–0.4	0.01–0.8	
DM			
Mean (SD)	8071.89 (2892.07)	10,884.85 (3011.82)	0.004
Median (IQR)	7943.67 (5992–8886.5)	10,738 (9092.75–12,774.5)	(f-test)
Range	4584.33–15,067	3830–16,341.25	
SM			
Mean (SD)	13.17 (3.17)	11.75 (4.52)	0.013
Median (IQR)	12.24 (11.36–13.91)	10.5 (9.8–11.76)	(Mann–Whitney U)
Range	9.04–21.18	8.59–35.08	
REG			
Mean (SD)	83.96 (7.48)	84.53 (6.83)	0.357
Median (IQR)	84.76 (81.12–86.41)	86.17 (82.81–88.97)	(Mann–Whitney U)
Range	66.67–96.77	60.66–92.46	

The ratio of incomplete data collection was 50% during the initial check and 33.9% during the follow-up. Factors such as patients' age, sex, diagnosis, and BCVA were

not found to be correlated with incomplete data acquisition. However, incomplete data collection was significantly associated with low DM ($p < 0.001$ during the initial check, $p = 0.004$ during the follow-up) and high SM ($p < 0.001$ during the initial check, $p = 0.013$ during the follow-up). Low REG was also identified as a factor contributing to incomplete data collection during the initial check ($p < 0.001$), but not during the follow-up ($p = 0.357$).

4. Discussion

Our study corroborates that the progression of CD, CRD, and STGD can be accurately tracked based on cone parameters with AO. We observed a deterioration in visual acuity (BCVA), a loss of cone density (DM), and an increase in cone spacing (SM) over a 6-year observation period. However, the changes in cone parameters did not correlate with the loss of BCVA in our study. We hypothesise that, due to the low standard deviation of the functional parameter used in our study (BCVA), the correlation of the morphological and functional parameters cannot be stated. The development of advancements in electrophysiology testing, such as multifocal electroretinography, as well as assessing the patients in early stages of disease, might be crucial for determining the real dependence of anatomical changes in photoreceptors on visual function.

Our goal was to discern whether differences existed in the adaptive optics cone parameters in eyes diagnosed with CD, CRD, and STGD. In both the initial exam of the study described in this article and in our other study [20], we found differences in DM, SM, and REG among the different diagnosis groups. However, these differences were not confirmed in the follow-up of our current study. We also did not find significant differences among the groups in terms of the DM, SM, and REG changes over time. This observation underscores the need for further longitudinal research on AO visualisation in eyes with IRDs, which would validate our findings.

The correlation between DM change and REG change may suggest a loss of quality in AO data with the progression of photoreceptor loss. However, since REG did not differ significantly between the initial check and the follow-up, we can infer that the quality of the obtained images of the cones was consistent across both examinations. More research is still required to confirm this correlation.

The highest BCVA was noted in the CRD group (0.32 on initial check, 0.28 on follow-up) and the lowest in the STGD group (0.13 on initial check, 0.09 on follow-up). The BCVA in the CD group was 0.17 on the initial check and 0.15 at the follow-up. Other clinical studies have confirmed that vision deterioration proceeds more slowly in CRD than in CD. Furthermore, nyctalopia is less common in patients with CRD [2,27]. However, in our study, BCVA deterioration over a 6-year period was not correlated with the diagnosis of CD, CRD, or STGD.

Changes in DM and SM over the six-year observation period were significantly higher in females than in males. This might be due to the higher percentage of females in the STGD group (57.1%, 16 women), compared to other groups. The percentages of females in the CD and CRD groups were 55.6% and 25%, corresponding to 5 and 2 women, respectively, indicating a small group size for reliable statistical analysis. To our knowledge, other studies have not reported a quicker progression of IRDs in females than in males. The observation of the greater prevalence of SM and DM changes in women with IRDs needs to be validated in future studies.

No inter-eye differences were noted in terms of cone density in our study, consistent with our previous study conducted on healthy eyes [16].

The rarity of inherited retinal dystrophies in the population constrained the number of patients in the study group. Several studies have compared AO imaging outcomes between eyes with IRDs and healthy eyes. For instance, Duncan et al. [28] contrasted 5 eyes with RP, 3 eyes with CRD, and 8 healthy eyes. Nakatake et al. [29] analysed 14 eyes with RP alongside 10 healthy controls. Additionally, Giannini et al. [30] included a range of conditions: 4 eyes with RP, 1 eye with best corrected macular dystrophy, 1 eye with occult macular dystrophy, 2 eyes with macular drusen, 4 eyes with nonproliferative

diabetic retinopathy, and 20 healthy subjects. However, none of these studies provided longitudinal observations.

To our knowledge, no study other than ours has longitudinally assessed eyes with CD, CRD, or STGD. However, other reports on various IRDs do exist. For instance, a study on 16 eyes with RCD confirmed the correlation of AO changes with retinal thickness and findings in microperimetry, as well as a significant decline in cone spacing over a 3-year observation in the study group with no significant decline in healthy subjects [31].

Ueda-Consolvo et al. [32] carried out a study on 12 eyes of six patients with RP, aged 19–63, confirming the deterioration in cone density over a 2-year follow-up. BCVA was found to deteriorate in only one of six patients. This study did not include healthy controls. An observational case series by Ziccardi et al. [33] suggested the possibility of monitoring the progression of RP based on three probands over two years. A more-recent study [34] offered a short-term observation with AO imaging of eight patients with RCD and 10 healthy eyes, confirming the change of DM over a 6-month observation period in rod-cone dystrophy, but did not provide a longitudinal observation of healthy subjects.

Another publication reported the outcomes of imaging the eyes with RCDs [22], including patients who underwent neparovovec (Luxturna[®]) gene therapy. While the study did not report quantitative parameters such as DM and SM, it pointed out a crucial practical aspect of AO imaging in IRDs: the ability to assess the effects of treatments, like gene therapies. Evaluating photoreceptor parameters, along with visual assessment and other auxiliary tests, allows for a quantifiable analysis of the impacts of therapeutic interventions.

The progression of photoreceptor changes due to non-genetic pathology was documented by Potic et al. [35], where the study group consisted of patients post-retinal detachment repair, and the follow-up time was 3 months.

Differentiation between various types of IRD has been made possible through the use of AO across different genotypes. Mastey et al. [19] examined 9 subjects with ACHM, 7 of whom had a mutation in the *ATF6* gene, 1 in *CNGA3*, and 1 in *CNGB3*. In two of the patients, the acquisition of high-quality images was not feasible. Yet, they were able to discern a characteristic clear foveal cone mosaic in *CNGA3* and *CNGB3* patients, in contrast to patients with an *ATF6* gene mutation, where hyporeflective structures, possibly retinal pigment epithelium cells, were identified. The unique characteristics of the photoreceptor mosaic in retinitis-pigmentosa-GTPase-regulator (RPGR)-associated retinopathy and Stargardt disease and the differentiation between them have been reported [6].

A possible limitation to our study is the broad age range of the patients: 13–61 years, which could potentially impact the consistency of our study group. Nonetheless, in healthy eyes, the correlation between a patient's age and cone density was not significant, as noted in our previous study [16]. There is no defined change rate in cone density and cone spacing. Foote et al. [31] found no change in cone spacing in healthy controls over a 3-year observation. Conversely, according to some authors, photoreceptor density appears to decrease over time. Our other study [15] describes the changes in AO parameters (mean cone density, cone spacing, cone regularity, and Voronoi analysis) over a two-year observation in healthy eyes and in patients with diabetes.

Another potential limitation of our study is the absence of a control group comprised of healthy eyes. The values of the photoreceptor parameters differed between our study and the study reporting a normative database of cone parameters of healthy eyes [16]. Longitudinal observations of eyes with IRDs and healthy controls are not commonplace, as outlined above. We believe that longitudinal studies comparing changes in DM and SM over time between eyes with IRDs and healthy eyes should be promoted.

One of the challenges encountered in adaptive optics (AO) imaging of eyes with inherited retinal diseases (IRDs) is the difficulty some eyes have in maintaining central fixation, which compromises the quality of the collected images. Additionally, when patients fixate eccentrically, the precise location of the captured image remains uncertain.

Daich-Varela et al. [10] underscored the challenge of obtaining standardised AO images for each specific IRD.

In a previous study, we identified low cone density as a risk factor for incomplete data acquisition due to the poor quality of the obtained images, rendering quantitative analysis of photoreceptor parameters impossible [20]. These results align with those presented in the current article, as they are based on a similar cohort of patients. In our current study, the rate of full image acquisition failures ranged from 33.9% to 50%. We describe the correlation of low cone density and high cone spacing with the risk of data collection failure. The impact of low cone regularity as a predictor for incomplete data analysis remains uncertain, as it was not confirmed in a follow-up assessment. Both the current and previous analyses did not establish a correlation between visual acuity, sex, or age and the risk of poor image quality. We suspect that the researchers' experience with the imaging device may impact the success of data collection, as the failure rate was higher during the initial assessment than during follow-up. Given the high percentage of eyes with IRDs, where obtaining high-quality images is often impossible, we propose considering average values of photoreceptor parameters collected from various quadrants rather than specific locations.

While the quality of imaging can be challenging in certain cases, it offers the ability to monitor disease progression, even in instances that are too advanced for successful standard monitoring with macular OCT, FAF, or electrophysiology testing.

5. Conclusions

We propose that adaptive optics is a dependable instrument in handling the complex task of tracking the progression of retinal diseases. Over the course of a 6-year observation, a significant change in the cone parameters DM and SM was recorded. The change in DM and SM was more pronounced in females than in males and appeared to be independent of diagnosis (STGD, CD, or CRD), BCVA, or age.

Our study group consisting of 55 eyes with IRDs, observed over a span of 6 years, is the largest and longest of its kind in terms of adaptive optics assessment of patients with IRDs. We anticipate that our findings will motivate other clinicians to incorporate this highly effective imaging tool into their practice. Presently, adaptive optics is predominantly used as a research method. We affirm that the data obtained with Rtx1™ are reliable, offering the potential for the long-term observation of disease progression. As the development of gene therapy in IRDs progresses, we believe that AO will serve as a valuable instrument for monitoring treatment efficacy.

Author Contributions: Conceptualisation, J.P.S. and A.Z.-Ż.; methodology, A.Z.-Ż.; software, K.S.; validation, A.Z.-Ż., K.S. and J.P.S.; formal analysis, A.Z.-Ż.; investigation, K.S., B.Ś. and A.Z.-Ż.; resources, K.S.; data curation, K.S. and B.Ś.; original draft preparation, K.S.; writing, K.S. and A.Z.-Ż.; review and editing, K.S., J.P.S., B.Ś. and A.Z.-Ż.; visualisation, J.P.S. and A.Z.-Ż.; supervision, A.Z.-Ż.; project administration, J.P.S.; funding acquisition, J.P.S. All authors have read and agreed to the published version of the manuscript.

Funding: This research received no external funding.

Institutional Review Board Statement: The study was conducted in accordance with the Declaration of Helsinki and approved by the Bioethics Committee of the Medical University of Warsaw (KB/87/2015, 7 April 2015).

Informed Consent Statement: Informed consent was obtained from all subjects involved in the study. In the case of patients younger than 18, the consent was given by the patient and his/her parent.

Data Availability Statement: Not applicable.

Conflicts of Interest: The authors declare no conflict of interest.

Abbreviations

The following abbreviations are used in this manuscript:

ATP	Adenosine triphosphate
cGMP	Cyclic guanosine monophosphate
GTP	Guanosine triphosphate
IQR	Interquartile range
MDPI	Multidisciplinary Digital Publishing Institute
DOAJ	Directory of open access journals
LD	Linear dichroism
SD	Standard deviation
OR	Odds ratio

References

- Vincent, A.; Wright, T.; Garcia-Sanchez, Y.; Kisilak, M.; Campbell, M.; Westall, C.; Héon, E. Phenotypic characteristics including in vivo cone photoreceptor mosaic in KCNV2-related “cone dystrophy with supernormal rod electroretinogram”. *Investig. Ophthalmol. Vis. Sci.* **2013**, *54*, 898–908. [\[CrossRef\]](#) [\[PubMed\]](#)
- Gill, J.S.; Georgiou, M.; Kalitzeos, A.; Moore, A.T.; Michaelides, M. Progressive cone and cone-rod dystrophies: Clinical features, molecular genetics and prospects for therapy. *Br. J. Ophthalmol.* **2019**, *103*, 711–720. [\[CrossRef\]](#) [\[PubMed\]](#)
- Wawrocka, A.; Skorzyc-Werner, A.; Wicher, K.; Niedziela, Z.; Ploski, R.; Rydzanicz, M.; Sykulski, M.; Kociecki, J.; Weisschuh, N.; Kohl, S.; et al. Novel variants identified with next-generation sequencing in Polish patients with cone-rod dystrophy. *Mol. Vis.* **2018**, *24*, 326–339. [\[PubMed\]](#)
- Ścieżyńska, A.; Oziębło, D.; Ambroziak, A.M.; Korwin, M.; Szulborski, K.; Krawczyński, M.; Stawiński, P.; Szaflik, J.; Szaflik, J.P.; Ploski, R.; et al. Next-generation sequencing of ABCA4: High frequency of complex alleles and novel mutations in patients with retinal dystrophies from Central Europe. *Exp. Eye Res.* **2016**, *145*, 93–99. [\[CrossRef\]](#)
- Tanna, P.; Strauss, R.W.; Fujinami, K.; Michaelides, M. Stargardt disease: Clinical features, molecular genetics, animal models and therapeutic options. *Br. J. Ophthalmol.* **2017**, *101*, 25–30. [\[CrossRef\]](#) [\[PubMed\]](#)
- Tanna, P.; Kasilian, M.; Strauss, R.; Tee, J.; Kalitzeos, A.; Tarima, S.; Visotcky, A.; Dubra, A.; Carroll, J.; Michaelides, M. Reliability and Repeatability of Cone Density Measurements in Patients With Stargardt Disease and RPGR-Associated Retinopathy. *Investig. Ophthalmol. Vis. Sci.* **2017**, *58*, 3608–3615. [\[CrossRef\]](#) [\[PubMed\]](#)
- Kong, X.; Fujinami, K.; Strauss, R.W.; Munoz, B.; West, S.K.; Cideciyan, A.V.; Michaelides, M.; Ahmed, M.; Ervin, A.M.; Schönbach, E.; et al. Visual Acuity Change Over 24 Months and Its Association With Foveal Phenotype and Genotype in Individuals With Stargardt Disease: ProgStar Study Report No. 10. *JAMA Ophthalmol.* **2018**, *136*, 920–928. [\[CrossRef\]](#)
- Schönbach, E.M.; Strauss, R.W.; Ibrahim, M.A.; Janes, J.L.; Birch, D.G.; Cideciyan, A.V.; Sunness, J.S.; Muñoz, B.; Ip, M.S.; Sadda, S.R.; et al. Faster Sensitivity Loss around Dense Scotomas than for Overall Macular Sensitivity in Stargardt Disease: ProgStar Report No. 14. *Am. J. Ophthalmol.* **2020**, *216*, 219–225. [\[CrossRef\]](#)
- Ong, J.; Zarnegar, A.; Corradetti, G.; Singh, S.R.; Chhablani, J. Advances in Optical Coherence Tomography Imaging Technology and Techniques for Choroidal and Retinal Disorders. *J. Clin. Med.* **2022**, *11*, 5139. [\[CrossRef\]](#)
- Daich Varela, M.; Esener, B.; Hashem, S.A.; Cabral de Guimaraes, T.A.; Georgiou, M.; Michaelides, M. Structural evaluation in inherited retinal diseases. *Br. J. Ophthalmol.* **2021**, *105*, 1623–1631. [\[CrossRef\]](#)
- Samelska, K.; Kupis, M.; Zaleska-Żmijewska, A.; Szaflik, J.P. Adaptive optics imaging in the most common inherited retinal degenerations. *Klin. Ocz.* **2021**, *123*, 74–79. [\[CrossRef\]](#)
- Gill, J.S.; Moosajee, M.; Dubis, A.M. Cellular imaging of inherited retinal diseases using adaptive optics. *Eye* **2019**, *33*, 1683–1698. [\[CrossRef\]](#) [\[PubMed\]](#)
- Zaleska-Żmijewska, A.; Wawrzyniak, Z.; Kupis, M.; Szaflik, J.P. The Relation between Body Mass Index and Retinal Photoreceptor Morphology and Microvascular Changes Measured with Adaptive Optics (rtx1) High-Resolution Imaging. *J. Ophthalmol.* **2021**, *2021*, 6642059. [\[CrossRef\]](#)
- Zaleska-Żmijewska, A.; Piątkiewicz, P.; Śmigielska, B.; Sokółowska-Oracz, A.; Wawrzyniak, Z.M.; Romaniuk, D.; Szaflik, J.; Szaflik, J.P. Retinal Photoreceptors and Microvascular Changes in Prediabetes Measured with Adaptive Optics (rtx1™): A Case-Control Study. *J. Diabetes Res.* **2017**, *2017*, 4174292. [\[CrossRef\]](#)
- Kupis, M.; Wawrzyniak, Z.M.; Szaflik, J.P.; Zaleska-Żmijewska, A. Retinal Photoreceptors and Microvascular Changes in the Assessment of Diabetic Retinopathy Progression: A Two-Year Follow-Up Study. *Diagnostics* **2023**, *13*, 2513. [\[CrossRef\]](#)
- Zaleska-Żmijewska, A.; Wawrzyniak, Z.M.; Ulińska, M.; Szaflik, J.; Dąbrowska, A.; Szaflik, J.P. Human photoreceptor cone density measured with adaptive optics technology (rtx1 device) in healthy eyes: Standardization of measurements. *Medicine* **2017**, *96*, e7300. [\[CrossRef\]](#)
- Wynne, N.; Heitkotter, H.; Woertz, E.N.; Cooper, R.F.; Carroll, J. Comparison of Cone Mosaic Metrics From Images Acquired With the SPECTRALIS High Magnification Module and Adaptive Optics Scanning Light Ophthalmoscopy. *Transl. Vis. Sci. Technol.* **2022**, *11*, 19. [\[CrossRef\]](#)

18. Song, H.; Rossi, E.A.; Yang, Q.; Granger, C.E.; Latchney, L.R.; Chung, M.M. High-Resolution Adaptive Optics in Vivo Autofluorescence Imaging in Stargardt Disease. *JAMA Ophthalmol.* **2019**, *137*, 603–609. [[CrossRef](#)]
19. Mastey, R.R.; Georgiou, M.; Langlo, C.S.; Kalitzeos, A.; Patterson, E.J.; Kane, T.; Singh, N.; Vincent, A.; Moore, A.T.; Tsang, S.H.; et al. Characterization of Retinal Structure in ATF6-Associated Achromatopsia. *Investig. Ophthalmol. Vis. Sci.* **2019**, *60*, 2631–2640. [[CrossRef](#)]
20. Samelska, K.; Szaflik, J.P.; Guskowska, M.; Kurowska, A.K.; Zaleska-Żmijewska, A. Characteristics of Rare Inherited Retinal Dystrophies in Adaptive Optics—A Study on 53 Eyes. *Diagnostics* **2023**, *13*, 2472. [[CrossRef](#)]
21. Song, H.; Rossi, E.A.; Latchney, L.; Bessette, A.; Stone, E.; Hunter, J.J.; Williams, D.R.; Chung, M. Cone and rod loss in Stargardt disease revealed by adaptive optics scanning light ophthalmoscopy. *JAMA Ophthalmol.* **2015**, *133*, 1198–1203. [[CrossRef](#)] [[PubMed](#)]
22. Sahel, J.A.; Grieve, K.; Pagot, C.; Authié, C.; Mohand-Said, S.; Paques, M.; Audo, I.; Becker, K.; Chaumet-Riffaud, A.E.; Azoulay, L.; et al. Assessing Photoreceptor Status in Retinal Dystrophies: From High-Resolution Imaging to Functional Vision. *Am. J. Ophthalmol.* **2021**, *230*, 12–47. [[CrossRef](#)] [[PubMed](#)]
23. Lombardo, M.; Serrao, S.; Devaney, N.; Parravano, M.; Lombardo, G. Adaptive optics technology for high-resolution retinal imaging. *Sensors* **2012**, *13*, 334–366. [[CrossRef](#)] [[PubMed](#)]
24. Muthiah, M.N.; Gias, C.; Chen, F.K.; Zhong, J.; McClelland, Z.; Sallo, F.B.; Peto, T.; Coffey, P.J.; da Cruz, L. Cone photoreceptor definition on adaptive optics retinal imaging. *Br. J. Ophthalmol.* **2014**, *98*, 1073–1079. [[CrossRef](#)]
25. Zaleska-Żmijewska, A.; Wawrzyniak, Z.M.; Dąbrowska, A.; Szaflik, J.P. Adaptive Optics (rtx1) High-Resolution Imaging of Photoreceptors and Retinal Arteries in Patients with Diabetic Retinopathy. *J. Diabetes Res.* **2019**, *2019*, 9548324. [[CrossRef](#)]
26. Polans, J.; Keller, B.; Carrasco-Zevallos, O.M.; LaRocca, F.; Cole, E.; Whitson, H.E.; Lad, E.M.; Farsiu, S.; Izatt, J.A. Wide-field retinal optical coherence tomography with wavefront sensorless adaptive optics for enhanced imaging of targeted regions. *Biomed. Opt. Express* **2017**, *8*, 16–37. [[CrossRef](#)]
27. Thiadens, A.A.H.J.; Phan, T.M.L.; Zekveld-Vroon, R.C.; Leroy, B.P.; van den Born, L.I.; Hoyng, C.B.; Klaver, C.C.W.; Roosing, S.; Pott, J.W.R.; van Schooneveld, M.J.; et al. Clinical course, genetic etiology, and visual outcome in cone and cone-rod dystrophy. *Ophthalmology* **2012**, *119*, 819–826. [[CrossRef](#)]
28. Duncan, J.L.; Zhang, Y.; Gandhi, J.; Nakanishi, C.; Othman, M.; Branham, K.E.H.; Swaroop, A.; Roorda, A. High-resolution imaging with adaptive optics in patients with inherited retinal degeneration. *Investig. Ophthalmol. Vis. Sci.* **2007**, *48*, 3283–3291. [[CrossRef](#)]
29. Nakatake, S.; Murakami, Y.; Funatsu, J.; Koyanagi, Y.; Akiyama, M.; Momozawa, Y.; Ishibashi, T.; Sonoda, K.H.; Ikeda, Y. Early detection of cone photoreceptor cell loss in retinitis pigmentosa using adaptive optics scanning laser ophthalmoscopy. *Graefes Arch. Clin. Exp. Ophthalmol.* **2019**, *257*, 1169–1181. [[CrossRef](#)]
30. Giannini, D.; Lombardo, G.; Mariotti, L.; Devaney, N.; Serrao, S.; Lombardo, M. Reliability and Agreement Between Metrics of Cone Spacing in Adaptive Optics Images of the Human Retinal Photoreceptor Mosaic. *Investig. Ophthalmol. Vis. Sci.* **2017**, *58*, 3127–3137. [[CrossRef](#)]
31. Foote, K.G.; De la Huerta, I.; Gustafson, K.; Baldwin, A.; Zayit-Soudry, S.; Rinella, N.; Porco, T.C.; Roorda, A.; Duncan, J.L. Cone Spacing Correlates with Retinal Thickness and Microperimetry in Patients With Inherited Retinal Degenerations. *Investig. Ophthalmol. Vis. Sci.* **2019**, *60*, 1234–1243. [[CrossRef](#)]
32. Ueda-Consolvo, T.; Ozaki, H.; Nakamura, T.; Oiwake, T.; Hayashi, A. The association between cone density and visual function in the macula of patients with retinitis pigmentosa. *Graefes Arch. Clin. Exp. Ophthalmol.* **2019**, *257*, 1841–1846. [[CrossRef](#)] [[PubMed](#)]
33. Ziccardi, L.; Giannini, D.; Lombardo, G.; Serrao, S.; Dell’Omo, R.; Nicoletti, A.; Bertelli, M.; Lombardo, M. Multimodal Approach to Monitoring and Investigating Cone Structure and Function in an Inherited Macular Dystrophy. *Am. J. Ophthalmol.* **2015**, *160*, 301–312. [[CrossRef](#)] [[PubMed](#)]
34. Roshandel, D.; Heath Jeffery, R.C.; Charnig, J.; Sampson, D.M.; McLenachan, S.; Mackey, D.A.; Chen, F.K. Short-Term Parafoveal Cone Loss Despite Preserved Ellipsoid Zone in Rod Cone Dystrophy. *Transl. Vis. Sci. Technol.* **2021**, *10*, 11. [[CrossRef](#)]
35. Potic, J.; Bergin, C.; Giacuzzo, C.; Daruich, A.; Pourmaras, J.A.; Kowalczyk, L.; Behar-Cohen, F.; Konstantinidis, L.; Wolfensberger, T.J. Changes in visual acuity and photoreceptor density using adaptive optics after retinal detachment repair. *Retina* **2020**, *40*, 376–386. [[CrossRef](#)]

Disclaimer/Publisher’s Note: The statements, opinions and data contained in all publications are solely those of the individual author(s) and contributor(s) and not of MDPI and/or the editor(s). MDPI and/or the editor(s) disclaim responsibility for any injury to people or property resulting from any ideas, methods, instructions or products referred to in the content.

Podsumowanie i wnioski

W ramach przedstawionej pracy przeprowadzono przegląd dostępnego piśmiennictwa dotyczącego zastosowania optyki adaptywnej w ocenie i monitorowaniu oczu z dziedzicznymi dystrofiami siatkówki.

W celu oceny zmian fotoreceptorów siatkówki przeprowadzono badanie przekrojowe oczu z chorobą Stargarda, dystrofią czopkowo-pręcikową i dystrofią czopkową.

Na podstawie uzyskanych wyników można stwierdzić, że parametry morfologiczne fotoreceptorów siatkówki w rzadkich dziedzicznych chorobach siatkówki różnią się od parametrów morfologicznych fotoreceptorów w zdrowych oczach. Ponadto, analiza progresji zmian wykazuje postęp degeneracji w obserwacji 6-letniej.

Zmiana parametrów fotoreceptorów jest niezależna od ostrości wzroku z najlepszą korekcją. Analiza progresji w czasie jest możliwa do obserwacji za pomocą optyki adaptywnej.

Wyniki cyklu prac niniejszej dysertacji pozwalają na sformułowanie wniosków o następującej treści:

1. Parametry czopków mierzone przy użyciu optyki adaptywnej w oczach z dziedzicznymi dystrofiami siatkówki różnią się od parametrów czopków w oczach zdrowych.
2. Gęstość czopków oraz odległość między czopkami w oczach z dziedzicznymi dystrofiami siatkówki nie są zależne od ostrości wzroku z najlepszą korekcją, wieku ani płci.
3. Parametry czopków w oczach z dziedzicznymi dystrofiami siatkówki nie pozwalają na rozróżnienie pomiędzy poszczególnymi dystrofiami.
4. Progresja zmian czopków w czasie jest możliwa do obserwacji przy użyciu optyki adaptywnej. Stopień progresji ubytku gęstości czopków, wzrostu odległości między czopkami i ubytku regularności mozaiki czopków nie różni się istotnie między zbadanymi jednostkami chorobowymi.
5. Stopień ubytku w czasie gęstości czopków w oczach z dziedzicznymi dystrofiami siatkówki nie jest skorelowany z obniżeniem ostrości wzroku z najlepszą korekcją.
6. Stopień ubytku w czasie gęstości czopków w oczach z dziedzicznymi dystrofiami siatkówki jest wyższy u kobiet niż u mężczyzn.
7. Obniżenie gęstości czopków w czasie jest skorelowane z obniżeniem regularności mozaiki czopków w oczach z dziedzicznymi dystrofiami siatkówki.
8. Ryzyko niepełnej jakości badania w oczach z dziedzicznymi dystrofiami siatkówki jest wyższe w oczach z niższą gęstością czopków oraz jest niezależne od ostrości wzroku z najlepszą korekcją.

Piśmiennictwo

1. Gill, J.S.; Georgiou, M.; Kalitzeos, A.; Moore, A.T.; Michaelides, M. Progressive cone and cone-rod dystrophies: Clinical features, molecular genetics and prospects for therapy. *Br. J. Ophthalmol.* 2019, 103, 711–720.
2. Hamel CP, Griffoin JM, Bazalgette C, et al. Molecular genetics of pigmentary retinopathies: identification of mutations in CHM, RDS, RHO, RPE65, USH2A and XLR51 genes. *J Fr Ophthalmol* 2000; 23: 985-995.
3. Thiadens, A.A.H.J.; Phan, T.M.L.; Zekveld-Vroon, R.C.; Leroy, B.P.; van den Born, L.I.; Hoyng, C.B.; Klaver, C.C.W.; Roosing, S.; Pott, J.W.R.; van Schooneveld, M.J.; et al. Clinical course, genetic etiology, and visual outcome in cone and cone-rod dystrophy. *Ophthalmology* 2012, 119, 819–826.
4. Tanna, P.; Kasilian, M.; Strauss, R.; Tee, J.; Kalitzeos, A.; Tarima, S.; Visotcky, A.; Dubra, A.; Carroll, J.; Michaelides, M. Reliability and Repeatability of Cone Density Measurements in Patients With Stargardt Disease and RPGR-Associated Retinopathy. *Investig. Ophthalmol. Vis. Sci.* 2017, 58, 3608–3615.
5. Tanna, P.; Strauss, R.W.; Fujinami, K.; Michaelides, M. Stargardt disease: Clinical features, molecular genetics, animal models and therapeutic options. *Br. J. Ophthalmol.* 2017, 101, 25–30.
6. Ścieżyńska, A.; Oziębło, D.; Ambroziak, A.M.; Korwin, M.; Szulborski, K.; Krawczynski, M.; Stawinski, P.; Szaflik, J.; Szaflik, J.P.; Płoski, R.; et al. Next-generation sequencing of ABCA4: High frequency of complex alleles and novel mutations in patients with retinal dystrophies from Central Europe. *Exp. Eye Res.* 2016, 145, 93–99.
7. Kong, X.; Fujinami, K.; Strauss, R.W.; Munoz, B.; West, S.K.; Cideciyan, A.V.; Michaelides, M.; Ahmed, M.; Ervin, A.M.; Schönbach, E.; et al. Visual Acuity Change Over 24 Months and Its Association With Foveal Phenotype and Genotype in Individuals With Stargardt Disease: ProgStar Study Report No. 10. *JAMA Ophthalmol.* 2018, 136, 920–928.
8. Schönbach, E.M.; Strauss, R.W.; Ibrahim, M.A.; Janes, J.L.; Birch, D.G.; Cideciyan, A.V.; Sunness, J.S.; Muñoz, B.; Ip, M.S.; Sadda, S.R.; et al. Faster Sensitivity Loss around Dense Scotomas than for Overall Macular Sensitivity in Stargardt Disease: ProgStar Report No. 14. *Am. J. Ophthalmol.* 2020, 216, 219–225.
9. Ong, J.; Zarnegar, A.; Corradetti, G.; Singh, S.R.; Chhablani, J. Advances in Optical Coherence Tomography Imaging Technology and Techniques for Choroidal and Retinal Disorders. *J. Clin. Med.* 2022, 11, 5139.
10. Daich Varela, M.; Esener, B.; Hashem, S.A.; Cabral de Guimaraes, T.A.; Georgiou, M.; Michaelides, M. Structural evaluation in inherited retinal diseases. *Br. J. Ophthalmol.* 2021, 105, 1623–1631.
11. Dreher, A.W.; Bille, J.F.; Weinreb, R.N. Active optical depth resolution improvement of the laser tomographic scanner. *Appl. Opt.* 1989, 28, 804–808.
12. Liang, J.; Williams, D.R.; Miller, D.T. Supernormal vision and high-resolution retinal imaging through adaptive optics. *J. Opt. Soc. Am. A Opt. Image Sci. Vis.* 1997, 14, 2884–2892.
13. Lombardo, M.; Serrao, S.; Devaney, N.; Parravano, M.; Lombardo, G. Adaptive optics technology for high-resolution retinal imaging. *Sensors* 2012, 13, 334–366.
14. Scoles, D.; Sulai, Y.N.; Langlo, C.S.; Fishman, G.A.; Curcio, C.A.; Carroll, J.; Dubra, A. In vivo imaging of human cone photoreceptor inner segments. *Investig. Ophthalmol. Vis. Sci.* 2014, 55, 4244–4251.
15. Song, H.; Latchney, L.; Williams, D.; Chung, M. Fluorescence adaptive optics scanning laser ophthalmoscope for detection of reduced cones and

- hypoautofluorescent spots in fundus albipunctatus. *JAMA Ophthalmol.* 2014, 132, 1099–1104.
16. Wynne, N.; Heitkotter, H.; Woertz, E.N.; Cooper, R.F.; Carroll, J. Comparison of Cone Mosaic Metrics From Images Acquired With the SPECTRALIS High Magnification Module and Adaptive Optics Scanning Light Ophthalmoscopy. *Transl. Vis. Sci. Technol.* 2022, 11, 19.
 17. Song, H.; Rossi, E.A.; Latchney, L.; Bessette, A.; Stone, E.; Hunter, J.J.; Williams, D.R.; Chung, M. Cone and rod loss in Stargardt disease revealed by adaptive optics scanning light ophthalmoscopy. *JAMA Ophthalmol.* 2015, 133, 1198–1203.
 18. Al-Khuzaei, S.; Shah, M.; Foster, C.R.; Yu, J.; Broadgate, S.; Halford, S.; Downes, S.M. The role of multimodal imaging and vision function testing in ABCA4-related retinopathies and their relevance to future therapeutic interventions. *Ther. Adv. Ophthalmol.* 2021, 13, 25158414211056384.
 19. Bensinger, E.; Rinella, N.; Saud, A.; Loumou, P.; Ratnam, K.; Griffin, S.; Qin, J.; Porco, T.C.; Roorda, A.; Duncan, J.L. Loss of Foveal Cone Structure Precedes Loss of Visual Acuity in Patients With Rod-Cone Degeneration. *Investig. Ophthalmol. Vis. Sci.* 2019, 60, 3187–3196.
 20. Wolfing, J.I.; Chung, M.; Carroll, J.; Roorda, A.; Williams, D.R. High-resolution retinal imaging of cone-rod dystrophy. *Ophthalmology* 2006, 113, 1019.e1.
 21. Foote, K.G.; De la Huerta, I.; Gustafson, K.; Baldwin, A.; Zayit-Soudry, S.; Rinella, N.; Porco, T.C.; Roorda, A.; Duncan, J.L. Cone Spacing Correlates With Retinal Thickness and Microperimetry in Patients With Inherited Retinal Degenerations. *Investig. Ophthalmol. Vis. Sci.* 2019, 60, 1234–1243.
 22. Chen, Y.; Ratnam, K.; Sundquist, S.M.; Lujan, B.; Ayyagari, R.; Gudiseva, V.H.; Roorda, A.; Duncan, J.L. Cone photoreceptor abnormalities correlate with vision loss in patients with Stargardt disease. *Investig. Ophthalmol. Vis. Sci.* 2011, 52, 3281–3292.
 23. Song, H.; Rossi, E.A.; Yang, Q.; Granger, C.E.; Latchney, L.R.; Chung, M.M. High-Resolution Adaptive Optics in Vivo Autofluorescence Imaging in Stargardt Disease. *JAMA Ophthalmol.* 2019, 137, 603–609.
 24. Duncan, J.L.; Zhang, Y.; Gandhi, J.; Nakanishi, C.; Othman, M.; Branham, K.E.H.; Swaroop, A.; Roorda, A. High-resolution imaging with adaptive optics in patients with inherited retinal degeneration. *Investig. Ophthalmol. Vis. Sci.* 2007, 48, 3283–3291.
 25. Song, H.; Rossi, E.A.; Stone, E.; Latchney, L.; Williams, D.; Dubra, A.; Chung, M. Phenotypic diversity in autosomal-dominant cone-rod dystrophy elucidated by adaptive optics retinal imaging. *Br. J. Ophthalmol.* 2018, 102, 136–141.
 26. Sahel, J.A.; Grieve, K.; Pagot, C.; Authié, C.; Mohand-Said, S.; Paques, M.; Audo, I.; Becker, K.; Chaumet-Riffaud, A.E.; Azoulay, L.; et al. Assessing Photoreceptor Status in Retinal Dystrophies: From High-Resolution Imaging to Functional Vision. *Am. J. Ophthalmol.* 2021, 230, 12–47.
 27. Palejwala, N.V.; Gale, M.J.; Clark, R.F.; Schlechter, C.; Weleber, R.G.; Pennesi, M.E. Insights into autosomal dominant stargardt-like macular dystrophy through multimodality diagnostic imaging. *Retina* 2016, 36, 119–130.
 28. Choi, S.S.; Doble, N.; Hardy, J.L.; Jones, S.M.; Keltner, J.L.; Olivier, S.S.; Werner, J.S. In vivo imaging of the photoreceptor mosaic in retinal dystrophies and correlations with visual function. *Investig. Ophthalmol. Vis. Sci.* 2006, 47, 2080–2092.
 29. Ueda-Consolvo, T.; Ozaki, H.; Nakamura, T.; Oiwake, T.; Hayashi, A. The association between cone density and visual function in the macula of patients with retinitis pigmentosa. *Graefes Arch. Clin. Exp. Ophthalmol.* 2019, 257, 1841–1846.

30. Ziccardi, L.; Giannini, D.; Lombardo, G.; Serrao, S.; Dell’Omo, R.; Nicoletti, A.; Bertelli, M.; Lombardo, M. Multimodal Approach to Monitoring and Investigating Cone Structure and Function in an Inherited Macular Dystrophy. *Am. J. Ophthalmol.* 2015, 160, 301–312.
31. Roshandel, D.; Heath Jeffery, R.C.; Charng, J.; Sampson, D.M.; McLenachan, S.; Mackey, D.A.; Chen, F.K. Short-Term Parafoveal Cone Loss Despite Preserved Ellipsoid Zone in Rod Cone Dystrophy. *Transl. Vis. Sci. Technol.* 2021, 10, 11.
32. Giannini, D.; Lombardo, G.; Mariotti, L.; Devaney, N.; Serrao, S.; Lombardo, M. Reliability and Agreement Between Metrics of Cone Spacing in Adaptive Optics Images of the Human Retinal Photoreceptor Mosaic. *Investig. Ophthalmol. Vis. Sci.* 2017, 58, 3127–3137.
33. Potic, J.; Bergin, C.; Giacuzzo, C.; Daruich, A.; Pournaras, J.A.; Kowalczyk, L.; Behar-Cohen, F.; Konstantinidis, L.; Wolfensberger, T.J. Changes in visual acuity and photoreceptor density using adaptive optics after retinal detachment repair. *Retina* 2020, 40, 376–386.
34. Hu, M.L.; Edwards, T.L.; O’Hare, F.; Hickey, D.G.; Wang, J.H.; Liu, Z.; Ayton, L.N. Gene therapy for inherited retinal diseases: Progress and possibilities. *Clin. Exp. Optom.* 2021, 104, 444–454.
35. Maguire, A.M.; Bennett, J.; Aleman, E.M.; Leroy, B.P.; Aleman, T.S. Clinical Perspective: Treating RPE65-Associated Retinal Dystrophy. *Mol. Ther.* 2021, 29, 442–463.

Opinia Komisji Bioetycznej



Komisja Bioetyczna przy Warszawskim Uniwersytecie Medycznym

Tel.: 022/ 57 - 20 -303
Fax: 022/ 57 - 20 -165

ul. Żwirki i Wigury nr 61
02-091 Warszawa

e-mail: komisja.bioetyczna@wum.edu.pl
www.komisja-bioetyczna.wum.edu.pl

KB/.....⁸⁷...../2015

Komisja Bioetyczna przy Warszawskim Uniwersytecie Medycznym
po zapoznaniu się z wnioskiem /wymienić wnioskodawcę/ - w dniu 07 kwietnia 2015r.
Prof. dr hab.n. med. Jacek P. Szaflik, Katedra i Klinika Okulistyki,
ul. Sierakowskiego 13, 03-709 Warszawa

dotyczącym: wyrażenia opinii w sprawie badania pt.: „Ocena morfologii i funkcji fotoreceptorów centralnej siatkówki oraz naczyń siatkówki w wybranych jednostkach chorobowych z zastosowaniem metody optyki adaptatywnej.”

wyraża następującą opinię

- stwierdza, że jest ono dopuszczalne i zgodne z zasadami naukowo-etycznymi*.
- stwierdza, że jest ono niedopuszczalne i niezgodne z zasadami naukowo-etycznymi.*

Uwagi Komisji-verte

Pouczenie-w ciągu 14 dni od otrzymania decyzji wnioskodawcy przysługuje Prawo odwołania do Komisji Odwoławczej za pośrednictwem Komisji Bioetycznej przy Warszawskim Uniwersytecie Medycznym.

Komisja działa na podstawie art.29 ustawy z dnia 5.12.1996r. o zawodzie lekarza /Dz.U.nr 28/97 poz.152 wraz z późn.zm./, zarządzenia MZiOS z dn.11.05.1999r. w sprawie szczegółowych zasad powoływania i finansowania oraz trybu działania komisji bioetycznych /Dz.U.nr 47 poz.480/, Ustawy prawo farmaceutyczne z dnia 6 września 2001r. (Dz.U.Nr 126, poz. 1381 z późn. zm.) Zarządzenie nr 56/2007 z dnia 15 października 2007 r.w sprawie działania Komisji Bioetycznej przy Warszawskim Uniwersytecie Medycznym /Regulamin Komisji Bioetycznej przy Warszawskim Uniwersytecie Medycznym/.

Komisja działa zgodnie z zasadami GCP.

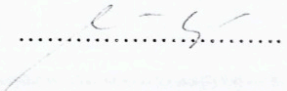
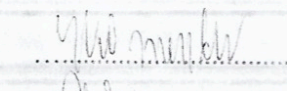
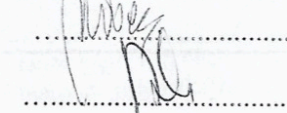
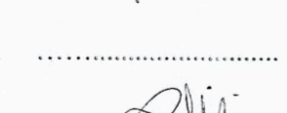
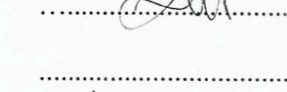
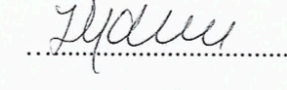
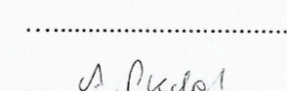
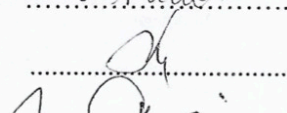
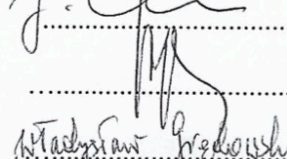
W załączeniu- skład Komisji oraz lista obecności.

Przewodnicząca
Komisji Bioetycznej

Prof. dr hab. n .med. Maria Roszkowska-Blaim

*niepotrzebne skreślić

strona podpisowa do uchwały Komisji Bioetycznej przy Warszawskim
Uniwersytecie Medycznym nr KB/.....⁸⁷..... z dnia 07 kwiecień 2015r.

1. Prof. dr hab. med. Maria ROSZKOWSKA-BLAIM 
2. Prof. dr hab. Barbara GAIKOWSKA
3. Prof. dr hab. med. Jadwiga KOMENDER 
4. Prof. dr hab. med. Bożenna WOCIAL 
5. Prof. nadzw. dr hab. med. Andrzej KAŃSKI 
6. Prof. dr hab. med. Jadwiga DWILEWICZ-TROJACZEK
7. Prof. dr hab. med. Zbigniew WIERZBICKI 
8. Prof. dr hab. med. Krzysztof J. FILIPIAK
9. Dr n. med. Zygmunt JAMROZIK 
10. Dr hab. n. med. Mariusz JASIK
11. Dr Agnieszka PIECHAL 
12. Mec. Ryszard PŁACZKOWSKI
13. Prof. dr hab. Joanna GÓRNICKA-KALINOWSKA 
14. Alicja JAWORSKA
15. Ksiądz Władysław GRĘDOWSKI 

Oświadczenia współautorów

Warszawa, 3.06.2024(miejsowość, data)

Lek. Katarzyna Samelska

OŚWIADCZENIE

Jako współautor pracy pt. *Adaptive optics imaging in the most common inherited retinal degenerations* oświadczam, iż mój własny wkład merytoryczny w przygotowanie, przeprowadzenie i opracowanie badań oraz przedstawienie pracy w formie publikacji obejmował: koncepcję artykułu, przygotowanie projektu pracy, zebranie danych, przygotowanie manuskryptu, sprawdzenie i edycję manuskryptu.

Mój udział procentowy w przygotowaniu publikacji określam jako 75%.

Jednocześnie wyrażam zgodę na wykorzystanie w/w pracy jako część mojej rozprawy doktorskiej.

Katarzyna Samelska
(podpis oświadczającego)

Notzeme 8.04.24.....(miejsowość, data)

Lek. Magdalena Kupis

OŚWIADCZENIE

Jako współautor pracy pt. *Adaptive optics imaging in the most common inherited retinal degenerations* oświadczam, iż mój własny wkład merytoryczny w przygotowanie, przeprowadzenie i opracowanie badań oraz przedstawienie pracy w formie publikacji obejmował:
przygotowanie manuskryptu, akceptację ostatecznej wersji manuskryptu.
Mój udział procentowy w przygotowaniu publikacji określam jako 5%.

Wkład lek. Katarzyny Samelskiej w powstawanie publikacji określam jako 75%,
obejmował on: koncepcję artykułu, przygotowanie projektu pracy, zebranie danych, przygotowanie manuskryptu, sprawdzenie i edycję manuskryptu.

Jednocześnie wyrażam zgodę na wykorzystanie w/w pracy jako część rozprawy doktorskiej lek. Katarzyny Samelskiej.

.....
(podpis oświadczającego)

Warszawa, 4.06.24 (miejsowość, data)

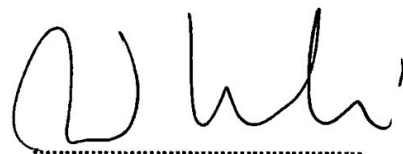
Prof. dr. hab. n. med.
Jacek. P. Szaflik

OŚWIADCZENIE

Jako współautor pracy pt. *Adaptive optics imaging in the most common inherited retinal degenerations* oświadczam, iż mój własny wkład merytoryczny w przygotowanie, przeprowadzenie i opracowanie badań oraz przedstawienie pracy w formie publikacji obejmował: sprawdzenie i edycję manuskryptu, akceptację ostatecznej wersji manuskryptu. Mój udział procentowy w przygotowaniu publikacji określam jako 10%.

Wkład lek. Katarzyny Samelskiej w powstawanie publikacji określam jako 75%, obejmował on: koncepcję artykułu, przygotowanie projektu pracy, zebranie danych, przygotowanie manuskryptu, sprawdzenie i edycję manuskryptu.

Jednocześnie wyrażam zgodę na wykorzystanie w/w pracy jako część rozprawy doktorskiej lek. Katarzyny Samelskiej.



(podpis oświadczającego)

Warszawa 2.04.24 (miejsowość, data)

Dr hab. n. med.
Anna Zaleska-Żmijewska

OŚWIADCZENIE

Jako współautor pracy pt. *Adaptive optics imaging in the most common inherited retinal degenerations* oświadczam, iż mój własny wkład merytoryczny w przygotowanie, przeprowadzenie i opracowanie badań oraz przedstawienie pracy w formie publikacji obejmował: sprawdzenie i edycję manuskryptu, akceptację ostatecznej wersji manuskryptu. Mój udział procentowy w przygotowaniu publikacji określam jako 10%.

Wkład lek. Katarzyny Samelskiej w powstawanie publikacji określam jako 75%, obejmował on: koncepcję artykułu, przygotowanie projektu pracy, zebranie danych, przygotowanie manuskryptu, sprawdzenie i edycję manuskryptu.

Jednocześnie wyrażam zgodę na wykorzystanie w/w pracy jako część rozprawy doktorskiej lek. Katarzyny Samelskiej.

Anna Zaleska-Żmijewska
.....
(podpis oświadczającego)

Warszawa, 3.06.24.....(miejsowość, data)

Lek. Katarzyna Samelska

OŚWIADCZENIE

Jako współautor pracy pt. *Characteristics of Rare Inherited Retinal Dystrophies in Adaptive Optics—A Study on 53 Eyes* oświadczam, iż mój własny wkład merytoryczny w przygotowanie, przeprowadzenie i opracowanie badań oraz przedstawienie pracy w formie publikacji obejmował: wybór metodyki, zebranie danych, przeprowadzenie częściowej analizy statystycznej, interpretację wyników, przygotowanie manuskryptu, sprawdzenie manuskryptu.

Mój udział procentowy w przygotowaniu publikacji określam jako 65%.

Jednocześnie wyrażam zgodę na wykorzystanie w/w pracy jako część mojej rozprawy doktorskiej.

Katarzyna Samelska
.....
(podpis oświadczającego)

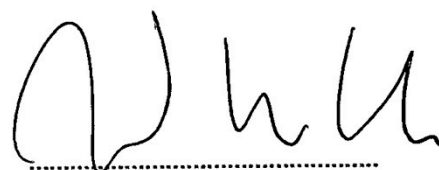
Warszawa 4.06.24 (miejscowość, data)

Prof. dr. hab. n. med.
Jacek. P. Szaflik

OŚWIADCZENIE

Jako współautor pracy pt. *Characteristics of Rare Inherited Retinal Dystrophies in Adaptive Optics— A Study on 53 Eyes* oświadczam, iż mój własny wkład merytoryczny w przygotowanie, przeprowadzenie i opracowanie badań oraz przedstawienie pracy w formie publikacji obejmował:
opracowanie koncepcji badania, wybór metodyki, nadzór merytoryczny nad poszczególnymi etapami badania, interpretację wyników, sprawdzenie i akceptację ostatecznej wersji manuskryptu, pozyskanie funduszy na opublikowanie artykułu.
Mój udział procentowy w przygotowaniu publikacji określam jako 10%.

Wkład lek. Katarzyny Samelskiej w powstawanie publikacji określam jako 65%, obejmował on:
wybór metodyki, zebranie danych, przeprowadzenie częściowej analizy statystycznej, interpretację wyników, przygotowanie manuskryptu, sprawdzenie manuskryptu.
Jednocześnie wyrażam zgodę na wykorzystanie w/w pracy jako część rozprawy doktorskiej lek. Katarzyny Samelskiej.



(podpis oświadczającego)

Warszawa, 9/04/24
.....(miejsowość, data)

Lek. Maria Guskowska

OŚWIADCZENIE

Jako współautor pracy pt. *Characteristics of Rare Inherited Retinal Dystrophies in Adaptive Optics— A Study on 53 Eyes* oświadczam, iż mój własny wkład merytoryczny w przygotowanie, przeprowadzenie i opracowanie badań oraz przedstawienie pracy w formie publikacji obejmował:

zebranie danych, sprawdzenie i akceptację ostatecznej wersji manuskryptu.

Mój udział procentowy w przygotowaniu publikacji określam jako 5%.

Wkład lek. Katarzyny Samelskiej w powstawanie publikacji określam jako 65%, obejmował on:

wybór metodyki, zebranie danych, przeprowadzenie częściowej analizy statystycznej, interpretację wyników, przygotowanie manuskryptu, sprawdzenie manuskryptu.

Jednocześnie wyrażam zgodę na wykorzystanie w/w pracy jako część rozprawy doktorskiej lek. Katarzyny Samelskiej.


.....
(podpis oświadczającego)

Warszawa, 20.05.24 (miejsowość, data)

Dr n. med. Anna K. Kurowska

OŚWIADCZENIE

Jako współautor pracy pt. *Characteristics of Rare Inherited Retinal Dystrophies in Adaptive Optics—A Study on 53 Eyes* oświadczam, iż mój własny wkład merytoryczny w przygotowanie, przeprowadzenie i opracowanie badań oraz przedstawienie pracy w formie publikacji obejmował:

nadzór merytoryczny, sprawdzenie i akceptację ostatecznej wersji manuskryptu.

Mój udział procentowy w przygotowaniu publikacji określam jako 5%.

Wkład lek. Katarzyny Samelskiej w powstawanie publikacji określam jako 65%, obejmował on:

wybór metodyki, zebranie danych, przeprowadzenie częściowej analizy statystycznej, interpretację wyników, przygotowanie manuskryptu, sprawdzenie manuskryptu.

Jednocześnie wyrażam zgodę na wykorzystanie w/w pracy jako część rozprawy doktorskiej lek. Katarzyny Samelskiej.



(podpis oświadczającego)

Warszawa, 8.04.24.....(miejsowość, data)

Dr hab. n. med.
Anna Zaleska-Żmijewska

OŚWIADCZENIE

Jako współautor pracy pt. *Characteristics of Rare Inherited Retinal Dystrophies in Adaptive Optics— A Study on 53 Eyes* oświadczam, iż mój własny wkład merytoryczny w przygotowanie, przeprowadzenie i opracowanie badań oraz przedstawienie pracy w formie publikacji obejmował:


opracowanie koncepcji badania, wybór metodyki, nadzór merytoryczny nad poszczególnymi etapami badania, interpretację wyników, sprawdzenie, edycję i akceptację ostatecznej wersji manuskryptu.

Mój udział procentowy w przygotowaniu publikacji określam jako 15%.

Wkład lek. Katarzyny Samelskiej w powstawanie publikacji określam jako 65%, obejmował on:

wybór metodyki, zebranie danych, przeprowadzenie częściowej analizy statystycznej, interpretację wyników, przygotowanie manuskryptu, sprawdzenie manuskryptu.

Jednocześnie wyrażam zgodę na wykorzystanie w/w pracy jako część rozprawy doktorskiej lek. Katarzyny Samelskiej.


.....
(podpis oświadczającego)

Warszawa, 3.06.24.....(miejsowość, data)

Lek. Katarzyna Samelska

OŚWIADCZENIE

Jako współautor pracy pt. *Progression of Rare Inherited Retinal Dystrophies May Be Monitored by Adaptive Optics Imaging* oświadczam, iż mój własny wkład merytoryczny w przygotowanie, przeprowadzenie i opracowanie badań oraz przedstawienie pracy w formie publikacji obejmował: wybór metodyki, zebranie danych, przeprowadzenie częściowej analizy statystycznej, interpretację wyników, przygotowanie manuskryptu, sprawdzenie manuskryptu.

Mój udział procentowy w przygotowaniu publikacji określam jako 70%.

Jednocześnie wyrażam zgodę na wykorzystanie w/w pracy jako część mojej rozprawy doktorskiej.

Katarzyna Samelska

(podpis oświadczającego)

Narzędzia, 4.06.2024(miejsowość, data)

Prof. dr. hab. n. med.
Jacek. P. Szaflik

OŚWIADCZENIE

Jako współautor pracy pt. *Progression of Rare Inherited Retinal Dystrophies May Be Monitored by Adaptive Optics Imaging* oświadczam, iż mój własny wkład merytoryczny w przygotowanie, przeprowadzenie i opracowanie badań oraz przedstawienie pracy w formie publikacji obejmował:

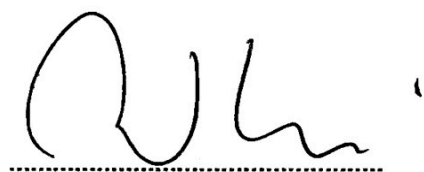
opracowanie koncepcji badania, wybór metodyki, sprawdzenie i akceptację ostatecznej wersji manuskryptu.

Mój udział procentowy w przygotowaniu publikacji określam jako 10%.

Wkład lek. Katarzyny Samelskiej w powstawanie publikacji określam jako 70%, obejmował on:

wybór metodyki, zebranie danych, przeprowadzenie częściowej analizy statystycznej, interpretację wyników, przygotowanie manuskryptu, sprawdzenie manuskryptu.

Jednocześnie wyrażam zgodę na wykorzystanie w/w pracy jako część rozprawy doktorskiej lek. Katarzyny Samelskiej.



.....
(podpis oświadczającego)

Warszawa 23.04.2021
.....(miejsowość, data)

Dr n. med. Barbara Śmigielska

OŚWIADCZENIE

Jako współautor pracy pt. *Progression of Rare Inherited Retinal Dystrophies May Be Monitored by Adaptive Optics Imaging* oświadczam, iż mój własny wkład merytoryczny w przygotowanie, przeprowadzenie i opracowanie badań oraz przedstawienie pracy w formie publikacji obejmował: zebranie danych, sprawdzenie i akceptację ostatecznej wersji manuskryptu. Mój udział procentowy w przygotowaniu publikacji określam jako 5%.

Wkład lek. Katarzyny Samelskiej w powstawanie publikacji określam jako 70%, obejmował on: wybór metodyki, zebranie danych, przeprowadzenie częściowej analizy statystycznej, interpretację wyników, przygotowanie manuskryptu, sprawdzenie manuskryptu. Jednocześnie wyrażam zgodę na wykorzystanie w/w pracy jako część rozprawy doktorskiej lek. Katarzyny Samelskiej.

B.Śmigielska
.....
(podpis oświadczającego)

Norowa 9.04.2024 (miejsowość, data)

Dr hab. n. med.
Anna Zaleska-Żmijewska

OŚWIADCZENIE

Jako współautor pracy pt. *Progression of Rare Inherited Retinal Dystrophies May Be Monitored by Adaptive Optics Imaging* oświadczam, iż mój własny wkład merytoryczny w przygotowanie, przeprowadzenie i opracowanie badań oraz przedstawienie pracy w formie publikacji obejmował: opracowanie koncepcji badania, wybór metodyki, nadzór merytoryczny nad poszczególnymi etapami badania, interpretację wyników, sprawdzenie i akceptację ostatecznej wersji manuskryptu. Mój udział procentowy w przygotowaniu publikacji określam jako 15%.

Wkład lek. Katarzyny Samelskiej w powstawanie publikacji określam jako 70%, obejmował on: wybór metodyki, zebranie danych, przeprowadzenie częściowej analizy statystycznej, interpretację wyników, przygotowanie manuskryptu, sprawdzenie manuskryptu. Jednocześnie wyrażam zgodę na wykorzystanie w/w pracy jako część rozprawy doktorskiej lek. Katarzyny Samelskiej.



(podpis oświadczającego)